Involvement of Gibberellin in growth and carbohydrate partitioning in developing pea (*Pisum sativum* L.) seeds

By

Kosala Dinuka Waduthanthri

A thesis submitted in partial fulfillment of the requirements for the degree of

Master of Science
in
Plant Science

Department of Agricultural, Food, and Nutritional Sciences

University of Alberta

Abstract

Gibberellins (GAs) are an important class of diterpenoid plant hormones that control various aspects of plant development including seed growth and development. The involvement of GAs during pea (*Pisum sativum*) seed development was studied by comparing GA deficient mutants; *lh*-2, *lh-1, le-3, ls-1* and a transgenic GA-overexpressor line (TG1) with their respective isogenic or transgenic controls. *lh*-2 was the most severe GA biosynthesis mutant studied, with marked reduction in seed bioactive GA levels, reduced seed growth, and high seed abortion (Swain et al., 1993, Planta 191:482). Seed coats of *lh-2* exhibited delayed hypodermal and reduced epidermal and ground parenchyma cell expansion compared to *LH* seed coats. *lh-2* cotyledonary storage parenchyma cell expansion was also reduced compared to the *LH* line. With respect to photoassimilate partitioning, starch accumulation (8 to 12 days after anthesis; DAA) in the seed coat and mobilization of seed coat starch to the embryo (14 to 20 DAA), as well as starch accumulation in the cotyledons, were dramatically reduced in the *lh-2* mutant compared to *LH*. The *lh-2* mutation delayed the transition of the liquid endosperm from a high to low glucose to sucrose state, and prolonged the complete absorption of the endosperm by the developing embryo by four days compared to that of *LH*. The other three GA biosynthesis mutants (*lh-1, le-3, and ls-1*) showed less severe effects on seed growth and development, and seed coat cell expansion. However, starch accumulation in the seed coat was markedly lower in *lh-1, le-3, and ls-1* than in their isogenic wild-type (from 8 to 12 DAA), and accumulation of starch in the embryo was delayed (14 to 20 DAA).

The GA-overexpressor line TG1 constitutively expresses *PsGA3ox1* (*LE*; a fully functional wild-type GA 3β-hydroxylase gene that encodes 3β-hydroxylase that converts GA_{20} to GA_1) in a semi-dwarf *lele* pea line ('Carneval'; *le-1*; single base-pair mutation in *PsGA3ox1*) (Reinecke et al., 2013, Plant Physiol 163:929). In the GA-overexpressor line

TG1, enhanced hypodermal, epidermal, ground parenchyma and branched parenchyma cell expansion was observed in the seed coat compared to the transgenic control C1. Starch accumulation in the seed coat cells was greater at 10 DAA and mobilization of seed coat starch to the embryo was enhanced from 16 to 20 DAA in TG1 compared to the transgenic control line. The accelerated assimilate partitioning into the seed in TG1 was correlated with larger seed size at maturity. These data support that GAs regulate specific aspects of seed coat and embryo development, and as a result, can modify photoassimilate partitioning into the developing seed.

Preface

Drs. Ozga and Reinecke (Plant BioSystems Group, Department of Agricultural, Food, and Nutritional Science, University of Alberta) designed the experiments presented in this thesis. I performed all experiments and obtained the data for all growth, histological, and carbohydrate studies. I provided and made the final micrographs for all tissues. I provided the plant material for gibberellin quantitation that was performed by the National Research Council Canada, Saskatoon, Canada. Dr. Harleen Kaur provided graphs for the growth, cell expansion and carbohydrate data presented in the thesis.

Acknowledgements

I would like to take this opportunity to thank the many people who have contributed to my graduate research. First and foremost I would like to sincerely thank my supervisor Professor Jocelyn Ozga for her guidance and suggestions throughout the duration of program. She has guided me through uncertainties and shared her experiences in a gentle and generous manner. Many thanks to my committee member, Dr. Janice Cooke for her constructive criticisms and support during my program. I am very thankful to Dr. Dennis Reinecke who was very generous with his time in sharing his experience and expertise. For technical help, Arlene Oatway was available to answer my questions and gave her advice when I needed to troubleshoot a problem, during microscopy studies. Further thanks go to Dr. Harleen Kaur and Dr. Alena Jin for helping me in numerous ways and for giving professional and technical advices. Indeed I was also lucky to meet numerous other nice people, including Dr. Kelvin Lien**,** Charitha Jayasinghe, Dakshina Ariyawansha, Gabor Botar, Szidonia Botar, Dhanuja Abeysingha and all my dear friends in the department who were always ready with their generous help and encouragement. My sincere gratitude goes to my wife Kethmi Jayawardhane for all her support, understanding and taking entire responsibilities of the family during my studies. Most importantly, my heartfelt gratitude goes to my parents for their unreserved love, inspiration, and never ending financial and emotional support throughout my life. Finally, my friend's loyal encouragement and sharing helped keep my life as a graduate student joyous and ever optimistic.

Contents

List of Tables

Table **Page**

Table **Page**

List of Figures

Figure **Page**

Figure **Page**

Figure **Page**

Figure **Page**

List of Abbreviations

Abbreviation	Definition
µmol	micro molar
ADP	Adenosine diphosphate
$CaCl_2$	calcium chloride
cDNA	complementary DNA
CDP	*ent*-copalyl diphosphate
CPS	*ent*-copalyl diphosphate synthase
CWI	cell wall-bound invertase
DAA	days after anthesis
DAP	days after pollination
DPX	distyrene, plasticiser and xylene mixture
EDTA	ethylenediaminetetraacetic acid
EtOH	ethanol
g	gram
GA	gibberellin
GGDP	geranyl geranyl diphosphate
KAO	kaurenoic acid oxidase
K_m	Michaelis-Menten constant
KO	*ent*-kaurene oxidase
KS	*ent*-kaurene synthase
LE	*LENGTH;* encodes *GA 3-oxidase*
LH	encodes *ent- kaurene oxidase*
LS	encodes *ent-copalyl diphosphate synthase*
MEP	methylerythritol 4-phosphate

Abbreviation	Definition
mg dwt	milligrams dry weight
min	minutes
mRNA	messenger ribonucleic acid
PIPES	piperazine-N,N′-bis (2-ethanesulfonic acid)
RNA	ribonucleic acid
SE	standard error of the mean
SLN	*SLENDER*; encodes *GA 2-oxidase*
WT	wild-type

INTRODUCTION

1. 1 Plant hormones and gibberellins

Plant hormones are signaling molecules that controlling diverse aspects of plant growth and development. They can elicit a physiological response depending on external or internal cues. Auxins, gibberellins (GAs), cytokinins, abscisic acid, ethylene and brassinosteroids are commonly recognized as the main classes of naturally occurring plant hormones (Depuydt and Hardtke, 2011).

GAs are a large group of tetracyclic diterpenoid compounds that occur in higher plants as well as some species of bacteria and fungi (Yamaguchi, 2008). Presently, there are 136 fully characterized GAs. However, only a few of the 136 known GAs have intrinsic biological activity. These include GA_1, GA_3, GA_4, GA_5, GA_6 and GA_7 (Sponsel and Hedden, 2010). GAs are regulators of many aspects of higher plant development including, stem elongation, seed germination, flower induction and fruit development (Ueguchi-Tanaka et al., 2007; Ozga et al., 2002). GA was first discovered in the fungus *Gibberella fujikuroi* from which this class of hormone derives its name. Certain strains of this fungus secrete GAs when they infect rice plants causing "foolish seedling disease" (extensive stem growth of the host plant). The predominant active form of the GA in the fungal secretion was found to be GA_3 (gibberellic acid; Hedden, 2012). In 1930, the active principle form of the fungal secretion was isolated in Japan, and 20 years later it was discovered that application of a pea seedling GA extract restores the wild type phenotype when apply to dwarf pea plants (Radley, 1956). The chemical structure of gibberellic acid was published in the 1950's by Cross et al. (1956).

1. 2 Gibberellin biosynthesis pathway

The naturally occurring GAs possess an *ent*-gibberellane carbon skeleton (Sponsel and Hedden, 2010). Synthesis of bioactive GAs in plants requires the involvement of three classes of enzymes; plastid located terpene cyclases, membrane-associated cytochrome P-450 monooxygenases and soluble 2-oxogluterate-dependent dioxygenases. The entire GA pathway can be subdivided into three major parts occurring in different cellular compartments.

1. Synthesis of *ent*- kaurene starting from isopentyl diphosphate precursors
2. Conversion of *ent*-kaurene to GA_{12}-aldehyde
3. Formation of bioactive GA_1 from GA_{12}-aldehyde

GA biosynthesis starts mainly in the plastids from the initial precursor methylerythritol 4-phosphate (MEP) which supplies isoprenoid units for the eventual formation of geranylgeranyl diphosphate (GGDP; Kasahara et al., 2002). GGDP is then converted to *ent*-kaurene by a two-step cyclization process. GGDP is converted first to bicyclic *ent*-copalyl diphosphate by *ent*-copalyl diphosphate synthase (CPS; Fig. 1.1). This intermediate is then converted to *ent*-kaurene by *ent*-kaurene synthase (KS; Hedden, 2012). In the second part of the GA biosynthesis pathway, which occurs in both plastids and the endoplasmic reticulum (Helliwell et al., 2001), *ent*-kaurene is converted to GA_{12}-aldehyde through a series of oxidization steps. First, *ent*-kaurene is oxidized to form *ent*-kaurenoic acid by *ent*-kaurene oxidase (KO) located on the plastid membrane. *ent*-Kaurenoic acid is then oxidized to *ent*-7α-hydroxy-kaurenoic acid by kaurenoic acid oxidase (KAO). Subsequently, *ent*-7α-hydroxy-kaurenoic acid is oxidized by GA_{12}-aldehyde synthase to GA_{12}-aldehyde (Hedden and Phillips, 2000; Fig. 1.1). All enzymes involved in this second phase of GA biosynthesis are membrane-associated cytochrome P450 monooxygenases (Sponsel and Hedden, 2010).

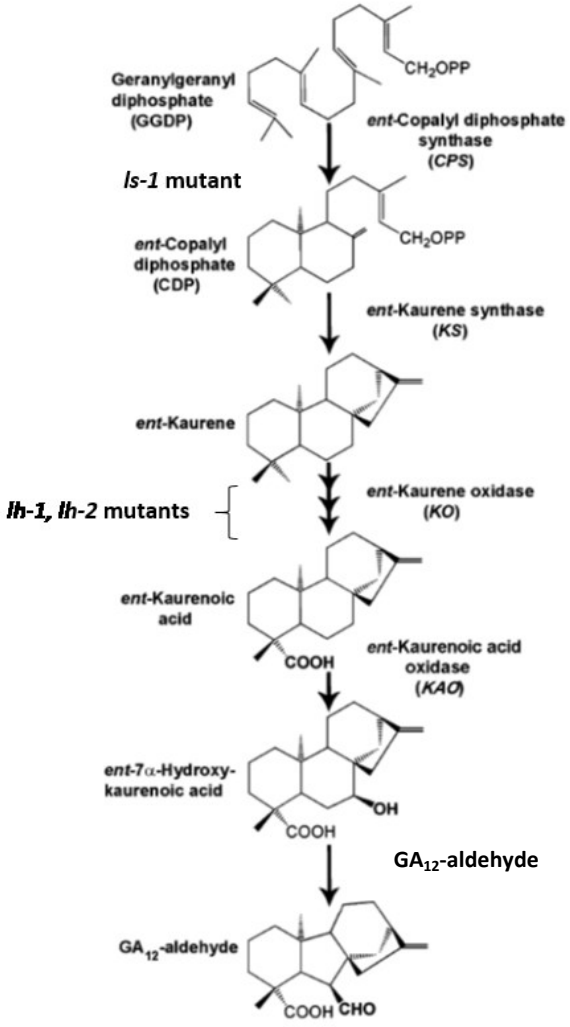

Figure 1.1: Gibberellin biosynthesis pathway from GGDP to GA_{12}-aldehyde. *ls-1* is a mutation in the *PsCPS* gene that affects the conversion of GGDP into CDP. *lh-1* and *lh-2* are mutations in the *PsKO1* gene that impair the oxidation of *ent*-kaurene to *ent*-kaurenoic acid (modified from Ayele et al., 2006).

GA 7-oxidases then catalyze the oxidation of GA_{12}-aldehyde to GA_{12}, the first GA fully committed to the GA biosynthesis pathway. GA_{12} can either be hydroxylated at the C-13 position (early 13-hydroxylation pathway) by GA 13-hydroxylase (Magome et al., 2013) producing GA_{53}, or it is not (non-13-hydroxylation pathway) in pea seeds (Nadeau et al., 2011; Fig. 1.2).

In the third part of the GA pathway, which occurs in the cytosol, GA_{12}, or GA_{53} are further oxidized to other C20-GAs, then C19-GAs (Fig. 1.2). The enzymes necessary for the conversions from GA_{12} or GA_{53} to bioactive GA_4 or GA_1, and their immediate precursors

GA_9 or GA_{20}, respectively, as well as their immediate inactive catabolic products (GA_9 to GA_{51}; GA_4 to GA_{34}; GA_{20} to GA_{29}; GA_1 to GA_8), are cytosolic 2-oxogluterate-dependent dioxygenases (Yamaguchi, 2008). The multi-functional enzyme GA 20-oxidase (GA20ox) sequentially oxidizes carbon 20 of GA_{12} or GA_{53} to an alcohol, then to an aldehyde, followed by loss of the C-20 carbon and formation of a lactone ring between C-4 and C-10, forming the C19-GAs GA_9 or GA_{20}, respectively (Yamaguchi, 2008). In pea, GA 20-oxidases are known to be encoded by *PsGA20ox1* (Martin et al., 1996; García-Martínez et al., 1997) and *PsGA20ox2* (Lester et al., 1996).

The growth-active GAs, GA_4 and GA_1, are formed by 3β-hydroxylation of GA_9 or GA_{20} respectively, catalyzed by GA 3-oxidases (GA3ox). In pea, GA 3-oxidases are known to be encoded by *PsGA3ox1* and *PsGA3ox2* (Martin et al., 1997; Lester et al., 1997; Weston et al., 2008). GA 2β-hydroxylation is the most common deactivation mechanism of bioactive GAs (Hedden, 2012). GA 2-oxidases (GA2ox) which are responsible for the irreversible deactivation of GAs by 2β-hydroxylation, are known to be encoded by *PsGA2ox1* and *PsGA2ox2* in pea (Lester et al., 1999; Martin et al., 1999). Data from recombinant expression of *PsGA2ox1* and *PsGA2ox2* cDNA in *E.coli* suggest that the *PsGA2ox1* gene product effectively converts GA_{20} to GA_{29} and GA_1 to GA_8. The *PsGA2ox2* gene product also converts GA_1 to GA_8, but it was much less effective in the catalyzing the conversion of GA_{20} to GA_{29} (Lester et al., 1999).

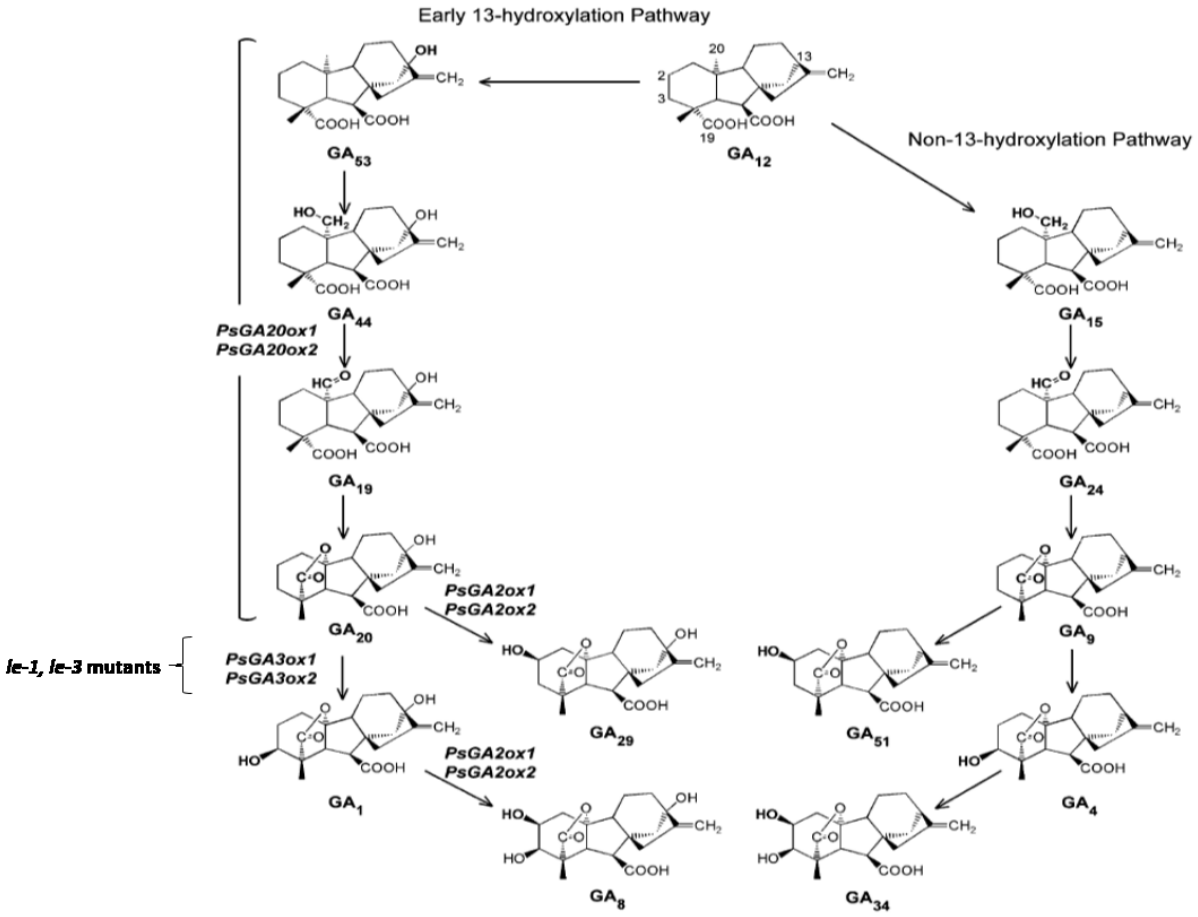

Figure 1.2: Non-13-hydroxylation and early 13-hydroxylation pathways of gibberellin biosynthesis. *le-1* and *le-3* are mutations in the *PsGA3ox1* gene that reduce the conversion GA_{20} and GA_9 into bioactive GAs, GA_1 and GA_4, respectively (source: Nadeau et al., 2011).

1.3 GA biosynthetic mutants and GA overexpressor plant lines

A number of GA biosynthetic mutants in pea (*Pisum sativum*) have been discovered and they have been very effective tools in understanding the GA biosynthesis pathway and the role of GAs in growth and development in this species (Hedden and Kamiya, 1997). Some of the pea GA biosynthesis mutants (*sln* mutants) elevate bioactive GA levels by inhibiting GA catabolism resulting in taller stem phenotypes (Reid and Ross, 1993). Other pea GA biosynthesis mutants (*le-3*, *lh-1*, *lh-2*, *ls-1*) impair the biosynthesis of bioactive GA resulting in shorter stem phenotypes (Fig. 1.3; Reid and Ross, 1993; Swain et al., 1995).

Figure 1.3: Phenotypes of 18-day old pea seedlings (18 days after imbibition) of LS LH LE3 wild type 107 (LS LH LE3 WT-107) and the GA biosynthesis mutants *lh-2, lh-1, le-3,* and *ls-1*; TG1 transgenic line (expresses *PsGA3ox1,* a fully functional wild-type GA 3β-hydroxylase gene in a semi-dwarf *le-1* pea line) and its transgenic control (C1).

1.3.1 *le* mutants

PsGA3ox1 corresponds to the Mendel *LE* locus in pea and it codes for a GA 3β-hydroxylase that converts GA_{20} and GA_9 into bioactive GAs, GA_1 and GA_4, respectively (Lester et al., 1997; Martin et al., 1997). *le-3* (previously le^{5839}; MacKenzie-Hose et al., 1998) and *le-1* are mutant alleles of the *LE* locus showing different degrees of dwarfism in pea (Lester et al., 1997). The *le-1* mutation is a guanine to adenine substitution at position 685 of *PsGA3ox1* leading to a change of alanine to threonine at amino acid position 229 of the encoded protein. The *le-3* mutation is due to a cytosine to thiamine substitution at position 826 of *PsGA3ox1*that results in a histidine to tyrosine substitution at amino acid position 276 of the encoded protein (Martin et al., 1997). Both of these point mutations are not located within the active site of the GA 3β-hydroxylase enzyme, but occur in close proximity to the conserved iron binding motif (His231-Asp233) common in the active site of 2-oxogluterate

dependent dioxygenases, thereby increasing the K_m value of the enzyme, and resulting in decreased enzyme activity and reduced bioactive GA production (Martin et al., 1997). The reduced GA content in the stems of *le-3* and *le-1* results in shorter internode length compared to the wild type and hence shorter plant stature (Fig. 1.3).

The pod growth of wild type pea and *le-1* mutants have been investigated previously and only minimal differences have been observed for the pod length. During the first few days after anthesis (until 4 DAA) growth of pea ovaries of wild type plants was advanced compared to the *le-1* mutants (Santes et al., 1993). The *le-1* mutation was also observed to reduce pea pod width and *le-1* pods exhibited a greater degree of tapering compared to wild type pods (Ross et al., 2003). The link between the *LE* locus and internode elongation is well documented, although the role of the *LE* locus in seed development has received less attention. The effects of *le-1* and *le-3* mutations on pea seed development have been studied previously. The *le-1* mutation reduces the GA_1 content in young seeds by 1.7 fold (MacKenzie –Hose et al., 1998). In contrast, young developing *le-3* seeds contain elevated levels of GA_1, GA_{20} and GA_{29} compared to wild-type seeds (Swain et al., 1995).

1.3.2 *ls-1* mutant

The *PsCPS* gene (*LS* locus) encodes a copalyl diphosphate synthase (CPS) in pea (Fig. 1.1). In the *ls-1* mutant, a guanine to adenine substitution in an intron of the *PsCPS* gene alters the consensus sequence of the 3' splice site and results in aberrant RNA splicing. As a result, high levels of truncated CPS protein with no apparent enzymatic activity are produced. As a consequence of this mutation, the conversion of GGDP to *ent*-copalyl diphosphate is reduced, leading to reduced GA content in the internodes of *ls-1* plants and approximately 75% reduction in internode length compared to wild type plants (Ait-Ali et al., 1997). The *ls-1* mutation has been reported to have minimal effects on pericarp growth, seed development or seed survival (MacKenze-Hose et al., 1998).

1.3.3 *lh-1* and *lh-2* mutants

lh-1 and *lh-2* are mutant alleles of the *LH* locus that encode the KO multifunctional enzyme responsible for the conversion of *ent*-kaurene to *ent*-kaurenoic acid (in pea; Fig. 1.1; Davidson et al., 2003). *lh-1* is a single point mutation in *PsKO1* that substitutes an adenine for a guanine, which replaces a highly conserved amino acid serine with an asparagine. Yeast strains expressing a *PsKO1* cDNA isolated from the *lh-1* did not metabolize *ent-kaurene* to *ent*-kaurenoic acid, whereas strains expressing a wild-type *PsKO1* cDNA were capable of

this conversion (Davidson et al., 2004). *lh-2* mutants have an intronic substitution of guanine to adenine at the beginning of an intron that, in turn, disrupts normal RNA splicing. *PsKO1* transcript from *lh-2* forms a matured mRNA product having an 83-bp intron with a stop codon in the reading frame that results in a 275-amino acid truncated putative protein that would be expected to be a null mutation. Even though both *lh-1* and *lh-2* mutations result in short-statured plants (Reid, 1986: Reid and Potts, 1986), the *lh-2* mutant has higher rates of seed abortion and smaller seeds at maturity, while the effect of the *lh-1* mutation on seed growth is transient, compared to the wild type (Swain et al., 1997). This may be due to the efficiency of RNA splicing in different plastidic environments present in seed tissues and vegetative tissues (Davidson et al., 2004). Furthermore, data suggest that developing seeds of *lh-2* mutants are deficient in utilizing available photoassimilate for seed development (Swain et al., 1997). Swain et al. (1997) suggested two possible models to explain the role of GAs in assimilate partitioning; GAs may directly promote assimilate uptake by developing seeds, or GAs may act indirectly through changes in seed growth.

1.3.4 GA overexpressor line TG1 and transgenic control

GA-overexpressor line TG1 was created by Reinecke et al. (2013); it constitutively expresses *PsGA3ox1* (*LE*; a fully functional wild-type GA 3β-hydroxylase gene driven by CaMV 35S promoter) in a semi-dwarf *lele* pea line ('Carneval'; *le-1*; single base-pair mutation in *PsGA3ox1*). Reinecke et al. (2013) reported that the *PsGA3ox1* transgenic line TG1 contained substantially elevated levels of *PsGA3ox1* (transgene and endogenous transcripts) and endogenous *PsGA20ox1* transcripts in the expanding internodes compared to a null control. Consistently, increased flux through $GA_{20} \rightarrow GA_1 \rightarrow GA_8$ occurred in the TG1 internodes and this was associated with increased internode length, as compared to the null control. Increased *PsGA3ox1* transcript abundance in young fruit (pericarp) was also associated with increased pericarp length (when pods with the same number of seeds were compared) in TG1 compared to a null control (Reinecke et al., 2013). Elevated expression of *PsGA3ox1* in the TG1 line was associated with larger embryos and seeds at maturity in TG1 compared to a null control (Wickramarathna, 2009).

1.4 Pea seed morphology and development

Legume seeds consist of three major parts: the maternally-derived seed coat, the endosperm and the embryo (Murray, 1987). The endosperm of pea is liquid and has a multinucleated cytoplasm (Marinos, 1970). The endosperm plays a major role before seed maturation acting as a nutrient reserve (Melkus et al., 2009). The embryo is made up of two types of tissues, cotyledons and the embryo axis (Van Dongen et al., 2003). The seed coat plays an important role in protecting the embryo and serving as a conduit to transport nutrients from the mother plant to the developing embryo (Melkus et al., 2009; Murray, 1987).

The pea seed coat consists of several discernible layers: the outer-most layer, the epidermis, a single subtending layer of hypodermal cells , multiple layers of chlorenchyma and ground parenchyma cells, and the inner-most layer made up of branched parenchyma cells (Nadeau et al., 2011). Pea seed coats undergo major histological changes from 8 days after anthesis (DAA) to 20 DAA, a period when the seed transitions from mainly maternal tissues to mainly embryonic tissues (Van Dongen et al., 2003; Nadeau et al., 2011). Pea seed coat growth of cv. I_3 (Alaska-type) mainly occurs prior to 12 DAA (Nadeau et al., 2011). The liquid endosperm obtains maximum volume by 12 DAA, and by 14 DAA, the endosperm is almost completely absorbed by the developing embryo (Nadeau et al., 2011). Epidermal cells of the seed coat differentiate into macrosclerids between 10 to 16 DAA. Seed coat hypodermal cells differentiate into hourglass-shaped cells between 10 to 14 DAA. Expansion of the seed coat ground parenchyma and chlorenchyma cells occurs from 10 to 14 DAA followed by a pause until 16 DAA and marked increased between 16 to 18 DAA (Nadeau et al., 2011). One of the most discernible histological changes observed in the developing 'I_3 (Alaska-type)' pea seed coat is the dramatic expansion of the branched parenchyma cells which occurs between 14 to 16 DAA (Nadeau et al., 2011). After 16 DAA, the branched parenchyma cell layer and inner layers of the ground parenchyma cells are compressed by the developing embryo. As a result, the branched parenchyma cells are no longer visible from approximately 18 to 20 DAA onward (Nadeau et al., 2011).

1.5 Phloem unloading into pea seeds and the post-phloem nutrient pathway

Phloem-imported nutrients enter the pea seed coat through the single vascular bundle of the funiculus that continues into the seed coat as the chalazal vein with two lateral vein branches. The chalazal vein of the seed coat is located along the integumentary fusion line, traverses approximately three-quarters of the seed circumference, and consists of a central

xylem bundle surrounded by phloem elements (Hardham, 1976). The two seed coat lateral vein branches contain only phloem and run more or less parallel to the embryo radicle. Phloem nutrients are reported to be symplastically unloaded from the seed coat vasculature into the seed coat ground parenchyma/chlorenchyma cells (Van Dongen et al., 2003). Since the pea embryo is not vascularly connected to the maternal seed coat tissue (Van Dongen et al., 2003; Melkus et al., 2009), the nutrients that are symplastically imported into the seed coat ground parenchyma/chlorenchyma cells must be unloaded into the seed coat apoplast for up-loading into the embryo (Van Dongen et al., 2003). Using *Vicia faba* as a model, Weber et al. (1997) suggested that during the pre-storage phase of seed development, cell wall invertase (CWI) is specifically expressed in the innermost layer of the seed coat parenchyma cells (likely homologous to the branched parenchyma of *Pisum*; Van Dongen et al. 2003). It was further postulated that CWI cleaves sucrose to glucose and fructose, increasing the negative value of the solute potential of the apoplast surrounding the inner cell layers of the seed coat. Therefore, a concentration gradient is created between the inner seed coat parenchyma cell layers where the phloem unloading occurs and the apoplast of these cells of *V. faba* (Weber et al., 1995). The resulting hexoses are then taken up by the cotyledons and resynthesized to sucrose. Therefore, Weber et al. (1995) suggested that seed coat cell wall bound invertase initially establishes sink strength in *V. faba* seeds. Furthermore, when the enlarging embryo contacts the seed coat (contact point), the inner seed coat cell layers are crushed and this is associated with a decline in seed coat cell wall invertase activity (Weber et al., 1995). It was proposed that the developmentally regulated degradation of this layer and associated loss of CWI activity initiates the nutrient storage phase of the cotyledons through a switch from high to low ratios of hexoses to sucrose in the environment surrounding the embryo (vacuolated endospermic space; Weber et al., 1997).

Sucrose uptake into *V. faba* and pea cotyledons is mediated by an epidermal cell uptake system (Borisjuk et al., 2004). As suggested by the intercellular movement of the symplastic tracer 5-(6)-carboxyfluorescein, a symplastic pathway connects the cotyledonary epidermal transfer cells to the storage parenchyma cells (Tegeder et al., 1999). Furthermore, sucrose/H+ symporters located in the cotyledonary epidermal transfer cells are suggested to be involved in acquisition of sucrose from the seed endospermic apoplast (Tegeder et al., 1999). The imported sucrose contributes to the production of starch, protein and lipids in the cotyledons during seed development (Weber et al., 1997). During the storage phase of pea cotyledon development, coordinate regulation of starch synthesizing enzymes including ADP-glucose

pyrophosphorylase and starch synthase converts sucrose in to starch (Smith et al., 1997; Denyer and Smith, 1992).

During *V. faba* cotyledon development, lower sucrose concentrations are found in non-differentiated premature regions and mature starch accumulating regions contain higher sucrose levels (Borisjuk et al., 2004). For pea, feeding sucrose to young embryos altered cotyledon development from a growth phase to a storage phase including the induction of starch accumulation and storage protein synthesis gene expression (Wang and Hedley, 1993). Therefore, it is thought that a high hexose to sucrose ratio is a signal for cell differentiation and a low hexose to sucrose ratio is a signal for up regulation of storage-associated genes triggering the embryo transition from an organ formation phase to a storage phase (Wang and Hedley, 1993), as mention in context to seed coat CWI above.

1.6 Involvement of GAs in pea seed growth, development and photoassimilate partitioning

Developing seeds are a rich source of GAs. Swain et al. (1997) showed the involvement of GA in early pea seed development using the *lh* GA biosynthesis mutants. In the *lh*-2 mutant, GA levels were reduced in shoots as well as in the young seeds. *lh*-2 seeds developed slowly and exhibited a high rate of seed abortion. Consistently, developing pea seeds treated with GA biosynthetic inhibitors show reduced mature seed weight and germination ability (Garcia-Martinez et al., 1987). Further evidence that suggests that GAs are required for seed development was reported by Nadeau et al. (2011) in the pea cultivar I_3 (Alaska-type). In this study, GA biosynthesis and catabolism gene expression and key GA profiles during the early seed filling stage (8-20 DAA) were correlated with morphological events as well as photoassimilate acquisition. Seed coat *PsGA20ox1* transcript abundance peaked at 10 DAA followed by a 3-fold increase in seed coat GA_{20} level by 12 DAA (GA_{20} is the immediate precursor of bioactive GA_1 and it is converted to GA_1 by GA 3β-hydroxylase). *PsGA3ox1* transcript level was low in the seed coat at 8 DAA, increasing to peak at 14 DAA; however seed coat GA_1 levels were greatest at 10 DAA, lower by 10-fold by 12 DAA, and they remained at this level until 14 DAA; GA_1 was undetectable in the seed coat by 16 DAA (Nadeau et al., 2011). It was hypothesized that the GA_1 detected in the seed coat at 10 DAA may be localized to the ground parenchyma cell layer where it acts to stimulate cell expansion at this stage. Furthermore, Nadeau et al. (2011) speculated that the high seed coat *PsGA3ox1* transcript levels at 14 DAA may be mainly localized to the seed coat branched parenchyma cells, and that the increased capacity to produce GA_1 drives the dramatic

expansion of cells in this layer from 14 to 16 DAA in the pea cultivar I_3 (Alaska-type; Nadeau et al., 2011). The expansion of the branched parenchyma layer was temporally correlated with a rapid decrease in seed coat sucrose level from 14 to 16 DAA postulated to be due to the uptake of sucrose and/or sucrose-derived hexose from the apoplast by the rapidly expanding branched parenchyma cells and the embryo (Nadeau et al. 2011). The data from Nadeau et al. (2011) in pea are consistent with those of Weber et al. (1995) in *V. faba* that suggest that the cleavage of phloem-derived sucrose into glucose and fructose in the seed coat (potentially by CWI in the branch parenchyma layer) acts to increase seed sink strength prior to and at the stage the embryo makes full contact with the seed coat.

Nadeau et al. (2011) also observed that starch-containing plastids were prevalent in the ground parenchyma and chlorenchyma cells of the pea seed coat at 12 DAA, and they decreased to minimal levels by 20 DAA (Nadeau et al., 2011). Nakayama et al. (2002) reported that GA_1 and/or GA_3 are localized around starch grains of *Pharbitis nill* (morning glory) seed coat cells. They also observed increased transcript abundance and localization of GA-inducible α-amylase (*PnAmy1*) transcript to the starch grains of the *Pharbitis nill* seed coat cells, suggesting that GA-inducible α-amylase is involved in starch grain digestion. In light of these data, Nadeau et al. (2011) hypothesized that the GA_1 present in pea seed coats may induce GA-inducible α-amylase starch grain digestion as part of the mechanism involved in starch mobilization from the seed coat to embryo during seed development.

In the pea embryo, *PsGA3ox1* and *PsGA3ox2* transcript profiles and trends in GA_1 levels at 10 to 16 DAA, and in embryo axes at 18 DAA, suggest localized GA_1-induced growth in these tissues (Nadeau et al., 2011). After 18 DAA, a shift from synthesis of GA_1 to that of GA_8 occurred in the embryo axis, suggesting that GA deactivation occurs to limit embryo axis growth and allow embryo maturation to proceed (Nadeau et al., 2011).

Overall, these data suggest that GAs play a role in pea seed coat and embryo growth, and development, and photoassimilate partitioning into the seed. However, to our knowledge a comprehensive study correlating GA-induced growth and carbohydrate partitioning into the pea seed has not been completed to date.

Research objectives

The goal of my thesis research was to test the hypothesis that GAs are involved in normal pea seed development and photoassimilate acquisition during the mid-phase of development. Physiological, analytical and histological techniques were used to compare GA biosynthetic mutants, and a transgenic GA overexpressor line, to their appropriate wild type or transgenic control lines to identify changes in the seed coats (from 8 to 20 DAA) and cotyledons (12 to 20 DAA) associated with GA-induced growth and development and carbohydrate partitioning into the seed. The follow specific objectives were addressed in this study:

- Objective 1: Determine if GAs affect the growth, morphology and cell expansion profiles of the seed coat and embryo over development (8 to 20 DAA).
- Objective 2: Determine if GAs affect assimilate partitioning into the seed. This will be accomplished by assessing starch, sucrose, and glucose profiles of the seed coat and cotyledons over development (8 to 20 DAA) using histological (iodine staining of starch) and analytical techniques. Additionally, in specific lines, sucrose and glucose levels will be assessed in the liquid endosperm when present in the seed, and protein content will be assessed in the embryos.

2. MATERIALS AND METHODS

2.1 Plant materials

Plant lines

Seeds of *Pisum sativum* L. Torsdag (LS LH LE3 WT-107) and seeds containing the *lh-1, lh-2, ls-1, and le-3* GA biosynthesis mutations generated in the Torsdag background were kindly provided by Dr. John Ross from the *Pisum sativum* Hobart collection maintained at the Department of Plant Science, University of Tasmania, Australia. Two independent mutational events in pea cv. Torsdag resulted in the alleles *lh-1* and *lh-2*. The *lh-1* mutant (line K511) was ethylmethane sulfonate-induced, and the *lh-2* mutant (line NGB5843) was ethyleneimine-induced by Dr. Klavdiya K. Sidorova (Institute of Cytology and Genetics, Novosibirsk, Russia; Reid, 1986; Swain and Reid, 1992). Another independent mutation in cv. Torsdag resulted in the *le-3* mutant (NGB5839 line) which was also produced by mutagenesis from cv. Torsdag, by Dr. K.K. Sidorova (Ross and Reid, 1991). The *ls-1* mutant (Hobart line 181) was also isolated from the wild type cultivar Torsdag (Reid, 1986). Seeds of the transgenic pea line TG1 (T6B [17-3] [A-2] [P-1]) that overexpress *PsGA3ox1* (*LE*; a fully functional wild-type GA 3β-hydroxylase gene) in the *Pisum sativum* L. cv. Carneval semi-dwarf *lele* background (Carneval; *le-1*; mutation that blocks 3β-hydroxylation of GA_{20} to GA_1; Reinecke et al., 2013) were obtained from the Ozga/Reinecke lab. Seeds of C1 (T6B [17-2] [A-13] [P-1,3]), a plant line that was subjected to the transformation process that provided the semi-dwarf *lele* 'Carneval' background as a control for the TG1 line were also obtained from the Ozga/Reinecke lab. The transgenic and transgenic control lines were from T4 and T5 seed generations .

Plant material for growth, carbohydrate, and protein content analyses

Seeds were planted at an approximate depth of 2.5 cm in 3-L plastic pots (3 seeds per pot) in Sunshine #4 potting mix (Sun Gro Horticulture, Vancouver, Canada) and sand (4:1). Plants were grown in a Conviron (Winnipeg, Canada) growth chamber using cool-white fluorescent lamps (F54/I5/835/HO high fluorescent bulbs, Phillips, Holland) 16 hours light/8 hours-dark photoperiod (19°C/17°C) with an average photon flux density of 385.5 μmol m^{-2} s^{-1} (measured with a QMSS-ELEC Quantum meter, Apogee instruments, Logan, USA). One week after emergence, plants were supplemented with Nutricote 13:13:13 slow release fertilizer (Chissa-Asahi Fertilizer Co., Ltd, Tokyo, Japan). All plant lines were grown in the

same growth chamber and planting of lines was sequenced to maximize overlap of lines to be directly compared within each parameter studied. Flowers were tagged at 0 days after anthesis (DAA) and 2 to 4 normally developing seeds per fruit (in the central region of the fruit) were harvested at 8, 10, 12, 14, 16, 18 and 20 DAA as identified by the date of anthesis and approximate whole seed fresh weight.

Seeds were harvested onto ice and whole seed fresh weights were recorded. Subsequently, seeds were dissected into seed coats (8 and 10 DAA) or seed coats and cotyledons (12, 14, 16, 18 and 20 DAA) and weighed. Additionally, to remove residual endosperm from the seed tissues that will be used for carbohydrate and cotyledon protein content analyses, seed coats and cotyledons from 8 to 14 DAA for LS LH LE3 WT-107, *lh-1, ls-1, le-3*, TG1 and C1, and from 8 to 18 DAA for *lh-2*, were rinsed three times in cold deionized water by sequentially immersing and mildly shaking tissue in three separate 20 mL vials containing approximately10 mL per vial placed on ice. The water in the vials was changed after approximately 3 tissues were rinsed. Seeds and seed tissues were then stored at -80^{o}C until further analysis.

2.2 Histology

Fresh seed coat tissues of LS LH LE3 WT-107, *lh-1, lh-2, ls-1, le-3*, TG1 and C1lines (8, 10, 12, 14, 16, 18 and 20 DAA) were obtained as described by Nadeau et al. (2011). Two parallel cuts from the top to bottom (where the funiculus is attached to the seed) of the seed were made as indicated in Figure 2.1. Seed coat tissues were trimmed to approximately 5 to 6 mm in length and 1.5 to 2 mm in width, prior to fixing. Cotyledon tissues of LS LH LE3 WT-107, *lh-1, lh-2, ls-1, le-3,* TG1 and C1 lines from 12 to 20 DAA were obtained from the area directly beneath the seed coat sections. Cotyledon tissues were trimmed to 5 to 6 mm in length, 3 to 4 mm in width, and 1.5 to 2 mm in thickness. Cotyledon and seed coat sections were obtained from both left and right halves of the seed. Cotyledon samples were obtained from regions away from the cotyledon-cotyledon interface.

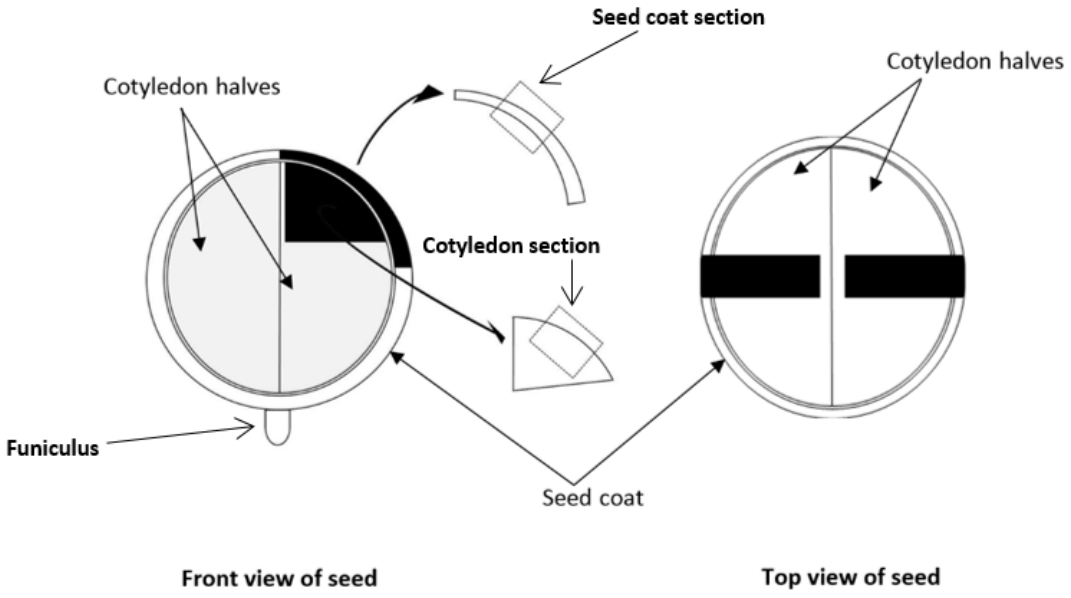

Figure 2.1: Diagram of pea seed cross-sections indicating orientations of cotyledon and seed coat sections used for histological analysis. Dark regions indicate the general region of excised tissues and the boxes within the excised tissue indicate the tissues used for microtome sectioning.

Fixation, embedding and sectioning of tissues was completed using a modified procedure described by Nadeau et al. (2011) and Ferraro et al. (2014). Tissue sections were fixed in an aqueous solution containing 0.2% gluteraldehyde (v/v), 3% paraformaldehyde (v/v), 2 mM $CaCl_2$, 10 mM sucrose and 25mM PIPES (piperazine-N,N′-bis (2-ethanesulfonic acid)) at pH 7. Fixation was carried out overnight under vacuum followed by two days at atmospheric pressure. Sections were then rinsed three times with 25mM PIPES buffer, followed by tissue dehydration using a graded ethanol series of 30% and 50% EtOH in 25 mM PIPES buffer (pH 7; v/v), followed by 70% EtOH in water (v/v) for 15 min each. Sections were sequentially infiltrated using Leica tissue processor 1020 (Leica Biosystems, Nussloch) as follows: 1 hour in 70% aqueous ethanol (v/v), 1 hour in 90% aqueous ethanol (v/v), 1.5 hours in 100% ethanol, 1.25 hours in ethanol:toluene 1:1 mixture, 0.5 hour in toluene, 2 hours in paraplast tissue embedding medium (Fisher Scientific, Houston, TX) and finally a second immersion in new paraplast tissue embedding medium for 2 hours.

Tissues were then embedded in proper orientation in paraffin blocks using a Tissue-TEK II Embedding centre (Tissue Tek, USA). Blocks were trimmed with stainless steel microtome blades (Feather safety razor co., Ltd, Osaka, Japan) to a maximum surface area of approximately 4 mm^2. Seed coat and cotyledon samples were sliced into 5 µm-thick sections using a Leica RM 2125 R25 microtome (Leica Biosystems, Nussloch, Germany), the sections

were placed into a 42-45^{0}C water bath (with approximately 0.05g of gelatine added to 2L of water to facilitate the adhesion of tissues to the slide) and incubated until sections were flat (no wrinkles present). Sections were then affixed onto clean slides and incubated overnight at 37^{0}C (Precision model 4 incubator, Precision scientific co., Chicago, USA). Removal of paraffin was performed on sections mounted on slides with two changes of toluene (5 min each), then sections were treated sequentially with 100% (two changes), 90%, 70%, and 50% aqueous EtOH (v/v), for 2 min each. Slides were then transferred to distilled water for 2 min before staining.

For determining cell area, prepared sections were stained with a 0.025% aqueous toluidine blue (w/v) solution for 20 seconds at room temperature. Slides were then briefly rinsed with distilled water to remove excess stain. Destaining of tissue was carried out by incubation in 95% aqueous EtOH for 2 min followed by two changes in 100% EtOH, 2 min each. Slides were then immersed in toluene for 5 min, then they were transferred into a new toluene bath before cover slips were added. Cover slips were mounted on the slides using DPX mounting media (BDH Chemicals, NY, USA). After drying slides overnight at 37^{0}C, they were observed under a Zeiss Axio Scope A1 light microscope (Zeiss, Germany), and micrographs were obtained using a microscope-mounted Optronics digital camera (Optronics, CA, USA) controlled by Picture Frame™ Application 2.3 software. Images were edited using Adobe Photoshop (Creative Cloud 2014) software and cell areas were estimated by manually outlining cells of micrographs using AxioVision SE64 software (Jena, Germany). A stage micrometer was photographed at different magnifications for obtaining scale bars. An average of 20 cells per technical replicate, two technical replicates per biological replicate, and a minimal of four biological replicates per tissue were used for determining cell cross-sectional area of seed coat tissues. For cotyledon storage parenchyma cells, an average of 16 cells per technical replicate, two technical replicates per biological replicate, and three biological replicates per sample were used for determining cell cross-sectional area.

For staining of starch grains, 3 to 4 drops of Gram's Iodine solution (1 g of iodine and 2 g of potassium iodide dissolved in 300 mL of water) was applied to the sections, cover slips were added, and the slides were incubated at 60^{0}C for two hours. Slides were observed using a Zeiss Axio Scope A1 light microscope and micrographs were obtained with an Optronics digital camera as described above. Representative micrographs for each developmental stage for each line were chosen from a pool of at least three biological replicates.

For protein body staining, slides were immersed in 1% (w/v) Amido black solution [1g of Amido black dissolved in 100 ml of 7% aqueous acetic acid (v/v)] for 1 min, then they were washed in 7% aqueous acetic acid (v/v), followed by distilled water. Stained tissues sections were covered with cover slips and incubated at 60^0C for two hours. Slides were observed under a Zeiss Axio Scope A1 light microscope and micrographs were obtained with an Optronics digital camera and images were edited using Adobe Photoshop as described above. Representative micrographs for each developmental stage for each line were chosen from a pool of at least three biological replicates.

2.3 Carbohydrate analysis

Seed coat and cotyledon tissues were lyophilized (Virtis Ultra 35L Freeze Dryer, Stone Ridge, New York, USA), then ground to a fine powder. Ground samples (30-50 mg; with a minimum of 6 seed coats and 8 cotyledons per sample) were extracted with 8 mL of 80% aqueous ethanol (v/v). The extract was placed at room temperature for 1 hour, then placed in a 75-80^0C water bath for 5 min, then centrifuged at 4,200 rpm for 15 min. After removing the supernatant, the pellet was re-extracted with 8 mL of 80% aqueous ethanol (v/v) and reprocessed as above, without waiting for 1 hour. The pellet was stored at -20^0C prior to starch analysis.

For determination of soluble sugars, supernatants were dried overnight under vacuum. The residue was dissolved in 4 mL of hexane followed by 4 mL of water for organic solvent partitioning to remove chlorophyll and lipids. The samples were partitioned 6 times (4 mL each) with hexane, and the aqueous phase was dried overnight under the vacuum. Dried samples were dissolved in 8 mL of water and stored in -20^0C until glucose and sucrose determination.

For sucrose determination, a 50µl sample aliquot was incubated with 100 µl of invertase [1500 units mL^{-1} invertase (Sigma Aldrich 4504) in 0.1 M acetic acid buffer, pH 4.6] at room temperature for 20 min to hydrolyze sucrose to glucose and fructose. Subsequently, 1.5 mL of glucose oxidase/peroxidase solution (GOPOD: 600 units L^{-1} glucose oxidase, 325 units L^{-1} peroxidase; Megazyme International, Ireland) was added and the samples were incubated for 20 min in 50^oC water bath. Absorbance of the samples was determined at 510 nm using a Spectra MAX190 spectrophotometer (Molecular Devices, Sunnyvale, California, USA) in a 96-well plate format (3 technical replicates per sample). A glucose standard curve was made from a dilution series of a 1mg mL^{-1} aqueous glucose stock solution for calibration. For glucose determination, a 200 µL sample aliquot was added to 1.5

mL of GOPOD solution, the solution was incubated at 50°C for 20 min, and glucose levels were determined spectrophotometrically as described above. For each sample, sucrose was determined by subtracting the value obtained for glucose of the no invertase treatment subsample from that of the invertase-treated subsample.

Total starch was determined based on the amyloglucosidase/α-amylase method (Megazyme International, Ireland). α-Amylase (3 mL of 300 units mL^{-1}; Megazyme International, Ireland, Catalog no. E-BLAAM) was added to the pellet, and the sample was vortexed and incubated in a boiling water bath for 6 min, while vortexing at 2 min intervals. After incubation, 50 µL of amyloglucosidase (3250 unites mL^{-1}; Megazyme International, Ireland) and 4 mL of 200 mM sodium acetate buffer (pH 4.5) were added to each sample. The samples were vortexed then incubated for 30 min at 50°C. After incubation, the volume of each sample was adjusted to 36 mL with deionized water. A 1 mL sample aliquot was centrifuged at 6000 rpm for 10 min, and a 50 µL aliquot from this solution was used for glucose determination as described above.

Liquid endosperm (at 10 and 12 DAA in LS LH LE3 WT-107, TG1, and C1, at 10, 12, 14 and 16 DAA in *lh-2*) was removed from the seeds using a micropipette and immediately frozen on dry ice for subsequent soluble sugar analysis. Prior to analysis, samples were diluted 10 times with Milli-Q water and centrifuged briefly. A 50µl sample aliquot of this solution was used for sucrose and glucose determination as described above.

2.4 Cotyledon protein content determination

Cotyledons from TG1 and C1 lines at 14, 16, 18 and 20 DAA (with a minimum of 8 cotyledons per sample) were lyophilized using a freeze dryer (Virtis Ultra 35L Freeze Dryer, Stone Ridge, New York, USA) for 7 days. Freeze dried cotyledons (three biological replicates) were ground to a fine powder. The nitrogen content was estimated in the samples (76-103 mg) using a nitrogen analyzer (model FP-428, Leco Instruments Ltd., Mississauga, ON, Canada). Caffeine (157 mg) and EDTA (Ethylenediaminetetraacetic acid; 102 mg) were used as standards for calibration. The total crude protein content of the cotyledons was calculated by multiplying the nitrogen content with a conversion factor of 6.25 (method 968.06; AOAC, 2005).

2.5 Gibberellin analysis of seeds and seed coats

Whole seeds (10 DAA) of WT-107, *lh-2*, *le-3*, C1 and TG1 lines, and seed coats (8 and 10 DAA) of C1 and TG1 lines were lyophilized (Virtis Ultra 35L Freeze Dryer, Stone Ridge, New York, USA) for 7 days. Freeze dried tissues were divided into two biological replicates and ground to a fine powder. Ground samples were sent to the National Research Council Canada, Saskatoon, Canada, for profiling of key GAs (GA_1, GA_8, GA_{20} and GA_{29}; approximately 50 mg dwt per sample used for analysis) using LC MS/MS quantitation with heavy-labelled GA internal standards. Technical details of the quantitation procedure are given at the following web-site:
http://www.nrc-cnrc.gc.ca/eng/solutions/advisory/plant_hormone.html (updated: June 30, 2015).

2.6 Statistical analyses

Probability values (P-values) were calculated using a two-tailed test (assuming unequal variance) for the comparisons of the WT-107 line with the GA biosynthesis mutant lines *lh-1, lh-2, ls-1*, *le-3*, and the GA overexpression line TG1 with the transgenic control C1 line for fresh weight (whole seed, seed coat and embryo; Table G.1), cell cross-sectional area (seed coat and cotyledon; Tables G.2 and G.3), glucose, sucrose and starch content (seed coat, cotyledon, and endosperm; Tables G.4, G.5 and G.6), and protein content (cotyledon; Table G.7). Statistical significance was declared at $P \leq 0.05$ for comparisons between plant lines.

3. RESULTS

3.1 Seed growth over development (8 to 20 DAA)

3.1.1 Seed growth of GA biosynthesis mutants *lh-1* and *lh-2* compared to WT-107 (*LH*)

In *LH*, whole seed growth (on a fresh weight basis) increased linearly from 8 to 20 DAA (Fig. 3.1A). From 8 to 12 DAA, increases in *LH* whole seed fresh weight were primarily driven by seed coat growth (Fig. 3.1B). At 14 DAA, the *LH* seed coat and embryo size (fresh weight) were equivalent, and by 16 DAA increases in whole seed fresh weight were mainly driven by embryo growth (Fig. 3.1B and C).

During rapid seed coat growth (from 8 to 14 DAA; Fig. 3.1B, a transient decrease in seed coat growth was observed in the *lh-1* at 8 and 10 DAA compared to *LH* (34 to 42%; $P \leq 0.05$; Fig. 3.1B). Embryo growth of *lh-1* was also lower at 14 (29%), 16 (19%), and 20 (6%) DAA; $P \leq 0.05$) than that of *LH* (also reflected in whole seed growth; Fig. 3.1A and C). The seed coat and embryo components of the seed become equivalent in size (fresh weight basis) at 14 DAA in *lh-1*, similar to that observed for *LH* (Fig. 3.1B and C). In contrast, the *lh-2* mutation markedly reduced whole seed (45 to 68 %; Fig. 3.1A), seed coat (15 to 72 %; Fig.3.1B) and embryo growth (67 to 97 %; Fig. 3.1C) from 8 to 20 DAA compared to that of *LH*. The seed coat and embryo of *lh-2* obtained approximate equivalent size (fresh weight) at 20 DAA compared to 14 DAA for *LH* (Fig. 3.1B and C).

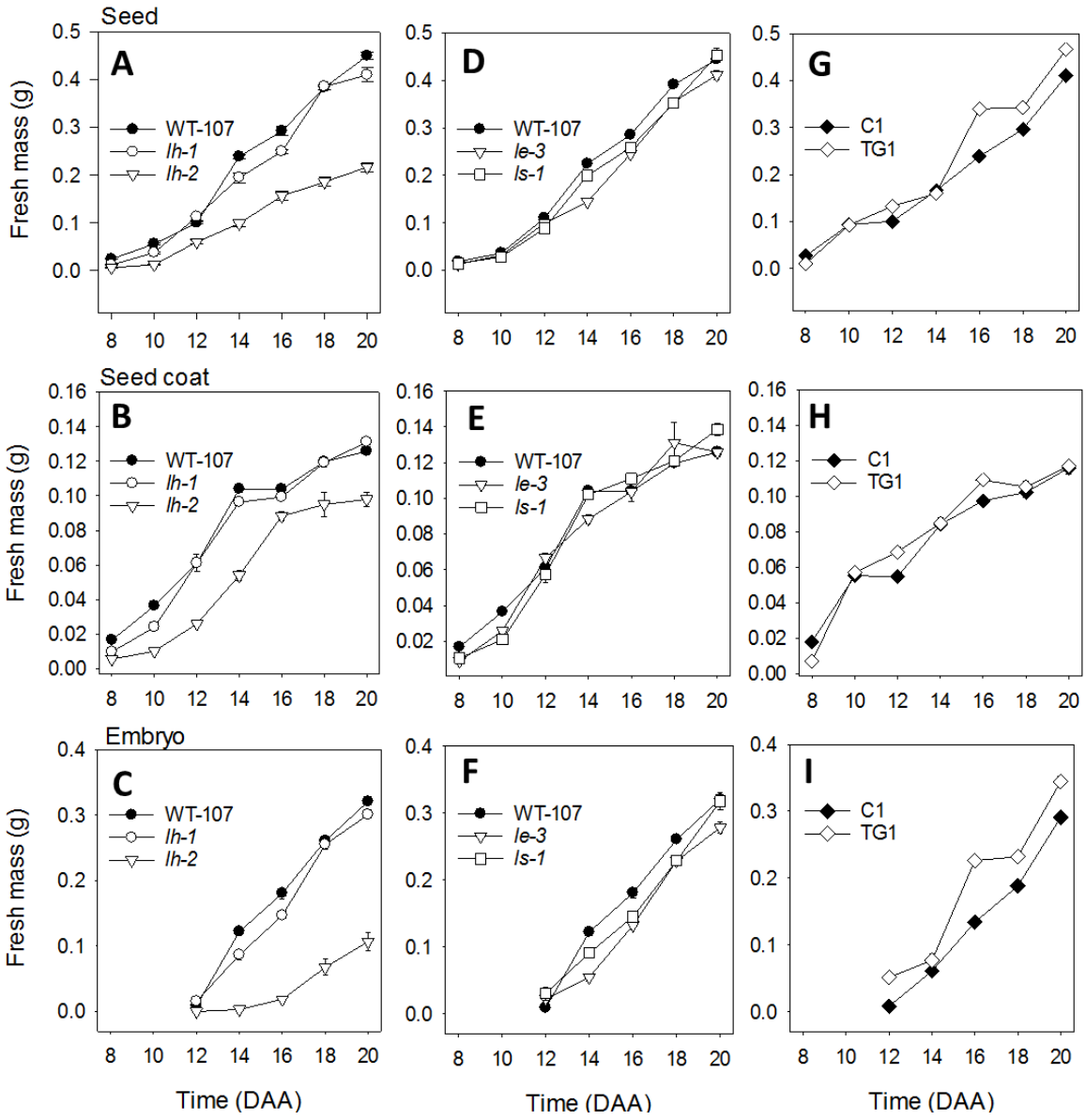

Figure 3.1: Pea seed growth over development (8 to 20 DAA) of the GA biosynthesis mutant lines, *lh-1*, *lh-2*, *le-3*, *ls-1*, and their isogenic wildtype line, WT-107 (*LH, LS, LE*), and the GA overexpressor line TG1 and its control line C1. Growth (in fresh weight) of whole seeds (A,D,G) seed coats (B,E,H) and embryos (C,F,I). Data are expressed as means ± SE; n=6 to 29 for whole seed, n=5 to 14 for seed coat, n=5 to 14 for embryo (except at 14 DAA in *lh*-2, where n=4). In some cases, standard error bars are not visible as they are obscured by symbols.

3.1.2 Seed growth of GA biosynthesis mutants *le-3* and *ls-1* compared to WT-107 (*LE/LS*)

The *le-3* mutation reduced the whole seed growth from 8 to 20 DAA (7 to 36 %; P≤0.05; with the exception of 10 DAA) compared to that of *LE* (WT-107; Fig. 3.1D). The reduction in *le-3* whole seed growth was reflected in reduced seed coat growth during the earlier part of this developmental phase [8 (48 %), 10 (29 %), and 14 (15 %) DAA; P≤0.05; Figure 3.1E], and reduced embryo growth from 14 to 20 DAA (12 to 55%; P≤0.05; Figure 3.1F) compared to that of *LE* (WT-107). The *le-3* seed coat and embryo size (fresh weight) became equivalent in size between 14 to 16 DAA (Fig. 3.1B and C; Table A.1). The *ls-1* mutant reduced whole seed growth from 9 to 23% at 8 and 12 to 18 DAA (Fig 3.1D; P≤0.05) compared to *LS* (WT-107). Reduced *ls-1* seed coat growth was observed at 8 and 10 DAA (37 to 43%; P≤0.05; Fig. 3.1E) and reduced *ls-1* embryo growth from 14 to 18 DAA (12 to 26%; P≤0.05; Fig. 3.1F), compared to that in *LS*. The seed coat and embryo of *ls-1* obtain similar size at 14 DAA, similar to that of *LS* (Fig. 3.1E and F; Table A.1).

3.1.3 Seed growth of GA overexpressor TG1 compared to C1 transgenic control

PsGA3ox1 overexpression (TG1 line) increased embryo growth (fresh weight) at 12 DAA, and from 16 to 20 DAA (18 to 69 %; P≤0.05) compared to the C1 transgenic control (Fig. 3.1I). This is consistent with the increased whole seed fresh mass observed in TG1 16 to 20 DAA (14 to 42%; Fig. 3.1G). The seed coat and embryo of both TG1 and C1 lines obtained approximate equivalent size (fresh weight) at 14 DAA (Fig. 3.1H and I; Table A.1).

3.2 Seed coat cell expansion and differentiation over development (8-20 DAA)

3.2.1 Seed coat cell expansion of GA biosynthesis mutants *lh-1* and *lh-2* compared to WT-107 (*LH*)

The timing of rapid cell expansion varied among the seed coat layers of *LH* from 8 to 20 DAA (Fig. 3.2A-E). Marked increases in cell expansion were observed from 10 to 12 DAA in the epidermal and chlorenchyma layers, from 10 to 14 DAA in the hypodermal layer, 8 to 14 DAA in the ground parenchyma layer, and from 10 to 12 DAA, and 14 to 16 DAA, in the branched parenchyma layer of *LH* seed coats (Fig. 3.2A-E). In contrast, cell expansion was reduced during the phase of rapid cell growth in all the seed coat cell layers of *lh-2* compared to that of *LH* (Fig. 3.2A-E). Specifically, marked reduction in cell expansion of *lh-2* was

observed from 8 to 14 DAA (19 to 32 %) in the epidermal layer, 12 to 16 DAA in the hypodermal layer (11 to 42 %), 12 to 14 DAA (18 to 34 %) in the chlorenchyma layer, and at 10 (49 %) and 14 (44 %) DAA in the ground parenchyma layer compared to that of *LH* ($P \leq 0.05$; Fig. 3.2A-E). With respect to development, hypodermal differentiation into hourglass-shaped cells occurred by 14 DAA in *LH* (WT-107), but was delayed from 14 to 16 DAA in *lh-2* (Fig. 3.3A and C).

In the less severe *LH* mutant *lh-1* (with respect to reduced bioactive GA levels), the only reduction in cell expansion in the seed coat layers was that of the ground parenchyma cells at 8 DAA compared to that of *LH* (54 %; $P \leq 0.05$; Fig. 3.2A-E).

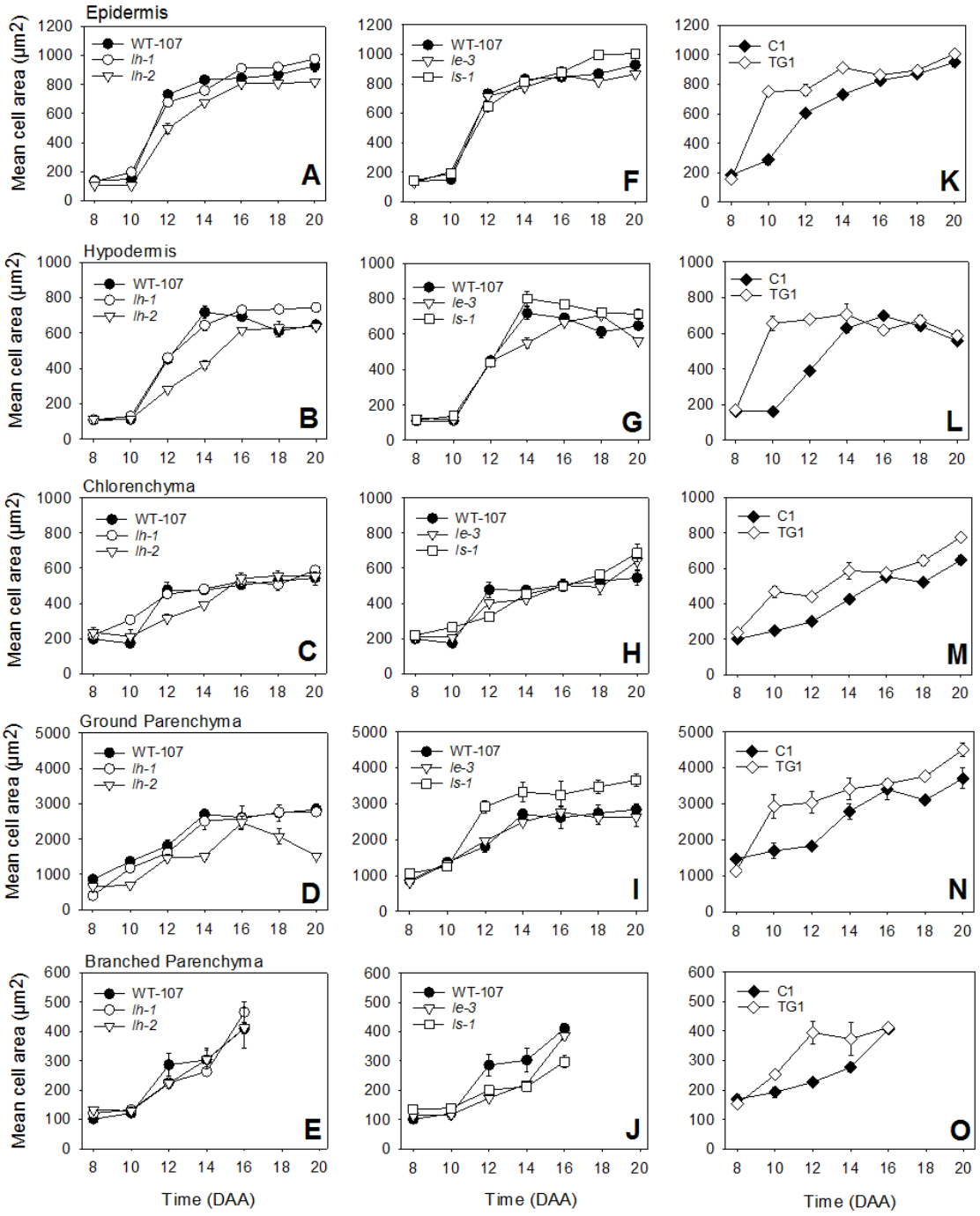

Figure 3.2: Seed coat cell expansion (cross-sectional area) over development (8 to 20 DAA) of the GA biosynthesis mutant lines, *lh-1*, *lh-2*, *le-3*, *ls-1*, and their isogenic wildtype line, WT-107 (*LH, LS, LE*), and the GA overexpressor line TG1 and its control line C1. Epidermis (A,F,K) hypodermis (B,G,L) chlorenchyma (C,H,M) ground parenchyma (D,I,N) branched parenchyma (E,J,O). The data are means ± SE, n = at least 4 biological replicates (average of 20 cells measured per technical replicate, two technical replicates per biological replicate). In some cases, error bars are obscured by data-points. The developing embryo crushes the innermost seed coat branch parenchyma cells after 16 DAA, so data at 18 and 20 DAA times are not presented.

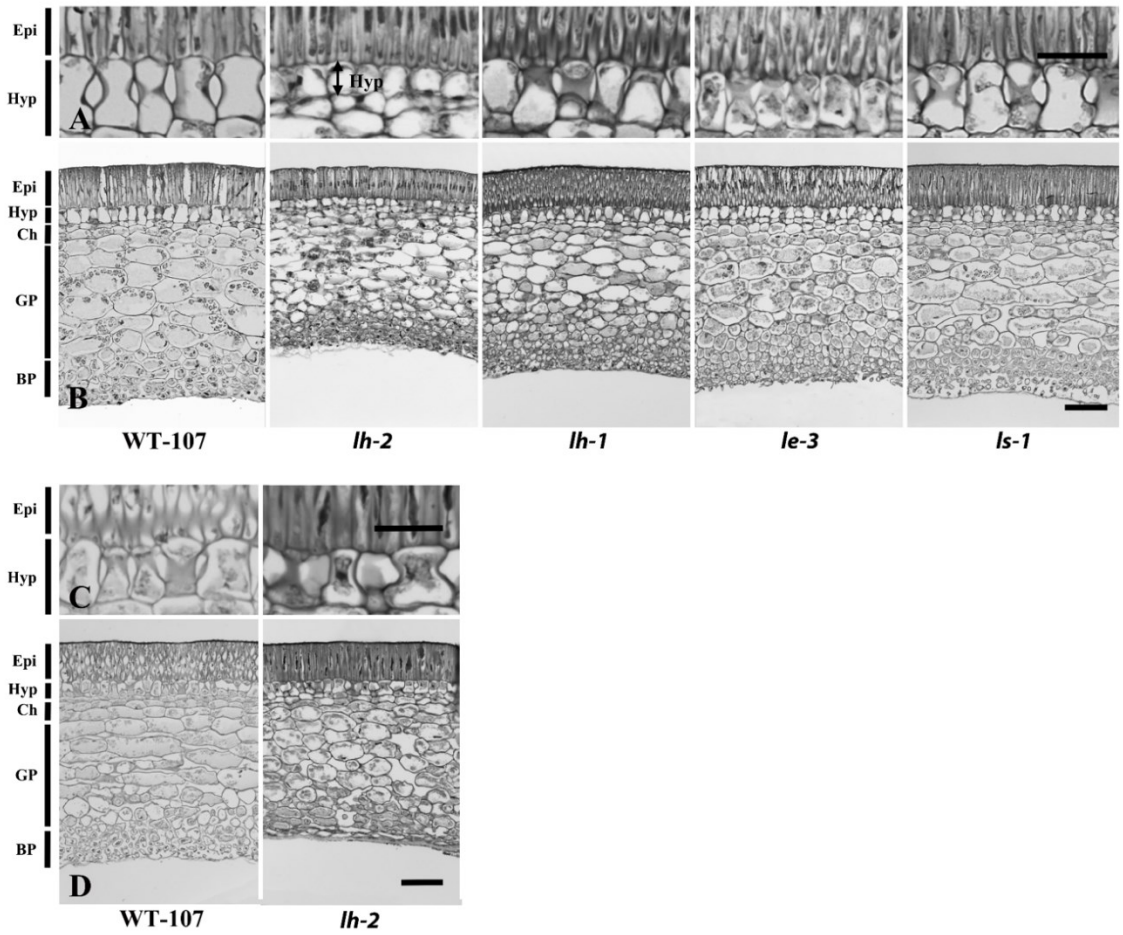

Figure 3.3: Representative micrographs of seed coats at 14 DAA (A and B) and 16 DAA (C and D) of the GA biosynthesis mutant lines, *lh-1*, *lh-2*, *le-3*, *ls-1*, and their isogenic wild-type line, WT-107 (*LH, LS, LE*). Micrographs were taken at 20X magnification and scale bars are 50 µm (A and C) and 100 µm (B and D). Epi, epidermis; Hyp, hypodermis; Ch, chlorenchyma; GP, ground parenchyma; BP, branched parenchyma.

3.2.2 Seed coat cell expansion of GA biosynthesis mutants *le-3* and *ls-1* compared to WT-107 (*LE/LS*)

The GA biosynthesis mutant *le-3* exhibited a similar pattern of seed coat cell layer expansion to that of its isogentic wild-type *LE* (WT-107), with the following noted exceptions (Fig. 3.2F-J). Reduced cellular expansion was observed in the *le-3* branched parenchyma cell layer at 12 DAA (40 %), and in the hypodermal (23 %) and chlorenchyma layers at 14 DAA (11 %) compared to that in *LE* (WT-107; $P \leq 0.05$; Fig. 3.2F-J). The GA biosynthesis mutant *ls-1* also showed a similar pattern of seed coat cell layer expansion to that of *LS* (WT-107; Fig. 3.2F-J), with the following noted exceptions. Cellular expansion was reduced in the *ls-1* chlorenchyma layer (32 %) and increased in the ground parenchyma

layer (38 %) at 12 DAA (Fig. 3.2H and I), and reduced in the branched parenchyma cell layer at 16 DAA compared to that of *LS* (WT-107; P ≤0.05; Fig. 3.2H-J). Fully differentiated hypodermal cells into hourglass shape was observed in *le-3* and *ls-1* seed coats at 14 DAA similar to that observed in *LE*/*LS* (WT-107; Fig. 3.3A).

3.2.3 Seed coat cell expansion of GA overexpressor line TG1 compared to C1 control

Enhanced *PsGA3ox1* expression in the TG1 transgenic line markedly increased cell expansion in all seed coat layers during the developmental period studied compared to the control C1 line (8 to 20 DAA; Fig. 3.2K-O). Specifically, increased cell expansion was observed in the GA overexpressor line TG1 from 10 to 16 DAA in the epidermal, 10 to 12 DAA in the hypodermal, 10 to 14 and 18 to 20 DAA in the chlorenchyma, 10 to 12 DAA and 18 DAA in the ground parenchyma, and 10 and 12 DAA in the branched parenchyma layers compared to that in the control line C1 (P ≤0.05; Fig. 3.2K-O). The hypodermal cells of TG1 were fully differentiated into hourglass-shaped cells by 10 DAA (Fig. 3.4A and B); however this occurred at 14 DAA in the control C1 line (Fig. 3.4C and D).

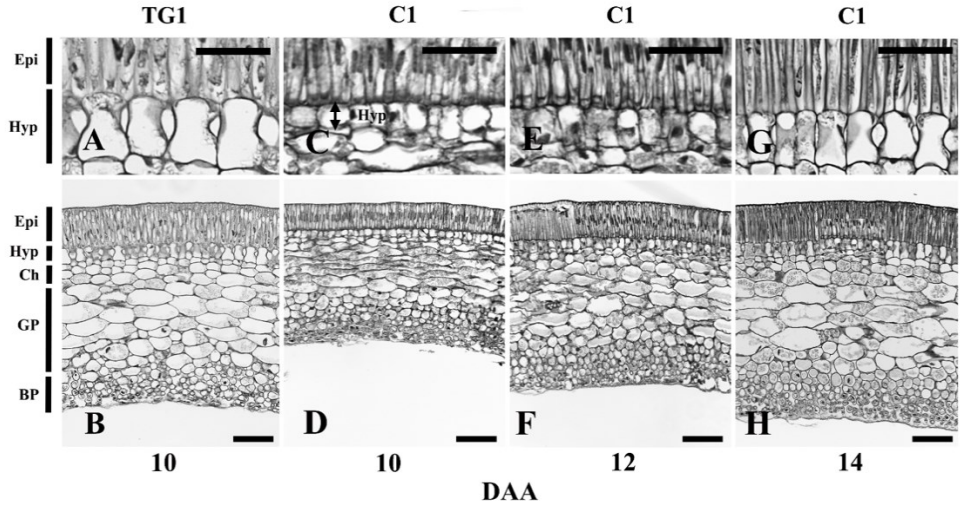

Figure 3.4: Representative micrographs of seed coats at 10 DAA of GA overexpressor line TG1 (A and B) and 10, 12 and 14 DAA of control line C1 (C-H). Micrographs were taken at 20X magnification and scale bars are 100 µm (B, D, F and H) and 50 µm (A, C, E and G). Epi, epidermis; Hyp, hypodermis; Ch, chlorenchyma; GP, ground parenchyma; BP, branched parenchyma.

3.3 Cotyledon cell expansion over development (12-20 DAA)

3.3.1 Cotyledon cell expansion of GA biosynthesis mutants *lh-1* and *lh-2* compared to WT-107 (*LH*)

In developing *LH* seeds, the liquid endosperm volume is maximum around 12 DAA and completely absorbed by the developing embryo by 14 DAA (data not shown). Consistently, from 12 to 16 DAA, the cotyledons of the *LH* embryo exhibited rapid storage parenchyma cell expansion (Fig. 3.5A). In *lh-2*, marked reduction in the cotyledonary storage parenchyma cell expansion occurred at 14 DAA (70%; P≤0.05; Fig. 3.5A), consistent with reduced *lh-2* embryo growth compared to that of *LH* (WT-107; Fig. 3.1C). The cell expansion of the cotyledonary storage parenchyma cells of *lh-1* was similar to that of *LH* from 12 to 20 DAA (Fig. 3.5A).

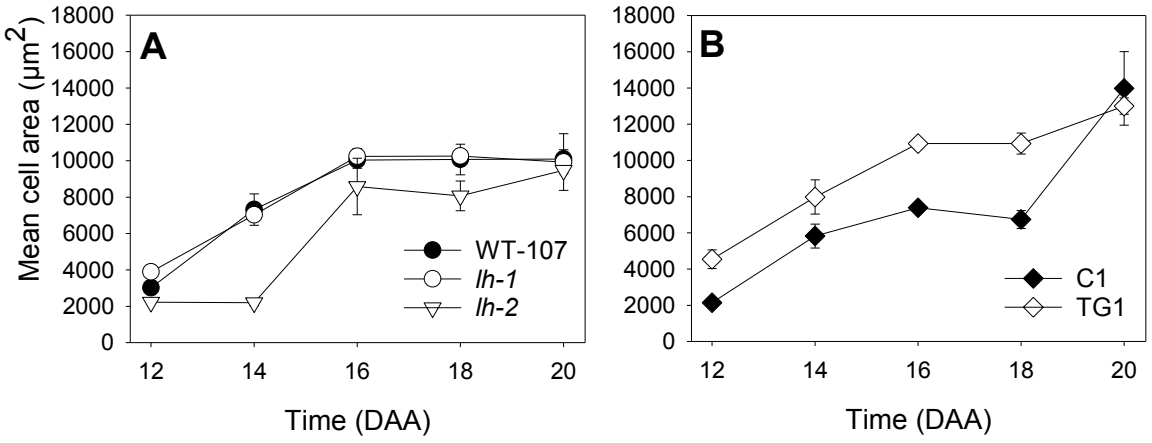

Figure 3.5: Average cross-sectional area of cotyledonary storage parenchyma cells from 12 to 20 DAA of the GA biosynthesis mutant lines *lh-1* and *lh-2* and their isogenic wildtype line, WT-107 (*LH, LE*), and the GA overexpressor line TG1 and its control line C1. The data are means ± SE, n = 3 biological replicates (an average of 16 cells per technical replicate, two technical replicates per biological replicate, and three biological replicates per sample were used for determining cell cross-sectional area). In some cases, error bars are obscured by data-points.

3.3.2 Cotyledon cell expansion of GA overexpressor TG1 compared to C1 control

Similar to the seed coat, enhanced *PsGA3ox1* expression in the TG1 transgenic line markedly increased cell expansion of the cotyledonary storage parenchyma cells (at 12, 16, and 18 DAA; 48-112 %; P≤0.05) compared to that observed in the control C1 line (Fig.

3.5B). This is consistent with the increased embryo growth (in fresh weight) observed in TG1compared to C1 during this period (Fig. 3.1I).

3.4 Seed coat starch, sucrose and glucose content over development (8-20 DAA)

3.4.1 Seed coat starch, sucrose and glucose content of GA biosynthesis mutants *lh-1* and *lh-2* compared to WT-107 (*LH*)

Histological and carbohydrate quantification data showed that starch transiently accumulated in, and was subsequently mobilized from, the pea seed coat from 8 to 20 DAA in the WT-107 (*LH*) line (Figs. 3.6A and 3.7C). Specifically, starch content in the *LH* seed coat remained relatively high from 8 to 12 DAA, then gradually decreased to minimal levels by 20 DAA (Figs. 3.6A and 3.7C). Glucose content in the *LH* seed coat was relatively low at 8 DAA, and it gradually decreased from 8 to 14 DAA, and it remained at the same level from 14 to 20 DAA (Fig. 3.7B). Sucrose levels in the *LH* seed coat increased during the earlier phase of seed coat development, when starch levels were high, peaking at 12 DAA (Fig. 3.7A). *LH* seed coat sucrose levels subsequently decreased as starch was mobilized from the seed coat to the developing embryo *(*Figs. 3.6A and 3.7A).

The starch content of *lh-2* seed coats was markedly lower during the earlier stages of seed coat development [8 (74%), 10 (71%), 12 (45%) and 14 (20%) DAA; $P \leq 0.05$] compared to that of *LH* (Figs. 3.6A, C and 3.7C). Subsequently, the initiation of starch mobilization from the *lh-2* seed coat to the embryo was delayed from 14 to 18 DAA compared to that of *LH* (Figs. 3.6A, C and 3.7C). Consistently, a substantial number of starch granules were visible in the *lh-2* seed coat at 20 DAA (Fig. 3.6C); however, by 25 DAA, no starch granules were observed in *lh-2* seed coats (see Appendix Fig. F.1). In *lh-1* seed coats, starch content was lower than that in *LH* at 8 and 10 DAA (62 to 79%; $P \leq 0.05$; Fig.3.7C), then increased to levels similar to that of *LH* by 12 DAA (Figs. 3.6B and 3.7C), and subsequently exhibited a similar trend in starch mobilization from the seed coat to the embryo as observed for *LH* (from 16 to 20 DAA; Figs. 3.6B and 3.7C).

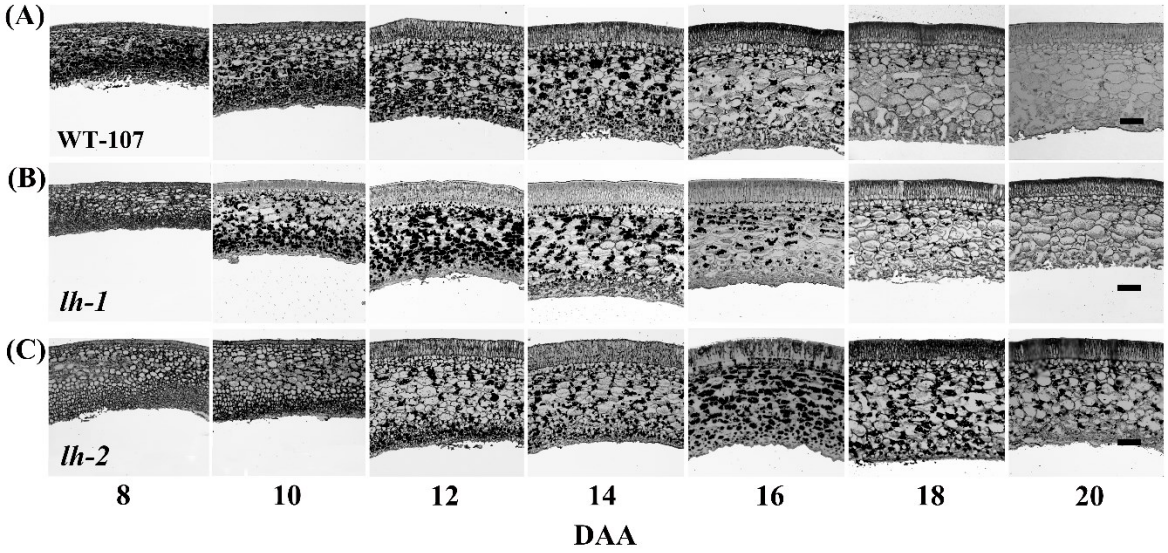

Figure 3.6: Representative micrographs of pea seed coat cross-sections from 8 to 20 DAA stained with iodine for starch grain visualization. (A) Isogenic wild-type line *LH* (WT-107); (B) GA biosynthesis mutant *lh-1*; (C) GA biosynthesis mutant *lh-2*. Micrographs were taken at 20X magnification and the scale bars are 100 μm.

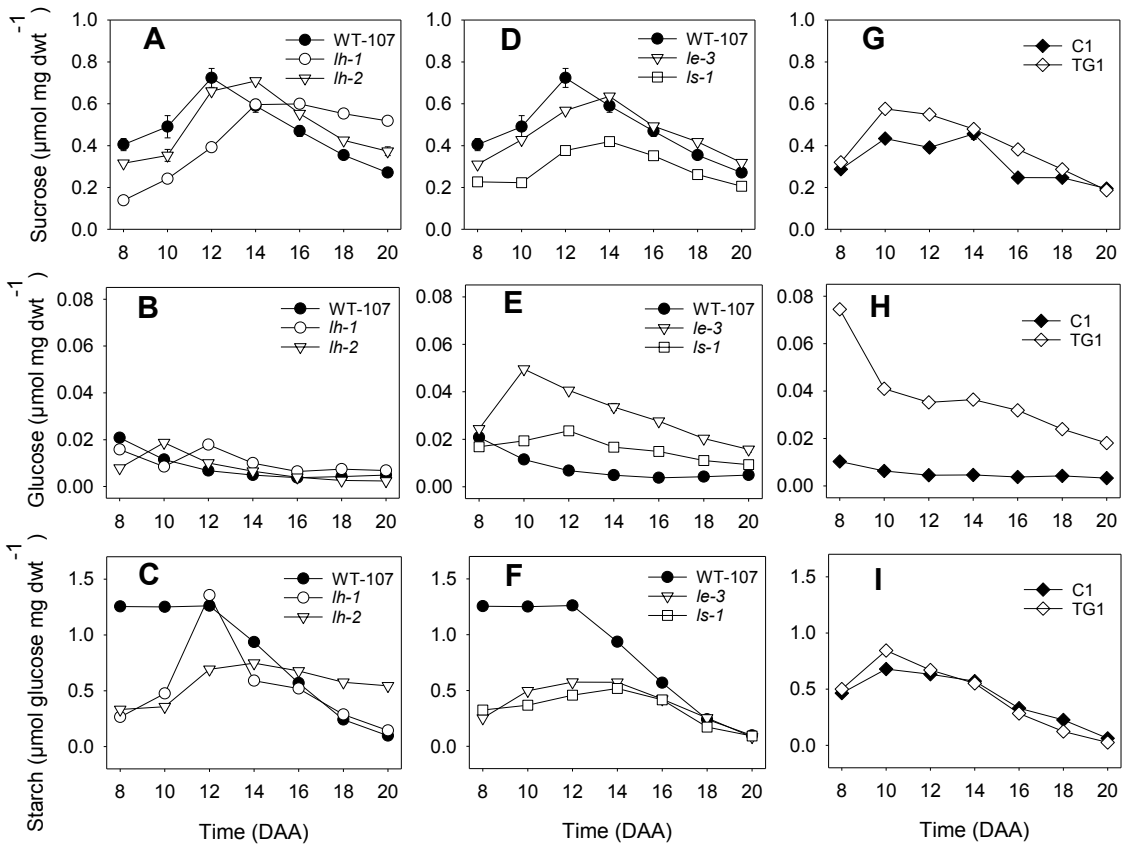

Figure 3.7: Starch, glucose and sucrose content in pea seed coats over the development (8 to 20 DAA) of the GA biosynthesis mutant lines *lh-1*, *lh-2*, *le-3*, and *ls-1* and their isogenic wildtype line WT- 107 (*LH, LS, LE*), and the GA overexpressor line TG1 and its control line C1. Sucrose (A, D, G) glucose (B, E, H) starch (C, F, I). Data are means ± SE; n= 3 biological replicates. In some cases, error bars are obscured by data-points.

Seed coat glucose levels in *lh-1* and *lh-2* were relatively similar to *LH* throughout development (8 to 20 DAA; Fig. 3.7B). Sucrose levels in the seed coat of *lh-1* were lower at 8, 10 and 12 DAA ($P \leq 0.05$; Fig. 3.7A), and higher at 14 to 20 DAA compared to that in *LH* ($P \leq 0.05$; Fig. 3.7A) Sucrose levels in *lh-2* seed coats were more similar to *LH* than those observed for *lh-1* from 8 to 20 DAA (Fig. 3.7A).

3.4.2 Seed coat starch, sucrose and glucose content of GA biosynthesis mutant *le-3* compared to WT-107 (*LE*)

In *le-3* seed coats, starch content was markedly lower from 8 to 16 DAA [8 (80%), 10 (60%), 12 (54%), 14 (39%) and 16 (26%) DAA; $P \leq 0.05$] to that of *LE* (WT-107; Fig. 3.7F).

Initiation of starch mobilization from the *le-3* seed coat to the embryo was delayed from 14 to 16 DAA compared to that of *LH* (Fig. 3.7F).

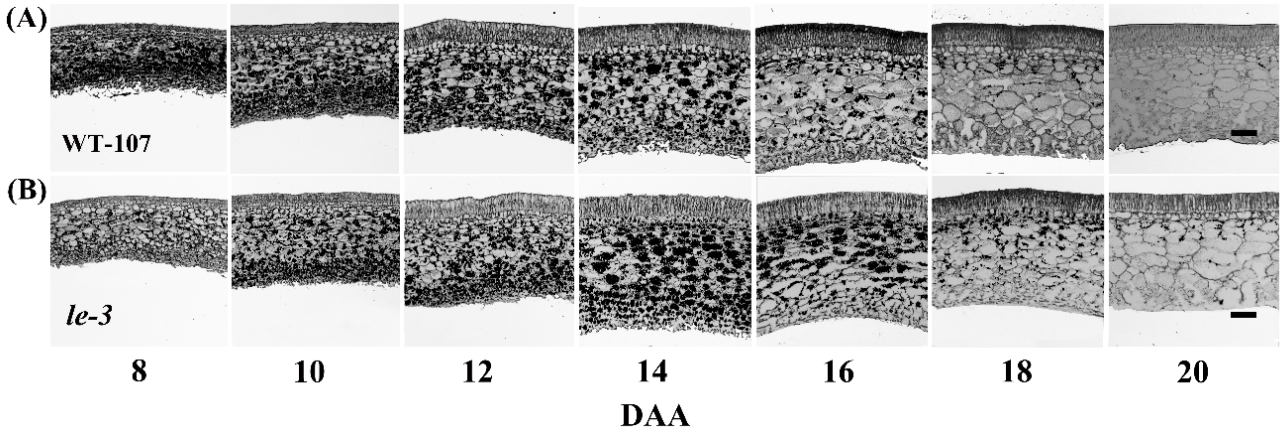

Figure 3.8: Representative micrographs of pea seed coat cross-sections from 8 to 20 DAA stained with iodine for starch grain visualization. (A) Isogenic wild-type line *LE* (WT-107); (B) GA biosynthesis mutant *le-3*. The micrographs were taken at 20X magnification and the scale bars are 100 μm.

Glucose level in the *le-3* seed coats was markedly elevated from 10 to 20 DAA (222 to 630%; P≤0.05) compared that in *LE* (WT-107; Fig.3.7E). However, *le-3* seed coat sucrose levels were relatively similar to those of *LE* from 8 to 20 DAA (Fig. 3.7D).

3.4.3 Seed coat starch, sucrose and glucose content of GA biosynthesis mutant *ls-1* compared to WT-107 (*LS*)

The seed coat starch profile of *ls-1* was similar to that of *le-3*, where markedly lower levels of starch were observed from 8 to 16 DAA [8 (74%), 10 (71%), 12 (64%), 14 (45%) and 16 (27%) DAA; P≤0.05] compared to that in the *LS* (WT-107; Fig. 3.7F). Initiation of starch mobilization from the *ls-1* seed coat to the embryo was delayed from 14 to 16 DAA compared to that of *LS* (Fig. 3.7F). Elevated glucose levels were observed in *ls-1* seed coats during the mid-phase of development (at 10, 12, 14 and 16 DAA; P≤0.05) compared to that in *LS* (WT-107; Fig. 3.7E). In contrast, sucrose levels in *ls-1* seed coats were lower than that in *LS* (WT-107) from 8 to 20 DAA (P≤0.05; Fig. 3.7D)

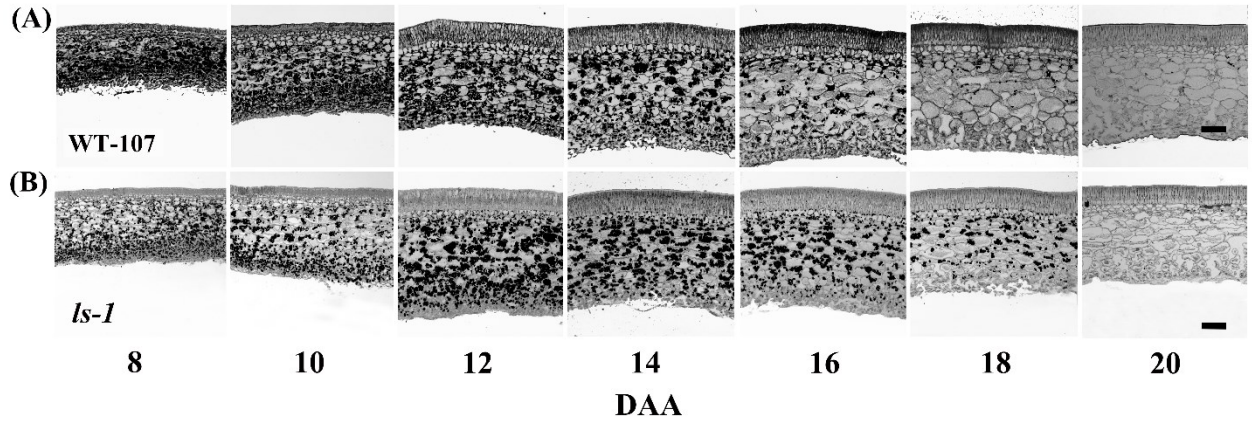

Figure 3.9: Representative micrographs of pea seed coat cross-sections from 8 to 20 DAA stained with iodine for starch grain visualization. (A) Isogenic wild-type line *LS* (WT-107); (B) GA biosynthesis mutant *ls-1*. The micrographs were taken at 20X magnification and the scale bars are 100 μm.

3.4.4 Seed coat starch, sucrose and glucose content of GA overexpressor TG1 compared to C1 control

Iodine stained seed coat and cotyledon micrographs and carbohydrate quantification data showed that starch transiently accumulates in, and subsequently is mobilized from the seed coat to the developing embryo, from 8 to 20 DAA in the C1 control line (Figs. 3.7I and 3.10A). Sucrose content in the C1 seed coat was higher from 8 to 14 DAA, then decreased (Fig. 3.7G), and the glucose level remained consistently low from 8 to 20 DAA (Fig. 3.7H).

The starch levels in TG1 seed coats were higher at 10 DAA (24 %; $P \leq 0.05$) and lower from 16 to 20 DAA (14 to 59 %; $P \leq 0.05$) compared to C1 control (Figs. 3.7I and 3.10B). Markedly higher levels of glucose were observed in the seed coats of TG1 from 8 to 20 DAA (447 to 745%; $P \leq 0.05$) compared to that in the control C1 line (Fig. 3.7H).

Sucrose levels in the TG1 seed coats were higher during the earlier phase of seed coat development, when starch levels were high, and sucrose levels decreased as starch was mobilized to the developing embryo *(*Fig. 3.7G and I). TG1 seed coat sucrose levels were also elevated at 10, 12, 16 and 18 DAA compared to that of C1 (16 to 54%; $P \leq 0.05$; Fig. 3.7G).

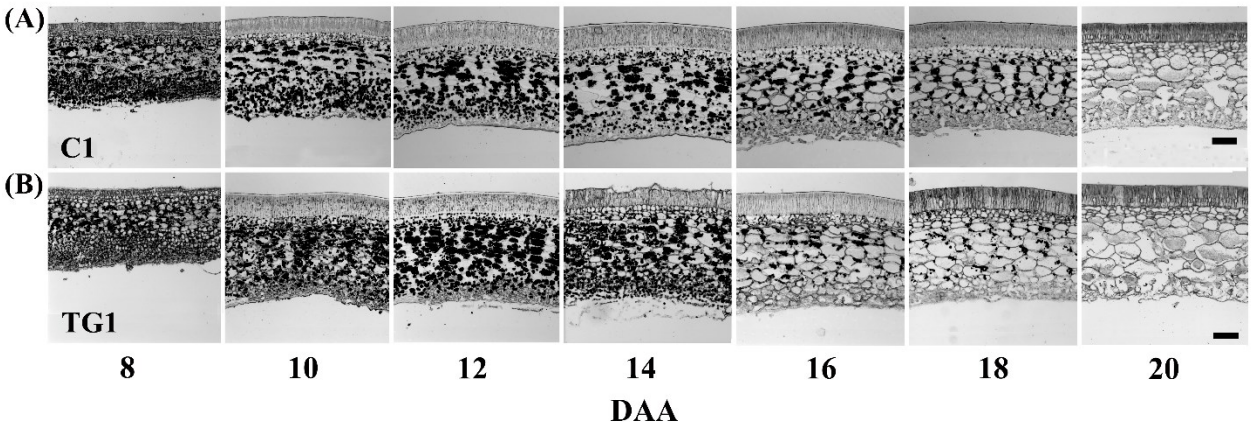

Figure 3.10: Representative micrographs of pea seed coat cross-sections from 8 to 20 DAA stained with iodine for starch grain visualization. (A) Control line C1; (B) GA overexpressor line TG1. The micrographs were taken at 20X magnification and the scale bars are 100 µm.

3.5 Cotyledon starch, sucrose and glucose content over development (12-20 DAA)

3.5.1 Cotyledon starch, sucrose and glucose content of GA biosynthesis mutants *lh-1* and *lh-2* compared to WT-107 (*LH*)

Histological and carbohydrate quantification data showed that starch increased in a linear manner in the WT-107 (*LH*) cotyledonary storage parenchyma cells from 12 to 20 DAA (Figs. 3.11A and 3.12C). Glucose content in the *LH* cotyledon remained relatively constant from 12 to 20 DAA (Fig. 3.12B). Sucrose levels in the *LH* cotyledons were higher from 12 to 16 DAA, then decreased (16 to 20 DAA; Fig. 3.12A).

The starch content of *lh-2* cotyledons was markedly lower compared to those of *LH* [16 (86%), 18 (64%) and 20 (63%) DAA; $P \leq 0.05$; Figs. 3.11C and 3.12C]. Consistently, fewer starch granules were observed in the *lh-2* cotyledonary sections from 16 to 20 DAA, than were observed in those of *LH* (WT-107; Fig. 3.11A and C). In *lh-1,* cotyledonary starch content was also lower at 14, 16 and 20 DAA, compared to *LH* [WT-107; 14 (81%), 16 (55%), 20 (28%) DAA; $P \leq 0.05$; Figs. 3.11B and 3.12C]. However, starch levels in *lh-1* at 16, 18 and 20 DAA stages were higher than those of *lh-2* (Figs. 3.11B, C and 3.12C). In general, cotyledonary glucose levels were not markedly affected by the *lh-1* mutation, with one exception, higher glucose levels were observed at 8 DAA in the *lh-1* cotyledons compared to that in *LH* (WT-107; Fig. 3.12B). Similar glucose levels were observed from 16-20 DAA in the cotyledons of *lh-2* and *LH* (WT-107; Fig. 3.12B).

Elevated sucrose levels were observed in *lh-1* cotyledons from 14 and 20 DAA [14 (29%), 16 (15%), 18 (31%) and 20 (44%) DAA; P≤0.05], and in *lh-2* cotyledons from 16 to 20 DAA [16 (10%), 18 (38%) and 20 (53%) DAA; P≤0.05] compared to that of *LH* (WT-107; Fig. 3.12A).

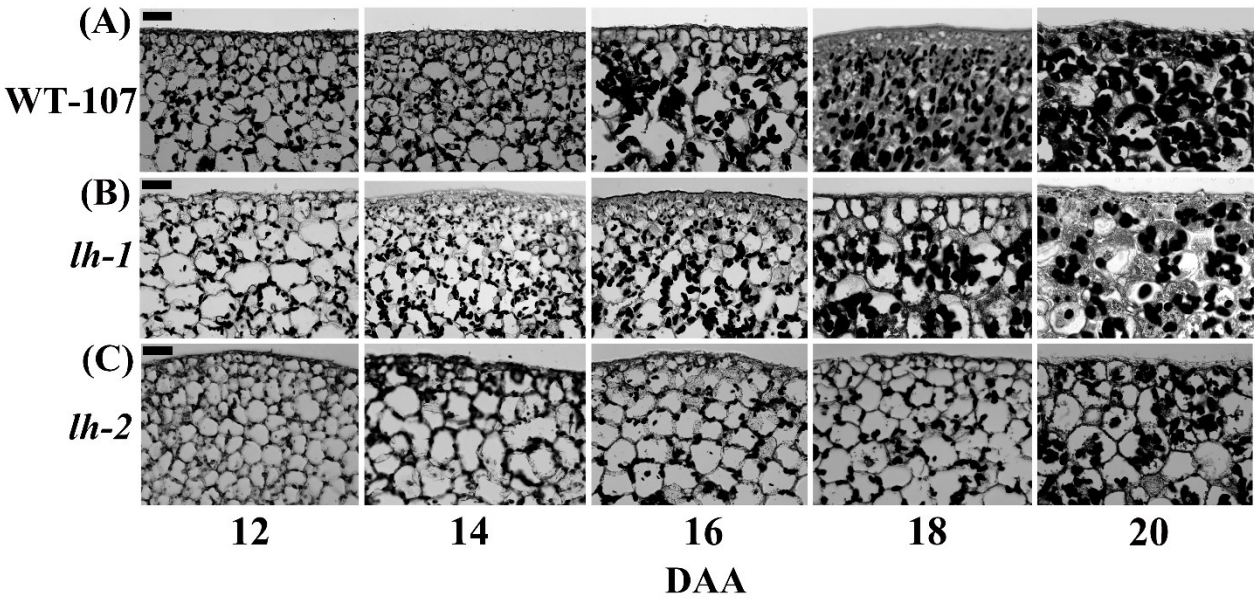

Figure 3.11: Representative micrographs of pea cotyledon cross-sections from 12 to 20 DAA stained with iodine for starch grain visualization. (A) Isogenic wild-type line *LH* (WT-107); (B) GA biosynthesis mutant *lh-1*; (C) GA biosynthesis mutant *lh-2*. The micrographs were taken at 40X magnification and the scale bars are 50 µm.

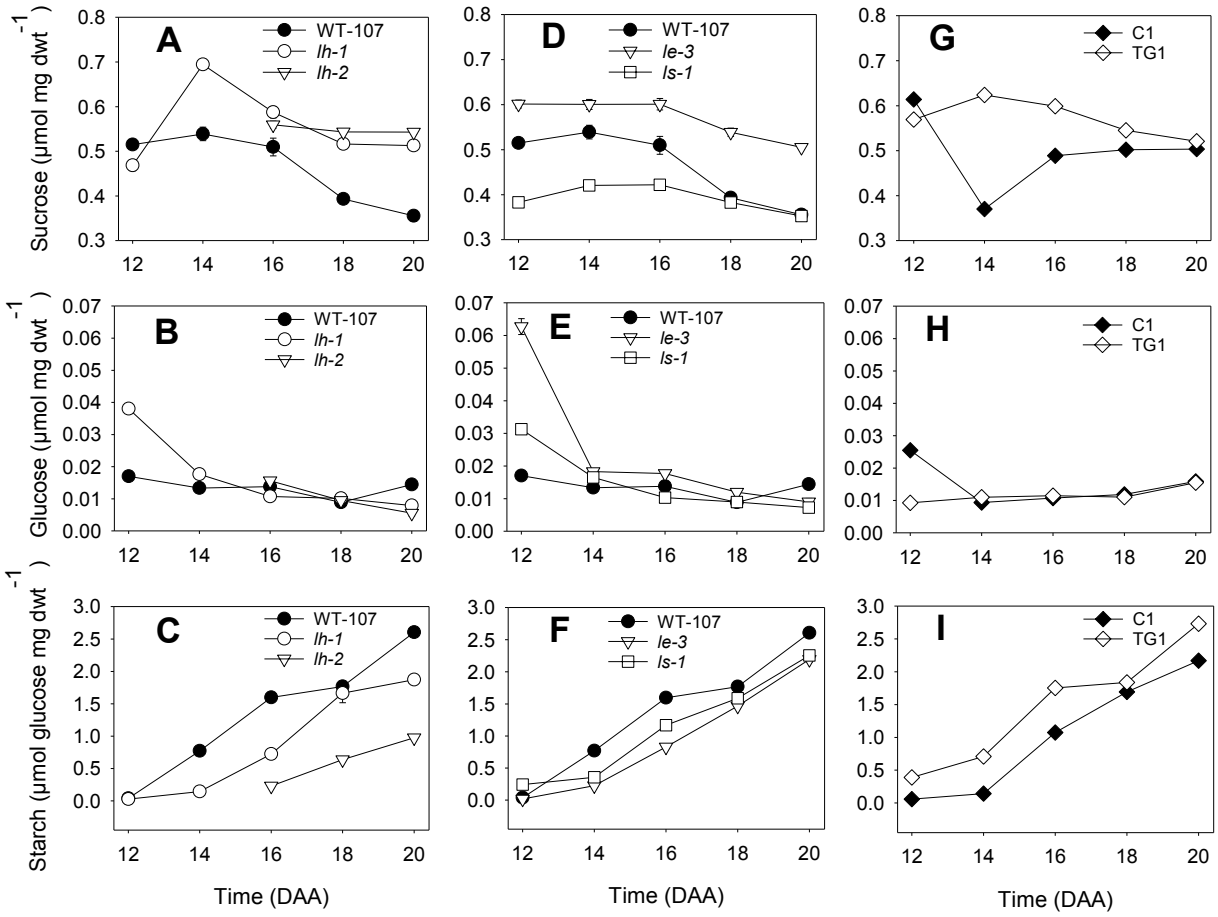

Figure 3.12: Starch, glucose and sucrose levels in cotyledons over development (12 to 20 DAA) of the GA biosynthesis mutant lines, *lh-1*, *lh-2*, *le-3*, *ls-1*, and their isogenic wildtype line, WT-107 (*LH, LS, LE*), and the GA overexpressor line TG1 and its control line C1. Sucrose (A, D, G) glucose (B, E, H) starch (C, F, I). Data are means ± SE n=3 biological replicates. In some cases, error bars are obscured by data-points.

3.5.2 Cotyledon starch, sucrose and glucose content of GA biosynthesis mutant *le-3* compared to WT-107 (*LE*)

Starch content was reduced in the cotyledonary storage parenchyma cells of *le-3* from 12 to 16 and 20 DAA compared to that in *LE* (16 to 71%; P≤0.05; Figs. 3.12F and 3.13B). In general, cotyledonary glucose levels were not markedly affected by the *le-3* mutation, with one exception, higher glucose levels were observed at 12 DAA in the *le-3* cotyledons compared to that in *LE* (WT-107; 268%; P≤0.05; Fig. 3.12E). Cotyledon sucrose levels remained high from 12 to 20 DAA in *le-3* compared to *LE* (WT-107; 11 to 42%; P≤0.05; Fig. 3.12D).

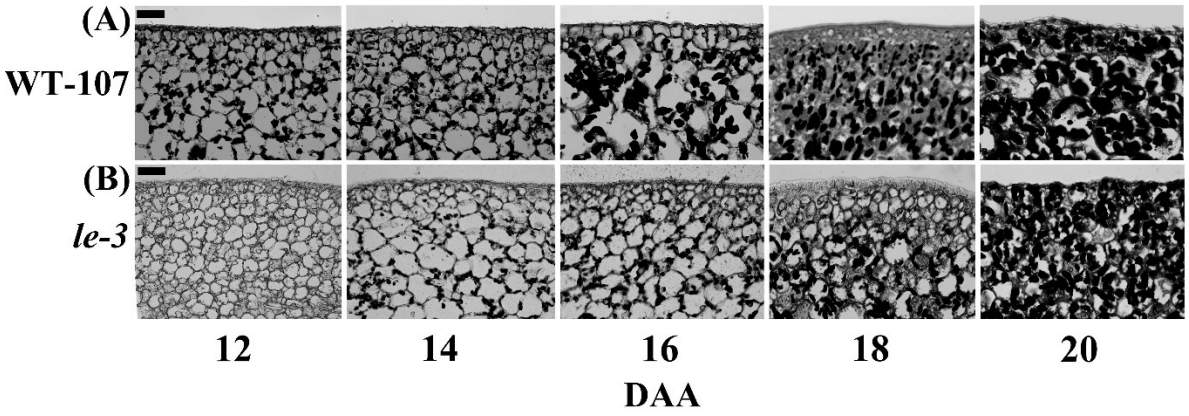

Figure 3.13: Representative micrographs of pea cotyledon cross-sections from 12 to 20 DAA stained with iodine for starch grain visualization. (A) Isogenic wild-type line *LE* (WT-107); (B) GA biosynthesis mutant *le-3*. The micrographs were taken at 40X magnification and the scale bars are 50 µm.

3.5.3 Cotyledon starch, sucrose and glucose content of GA biosynthesis mutant *ls-1* compared to WT-107 (*LS*)

The *ls-1* mutation reduced starch accumulation in the cotyledon storage parenchyma cells at 14, 16 and 20 DAA (10 to 54%; P≤0.05) compared to that in *LS* (WT-107; Figs. 3.12F and 3.14B). Cotyledonary glucose levels in *ls-1* at 12 and 14 DAA were higher [12 (84%) and 14 (24%) DAA; P≤0.05] than those of *LS* (Fig. 3.12E). Sucrose levels were lower in *ls-1* cotyledons at 12, 14 and 16 DAA (17 to 26%; P≤0.05) compared to those of *LS* (WT-107; Fig. 3.12 D)

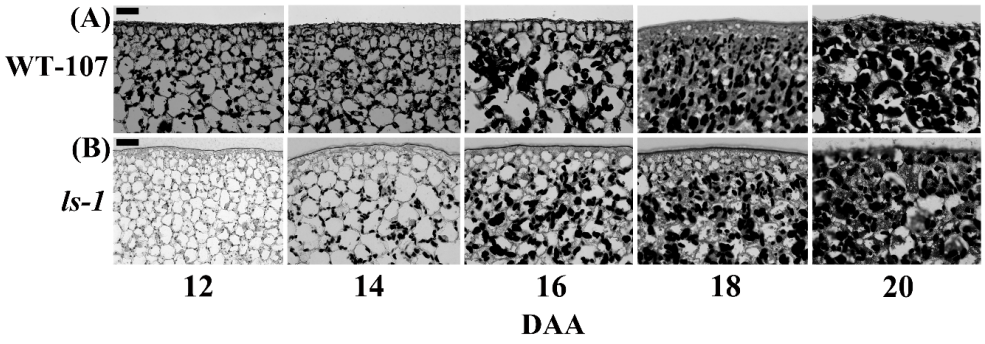

Figure 3.14: Representative micrographs of pea cotyledon cross-sections from 12 to 20 DAA stained with iodine for starch grain visualization. (A) Isogenic wild-type line *LS* (WT-107); (B) GA biosynthesis mutant *ls-1*. The micrographs were taken at 40X magnification and the scale bars are 50 µm.

3.5.4 Cotyledon starch, sucrose and glucose content of GA overexpressor TG1 compared to C1 control

Starch content in cotyledonary storage parenchyma cells increased with development from 12 to 20 DAA, with the GA overexpressor line TG1 consistently accumulating greater levels of starch (9% to 569%; P≤0.05) than is transgenic control C1 (Figs. 3.12I and 3.15A and B). In general, cotyledonary glucose levels were not markedly affected by *PsGA3ox1* (TG1), with one exception, lower glucose levels were observed at 12 DAA in the TG1 cotyledons compared to that in C1 (64 %; P≤0.05; Fig. 3.12H). Elevated levels of sucrose were observed in the cotyledons of the *PsGA3ox1* over-expression line TG1 at 14, 16 and 18 DAA [14 (68%), 16 (23%) and 18 (9%) DAA; P≤0.05] compared to that in C1 (Fig. 3.12G).

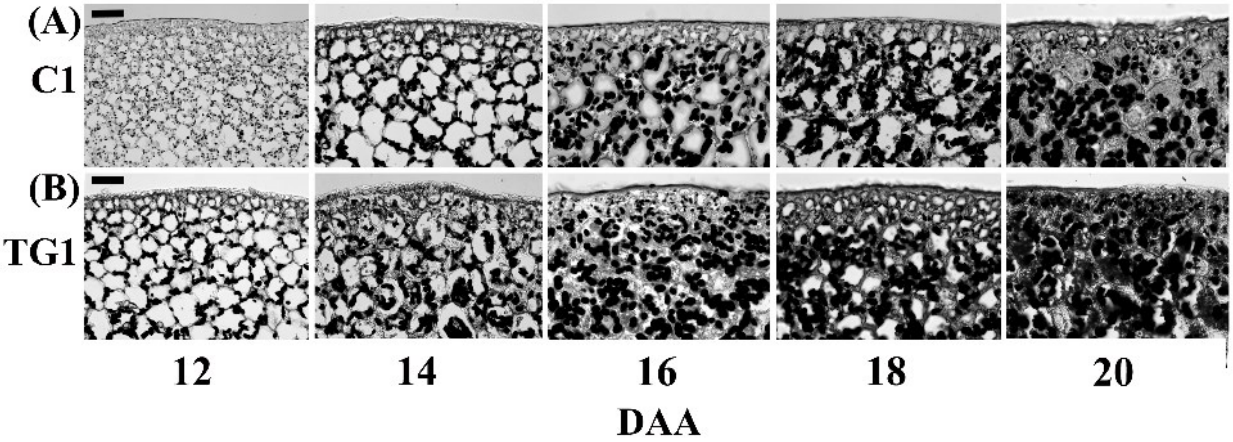

Figure 3.15: Representative micrographs of pea cotyledon cross-sections from 12 to 20 DAA stained with iodine for starch grain visualization. (A) Control line C1; (B) GA overexpressor line TG1. The micrographs were taken at 40X magnification and the scale bars are 50 μm.

3.6 Sucrose and glucose profiles in the endosperm

The sucrose level did not change in the liquid endosperm of *LH* seeds from 10 to 12 DAA, and it was at least 3-fold higher than that of glucose (Fig. 3.16A and B). However, the *LH* endosperm glucose level did decrease from 10 to 12 DAA resulting in a lower glucose: sucrose ratio in the endosperm at 12 DAA (Fig. 3.16C). By 14 DAA, the endosperm was completely absorbed by the developing *LH* embryo. In contrast, the delay in seed development in *lh-2* resulted in the presence of liquid endosperm in *lh-2* seeds at least until 16 DAA. Glucose levels were higher than sucrose levels in the endosperm of *lh-2* 10 to 14

DAA (Fig. 3.16B). Also, sucrose levels in the *lh-2* endosperm were lower than those in *LH*, even at 16 DAA (Fig. 3.16A).

Similar to *LH*, sucrose level did not change in the liquid endosperm of TG1 and C1 seeds from 10 to 12 DAA, and it was at least 3-fold higher than that of glucose (Fig. 3.16A and B). However, the endosperm glucose level did decrease from 10 to 12 DAA resulting in a lower glucose: sucrose ratio in the endosperm of TG1 and C1 seeds at 12 DAA (Fig. 3.16C). By 14 DAA, the endosperm is completely absorbed by the developing TG1 and C1 embryos.

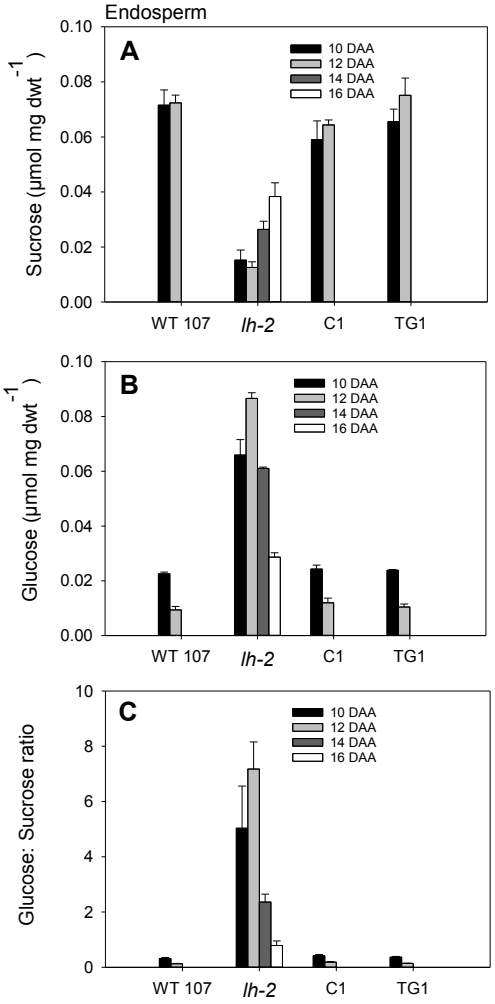

Figure 3.16: Sucrose (A), glucose (B) and glucose: sucrose ratio (C) in the endosperm of the GA biosynthesis mutant *lh-2* and its isogenic wild-type line WT-107 (*LH*), and the GA overexpressor line TG1 and its control line C1. For *LH*, C1 and TG1, data for 10 and 12 DAA stages are shown; for *lh-2* data for 10 to 16 DAA stages are shown. Data are means ± SE, n= 3 biological replicates.

3.7 Protein accumulation in cotyledonary storage parenchyma cells in TG1 and C1 control

Accumulation of proteins in pea cotyledonary storage parenchyma cells was observed using amido black staining of cotyledon sections (Fig. 3.17). The protein content (mg protein per 100 mg dwt) gradually decreased as the cotyledons increase in size from 14 to 18 DAA in both TG1 and C1 lines (Fig. 3.18A). However, at 20 DAA, protein levels did not decrease in TG1 cotyledons, even though they continued to increase in size (Fig. 3.18A). When expressing protein content on a per cotyledon pair basis, TG1 embryos contained higher protein than C1, due to its larger embryo size compared to that of C1 (Fig. 3.18B).

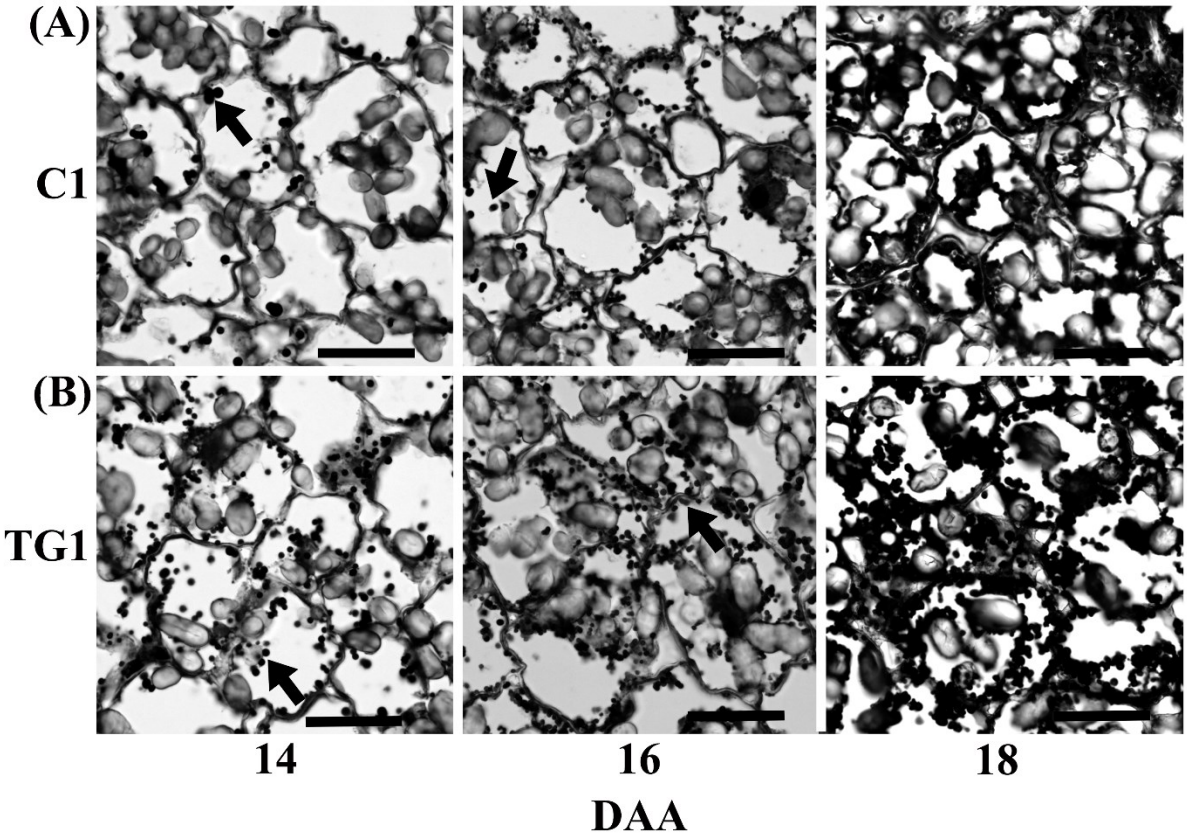

Figure 3.17: Representative micrographs of pea cotyledon cross-sections from 14 to 20 DAA stained with Amido black for the visualization of protein vacuoles. (A) Control line C1; (B) GA overexpressor line TG1. Arrows indicate Amido black-stained protein vacuoles. The micrographs were taken at 40X magnification and the scale bars are 100 μm.

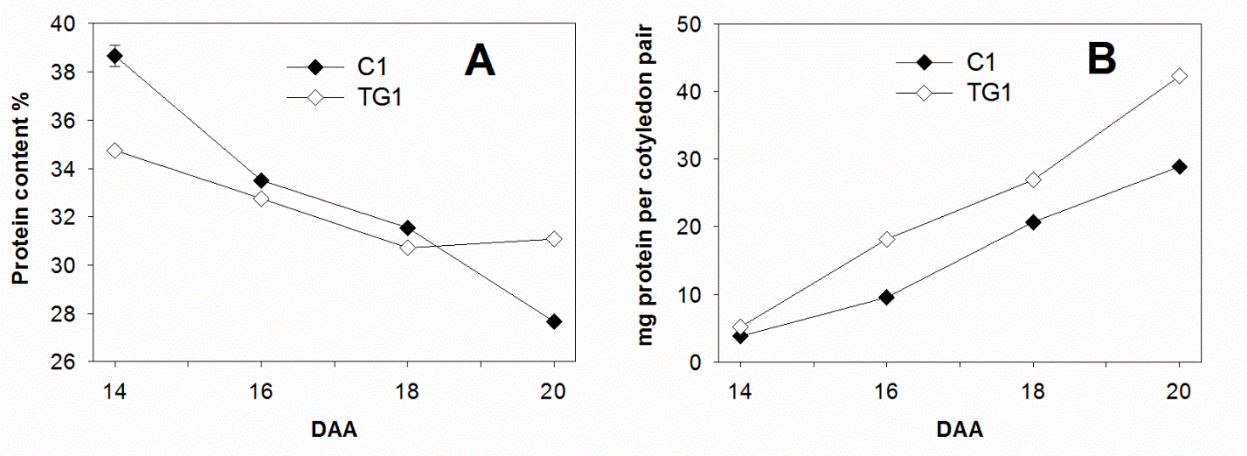

Figure 3.18: Protein accumulation in cotyledon from 14 to 20 DAA in the GA overexpressor line TG1 and the control line C1. (A) Percent protein content (mg of protein per 100 mg dry cotyledon weight). (B) Protein content per cotyledon pair. Data are means ± SE, n= 3 biological replicates. In some cases, error bars are obscured by data-points.

3.8 GA content in 10 DAA whole seeds of WT-107, *lh-2, le-3*, TG1 and C1, and in the seed coats of 8 and 10 DAA seeds of TG1 and C1

Growth active GA_1 and its immediate inactivated metabolite, GA_8, were detected in 10 DAA *LH* seeds (Table 3.1). In contrast, GA_1 was not detected, and GA_8 levels were lower (2-fold), in 10 DAA *lh-2* seeds compared to that in *LH*. Seeds of *le-3* (10 DAA) had higher levels of GA_1 and lower levels of GA_8 than that in *LE* seeds (Table 3.1). *PsGA3ox1* overexpression increased GA_1 levels in 8 DAA seed coats and GA_8 levels in 8 and 10 DAA seed coats of TG1 compared to that in C1 (Table 3.1). These data suggest that *PsGA3ox1* overexpression increased the flow through to bioactive GA_1 in rapidly expanding seed coats of pea. Overexpression of *PsGA3ox1* in *le-1* (TG1 line) decreased GA_{20} and GA_{29} levels in the whole seed, but increased their levels in the seed coat at 10 DAA (compare TG1 to C1; Table 3.1).

The *le-3* and *le-1* (C1) lines contained higher GA_{29} levels in 10 DAA seeds (than *LE*) as these mutations are in the gene that codes for GA 3-oxidase that converts GA_{20} to GA_1, so elevated levels of GA_{20} (due to the block in conversion of GA_{20} to GA_1) are removed from the GA biosynthesis pathway by conversion to the inactive metabolite GA_{29}.

Table 3.1. Abundance of 13-hydroxylated GAs; GA_1, GA_8, GA_{20} and GA_{29} in 10 DAA whole seeds of WT-107, *lh-2, le-3,* C1 and TG1 , and seed coats of 8 and 10 DAA TG1 and C1. Data are means ± SD; n=2; nd= not detected (endogenous GA not detected, but internal standard recovered).

Genotype	DAA	GA_1	GA_8	GA_1+ GA_8	GA_{20}	GA_{29}	GA_{20}+GA_{29}
				ng $gdwt^{-1}$			
Whole seed							
WT-107	10	17 ± 2	25 ± 8	42 ± 6	22 ± 5	59 ± 2	81 ± 7
lh-2	10	nd	12 ± 4	-	23 ± 10	34 ± 10	57 ± 0
le-3	10	39 ± 5	10 ± 1	49 ± 6	13 ± 4	128 ± 21	140 ± 25
C1(*le-1*)	10	10 ± 0	32 ± 5	43 ± 5	50 ± 3	220 ± 18	270 ± 21
TG1	10	12 ± 1	48 ± 16	59 ± 15	35 ± 5	164 ± 18	200 ± 13
Seed coat							
C1(*le-1*)	8	35 ± 1	86 ± 5	121 ± 5	91 ± 2	183 ± 14	274 ± 16
	10	11 ± 4	27 ± 4	38 ± 0	45 ± 1	161 ± 12	207 ± 11
TG1	8	47 ± 1	112 ± 2	159 ± 1	112 ± 35	293 ± 35	406 ± 70
	10	13 ± 2	49 ± 2	62 ± 0	65 ± 1	318 ± 6	383 ± 6

4. DISCUSSION

Viable mature seeds are produced by extensive coordination among seed coat, embryo (cotyledons and embryo axis) and endosperm during the seed development process. These tissues are subjected to unique structural and physiological changes throughout their development. In this thesis, genetic and biochemical approaches have been used to investigate the roles of GAs during the seed developmental process.

4.1 Effect of *lh-2* mutation on growth and carbohydrate partitioning in the seed

The reduction in seed fresh weight as the result of the *lh-2* (formerly lh^i) mutation observed in 7-19 DAA seeds (Swain et al., 1993, 1995, 1997), was confirmed, and determined to be the result of reduced seed coat and embryo growth from 8 to 20 DAA (Fig. 3.1A-C). The *lh-2* mutation reduced the amount of GA_1 in 10 DAA seeds to undetectable levels, and its immediate catabolite, GA_8, by 2-fold compared to that in *LH* (Table 3.1). As *lh-2* is a mutation in *ent*-kaurene oxidase, a step in the GA biosynthetic pathway that occurs prior to the formation of GA_{20} (see Fig. 1.1), it is likely that reduced levels of precursors for the production of GA_{20} minimizes the amount of GA_{20} that is catabolized to GA_{29}, an inactive GA metabolite in 10 DAA *lh-2* seeds (Table 3.1). These data are consistent with those of Swain et al., 1995 where they reported that the *lh*-2 mutation reduced GA_1, GA_3, GA_8, and to a lesser extent, GA_{20} and GA_{29} levels in young developing pea seeds (at 7, 9 and 11 DAA) compared to that in *LH* seeds. Fertilization of *lh-2* plants with *LH* pollen (resulting in *LH lh-2* embryo, *lh-2 lh-2* seed coat) increased seed weight at maturity and seed survival compared to seeds from the self-pollinated *lh-2* plants (Swain et al., 1995). Seeds (6 DAA) from the *lh-2*♀ *x LH*♂ cross had higher GA_1 and GA_3; however, the level of bioactive GA_1 was not fully restored to that in the seeds of the self-pollinated *LH* plants, and GA_8, GA_{20} and GA_{29} were not increased compared to seeds from self-fertilized *lh-2* plants (Swain et al., 1995). These data suggested that the *lh-2* mutation reduces GA_1 and GA_3 synthesized in the embryo and/or endosperm and GA_1, GA_8, GA_{20} and GA_{29} levels in the seed coat of young developing seeds compared to *LH* (Swain et al., 1995).

To investigate the tissue-specific effects of reduced bioactive GA levels on growth and cellular expansion of tissues that comprise the pea seed coat and embryo from 8 to 20 DAA, seeds of self-fertilized *lh-2* plants were compared to those of wild-type *LH* plants. In general, cellular development and expansion of the seed coat layers of *LH* were similar to that described by Nadeau et al. (2011) for *Pisum sativum* cv. I_3-Alaska-type and Van Dongen et

al. (2003) for *cv.* 'Marzia'. Nadeau et al. (2011) also observed marked rapid cell expansion in the branched parenchyma cell layer of the seed coat from 14 and 16 DAA in cv. I_3-Alaska-type seeds. Increased cell expansion in this layer was also observed in *LH* seed coats from 14 to 16 DAA (Fig. 3.2E), but to a much lesser extent than that observed in cv. I_3-Alaska-type (14 to 15; see Appendix Fig. E.1). In *lh-2*, our data suggests that the lower levels of bioactive GA_1 in developing *lh-2* seeds reduced cellular expansion during the phase of rapid cell growth in the epidermal, hypodermal, chlorenchyma, and ground parenchyma seed coat cell layers resulting in reduced tissue growth compared to that of *LH* (Figs. 3.1B and 3.2A-E).

The differentiation of the hypodermal cells into 'hourglass' shape between 12 and 14 DAA marked one of the most distinctive morphological changes in *LH* pea seed coats (Fig. 3.3A). This event was previously documented by Nadeau et al. (2011), where they reported that hypodermal cells were fully differentiated by 14 DAA in pea seed coats of cv. I_3 (Alaska-type). In contrast, hypodermal layer differentiation into 'hourglass-shaped cells was delayed by two days in *lh-2* compared to *LH* (Fig. 3.3A and C), suggesting that delayed hypodermal cell expansion (Fig. 3.2B) was the result of lower bioactive GA levels in *lh-2* seeds.

Concurrent with delayed seed coat cell expansion, a reduction in storage parenchyma cell expansion in *lh-2* cotyledons was observed at 14 DAA compared to those of *LH* (Fig. 3.5A). These data suggest that reduced bioactive GA levels during early seed development in the embryo and endosperm of *lh-2* (Swain et al., 1995), delay the growth and cellular expansion of the cotyledonary cells during the rapid phase of embryo expansion and the time to reach equivalent embryo: seed coat fresh mass (14 DAA for *LH* and 18 DAA for *lh-2*; See Table A.1).

Sucrose is the principal sugar that is transported from the vascular tissues to the sink organs and between cells in pea (Denyer and Smith, 1992). Sucrose enters the seed coat through the phloem of the vascular bundle and is unloaded symplastically into the ground parenchyma and chlorenchyma cells of the pea seed coat (Van Dongen et al., 2003). Sucrose has a number fates within the seed coat cells of the ground parenchyma and chlorenchyma layers. Incorporation of ^{14}C-labelled sucrose into isolated pea fruits (via the cut petiole of the nearest leaf) resulted in accumulation of ^{14}C first in the seed coat and then in the embryo of the seed. Sucrose, starch and amino acids were the main ^{14}C-labelled compounds in the seed coat, confirming that part of sucrose unloaded into the seed coat is metabolized within the

seed coat for starch synthesis and amino acid metabolism (amino acids coming into the seed coat through the phloem are processed primarily to produce new amino acids including alanine, glutamine and threonine; Rochat and Boutin, 1992). Sucrose depletion in seed coat lowers sap osmotic pressure (pressure exerted by a dissolved substance in virtue to its molecular motion) with a corresponding loss in water and fall in hydrostatic pressure (pressure exerted by a fluid) at the seed end of the post-phloem pathway (Patrick and Offler, 2001). The hydrostatic pressure difference drives bulk flow of water and dissolved nutrients through the phloem from source to sink and the bulk flow volume imported into seed is mainly determined by the hydrostatic pressure created at the seed-end of the phloem pathway (Patrick and Offler, 2001). Hence higher rate of sucrose depletion in the filial tissues promotes higher amount of nutrient release from the phloem into the seed coat (Patrick and Offler, 2001). Therefore the demand for sucrose in the seed coat is communicated as a turgor signal which promotes nutrients unloading from the phloem into the seed coat.

Earlier in seed development, when the seed coat is the main sink tissue of the developing seed, sucrose is converted to starch in plastids of the chlorenchyma and ground parenchyma cells of the seed coat to maintain a net flow of sucrose into the seed from source tissues (Rochat and Boutin, 1992). Consistently, from 8 to 12 DAA, high levels of starch were observed in the seed coat (see *LH*, Figs. 3.6A and 3.7C). When the embryo fully contacts the seed coat (14 DAA for *LH*), the embryo has become the main sink tissue, and the starch is mobilized from the seed coat to the embryo, where the embryo maintains the gradient favoring sucrose flow from source tissues into the seed by converting sucrose to starch *in situ*.

Similar levels of sucrose and lower levels of starch (from 8 to 14 DAA) observed in seed coats of *lh-2* compared to *LH* shows that the process of conversion of sucrose into starch has been affected in *lh-2* seed coat and this is most likely a reflection of the reduced growth of *lh-2* seeds compared to that of *LH*. Reduced seed growth would decrease the amount of sucrose and glucose imported into the seed coat resulting in less substrate to be converted to starch in the seed coats of *lh-2* compared to that of *LH*.

Results from fluorescent symplast tracer HPTS (8-hydroxypyrene-1,3,6-trisulfonic) experiment suggests that sucrose in the ground parenchyma and chlorenchyma cells moves symplastically cell to cell through plasmodesmata toward, but has minimal symplastic transport into, the branched parenchyma cells in pea (Van Dongen et al., 2003). Sucrose is then transferred to the apoplast of seed coat cells (Weber et al.,1997). Weber et al. (1997) proposed that in *Vicia faba*, CWI is specifically expressed in the thin-walled parenchyma

layer (homologous to the branched parenchyma cells of pea seed coat; Van Dongen et al., 2003) during the pre-storage phase of seed development. Furthermore, Weber et al., (1997) proposed that the developmentally regulated degradation of this layer (with loss of CWI activity) initiates the embryo storage phase as this switches the surrounding environment of embryo from high to low ratios of glucose to sucrose. A transition from high to low ratios of glucose to sucrose was observed in the liquid endosperm of *LH* between 10 to 12 DAA (Fig. 3.16C). The transition of the seed apoplastic solute/endosperm from high to low ratios of glucose to sucrose was delayed in *lh-2* by four days compared to that of endosperm of *LH*. Therefore it is most likely that delayed transition of endosperm from high to low ratios of glucose to sucrose delayed the initiation of the storage phase of the *lh-2* embryo compared to *LH*.

The epidermal cells of the cotyledon play a key role in up-take of sugars and other nutrients from the endospermal space for growth and storage in parenchyma cells of the cotyledons during the seed development (Tegeder et al., 1999). During the storage phase of cotyledon development, cotyledonary epidermal transfer cells function mainly in sucrose up-take through Sucrose/H+ symporters encoded by *PsSUT1* in pea (Tegeder et al., 1999). Imported sucrose moves from cotyledonary epidermal cells to the storage parenchyma cells through the symplastic pathway as the movement of symplastic tracer 5-(6)-carboxyfluorescein suggests that the symplastic pathway connects the epidermal transfer cells to the cotyledonary storage parenchyma cells (Tegeder et al., 1999). Sucrose is then converted to starch during the storage phase of cotyledon development by the coordinate regulation of sucrose synthase (Weber et al., 1997) and starch synthesizing enzymes including ADP-glucose pyrophosphorylase (Denyer and Smith, 1992).

Higher levels of sucrose and lower levels of starch observed in the cotyledonary storage parenchyma cells in *lh-2* from 8 to 20 DAA (Figs. 3.12 A and C) most likely are a reflection of the reduced growth rate (due to lower bioactive GA levels) of *lh-2* seeds (seed coat and embryo; Fig. 3.1 B and C) reducing the sink strength of the seed, compared to that of *LH* seeds (Fig. 3.1 B and C).

4.2 Effect of *lh-1* mutation on growth and carbohydrate partitioning in the seed

The *lh-1* mutation reduced the bioactive GA_1 level in young developing (7 DAA) seeds by 54% in contrast to *lh-2* mutation which reduce the bioactive GA_1 levels in young

developing pea seeds by 84 % (7 DAA; Swain et al., 1993). These authors reported that the *lh-1* mutation had minor effects on seed growth compared to *LH*. Furthermore, Swain et al. (1997) found that when *lh-2* plants were fertilized with *lh-1* pollen the resultant *lh-2 lh-1* embryos were larger (fresh weight) from 16 to 24 DAP (days after pollination; pollination occurs 24-36 hours prior to anthesis in pea; Cooper, 1938) compared to that of the *lh-2 lh-2* embryos resulting from self-fertilization of *lh-2* plants, but smaller than *lh-2 LH* embryos resulting from *lh-2* plants fertilized with *LH* pollen. Embryo weight was also lower in *lh-1 lh-1* embryos compared to *lh-1 LH* embryos (resulting from *lh-1* plants fertilized with *LH* pollen) from 16-19 DAP (Swain et al., 1997). Swain et al. (1997) concluded that both the *lh-1* and *lh-2* mutations reduce embryo growth around the contact point stage of development; however, the effect of *lh-1* on embryo and seed growth is transient, as *LH* and *lh-1* seed weight at maturity were similar (in contrast to that of *lh-2*). The results of this study are in agreement with the observations and general conclusions reported by Swain et al. (1993). In this study, *lh-1* had relatively minor effects on seed coat and embryo growth (from 8 to 20 DAA) compared to *LH*, in contrast to that observed for *lh-2* (Fig. 3.1 A-C). However, the *lh-1* mutation reduced seed coat fresh weight growth (8 and 10 DAA; Fig. 3.1B) and ground parenchyma cell expansion (at 8 DAA; Fig. 3.2D), and embryo fresh weight growth (14 to 20 DAA) during the rapid development phase of these tissues compared to *LH* (Fig. 3.1B). Hypodermal layer differentiation into 'hourglass-shaped cells in the seed coat and the time to reach equivalent seed coat and embryo size in the seeds (14 DAA) were similar in *lh-1* and *LH* (Fig. 3.3A and B), suggesting the GA_1 deficiency in *lh-1* seeds minimally affects seed development during the period studied.

At 8 and 10 DAA, reduction in seed coat fresh weight growth in *lh-1* was associated with reduced seed coat starch and sucrose accumulation compared to that of *LH* (Fig. 3.7A and C). Furthermore, from 14 to 20 DAA, reduced embryo growth was associated with reduced starch accumulation and elevated sucrose levels in cotyledons of *lh-1* compared to that of *LH* (Fig. 3.12 A and C). These data suggest that reduced bioactive GA levels as the result of the *lh-1* mutation reduced seed coat growth, and as a result reduced import of sucrose into the seed coat during early developmental stages (8-10 DAA). Consistently, less sucrose availability in the *lh-1* seed coats (8-10 DAA) resulted in lower starch accumulation in the seed coat cells at this stage. As the embryo entered into the storage phase of development (by 14 DAA), the lag in embryo growth in *lh-1,* as the result of lower bioactive GA levels, also likely leads to reduced starch accumulation and elevated sucrose levels in the

lh-1 cotyledons (as the sucrose taken up by the cotyledons is not rapidly converted to starch) compared to those of *LH*.

4.3 Effect of *ls-1* mutation on growth and carbohydrate partitioning in the seed

Plants with the *ls-1* mutation produced lower levels of GA_1, GA_8, GA_{20} and GA_{29} in 5 to 9 DAA developing seeds (Swain et al., 1995). Swain et al. (1995) made crosses that created embryos with *LS ls-1* (*ls-1*♀ x *LH*♂) and *ls-1 ls-1* (self-fertilized; *ls-1*♀ x *ls-1*♂) genotypes with an *ls-1 ls-1* seed coat genotype. These authors found reduced GA_1, GA_8, GA_{20} and GA_{29} levels in 6 DAA seeds developing on *ls-1* plants, regardless of pollen genotype. The authors concluded that the reduced GA levels in young developing *ls-1* seeds from self-pollinated *ls-1* plants compared to *LS* are due to reduced levels of these GAs in the seed coat, but not the embryo. Swain et al., 1995 observed that the average seed fresh weight of seeds obtained from self-pollinated *ls-1* plants at 5, 7 and 9 DAA, were, in general, similar to those of the wild-type *LS* line. In this study, the *ls-1* mutation reduced whole seed growth at 8 and 12 to 18 DAA compared to *LS* (WT-107; Fig. 3.1D). The reduction in whole seed growth in *ls-1* at these stages reflects reduced seed coat growth at 8 and 10 DAA, and embryo growth from 14 to 18 DAA (Fig. 3.1 E and F). Reduced seed coat cell expansion was only observed in the hypodermal and chlorenchyma layers (from 8 to 12 DAA) of *ls-1* compared to that of *LS*, concomitant with reduced seed coat growth. However, marked reduction in starch levels, with increased glucose (10 to 20 DAA) and sucrose levels (from 8 to 20 DAA) was observed in the seed coats of *ls-1* compared to that of *LS* (Fig. 3.7 D-F). Therefore, it appears that bioactive GA deficiency caused by *ls-1* mutation in the seed coat had a relatively small effect on cellular expansion and tissue growth, but a marked impact on carbohydrate partitioning in the seed coat tissues. The general trend of carbohydrate partitioning in the seed suggests that lower bioactive GA resulted in reduced import of sucrose into the seed coat, which likely lead to the reduced embryo growth observed in *ls-1* compared to that of *LS* (16 to 20 DAA; Fig. 3.1F).

4.4 Effect of *le-3* mutation on growth and carbohydrate partitioning in the seed

Swain et al., 1995 observed that le^{5839} (also known as *le-3*; MacKenzie-Hose et al., 1998) mutation slightly increases the level of bioactive GA_1 in 6 DAA seeds, compared to *LE*

seeds. These authors also detected higher levels of GA_{20} and GA_{29} in 6 DAA seeds. Based on the GA quantification data and seed fresh weight of 6 DAA seeds, Swain et al. (1995) concluded that the *le-3* mutation does not modify seed development or seed weight compared to *LE*. In agreement with the effect of *le-3* mutation on GA_1 level reported by Swain et al. (1995), a two fold increase in GA_1 level was observed in 10 DAA *le-3* seeds compared to *LE* seeds (Table 3.1). A slight reduction of whole seed growth was observed in *le-3* compared to *LE* in the present study (Fig. 3.1D). The reduction in *le-3* whole seed growth was mainly reflected in reduced seed coat growth during the earlier part of the developmental phase (8 ,10 and 14 DAA) and in reduced the embryo growth from 14 to 20 DAA (Fig. 3.1E and F). The *le-3* mutation had minimal effect on seed coat cell expansion when compared to the *LE* (Fig. 3.2F-J). However, marked reduction in starch levels (14 to 16 DAA; Fig. 3.7F), with increased glucose (10 to 20 DAA) levels (from 8 to 20 DAA) were observed in the seed coats of *le-3* compared to those of *LE* (Fig. 3.7 D-F). It has been shown that post-bloom application of GA_3 to seed less grape (Sultana) increases hexose content and soluble invertase activity throughout the growing period, compared to the GA_3 un-treated control. Particularly GA_3 application increased hexose content by 102% and invertase activity by 60% at ripening and these effects were positively correlated with the berry size (Pérez and Gómez, 2000). It is possible that elevated GA_1 level in *le-3* seeds increased soluble invertase activity which led to higher glucose levels in *le-3* seed coats compared to that of *LE*.

Higher levels of sucrose and lower levels of starch observed in the cotyledonary storage parenchyma cells in *le-3* from 14 to 20 DAA (Figs. 3.12 D and F) most likely are a reflection of the reduced growth rate (due to lower bioactive GA levels) of the *le-3* embryo reducing the sink strength of the seed, compared to that of *LE* seeds (Fig. 3.1F). As a result, the content of starch accumulated in the embryo is reduced.

4.5 Effect of *PsGA3ox1* overexpression on growth and carbohydrate partitioning in the seed

Overexpression of *PsGA3ox1*, which encodes a GA 3β-hydroxylase which converts GA_{20} to bioactive GA_1, increased the flow through to bioactive GA_1 (in rapidly developing seeds; Table 3.1), and embryo growth (12 to 20 DAA) compared to the control (C1; Fig. 3.1I), consistent with the larger seed size observed at maturity for TG1 by Wickramarathna (2009).

With respect to tissue specificity, *PsGA3ox1* overexpression increased cell expansion during the rapid phase of tissue growth in all seed coat cell layers during the period studied (8-20 DAA; Fig. 3.2K-O). Overexpression of *PsGA3ox1* also advanced seed coat development. The hypodermal cells of the seed coat of TG1 differentiated into hourglass shape in TG1 four days earlier than those of its control C1 (Fig. 3.4A-D). Concurrent with enhanced seed coat cell expansion, cotyledonary storage parenchyma cell expansion was also enhanced in TG1 (at 12, 16 and 18 DAA) compared to those of C1 (Fig. 3.5 B) Overall, these data suggest that elevated levels of bioactive GA due to *PsGA3ox1* overexpression enhanced the growth and cellular expansion in both the seed coat and cotyledons during the mid-phase of seed development. The amount of imported sucrose from the phloem into seed coat remained higher (at 10, 12, 16 and 18 DAA; Fig. 3.7G) in TG1 compared to C1 as the more rapidly growing TG1 seeds have a higher demand for nutrients. As a result, higher levels of starch (at 10 DAA; Fig. 3.7I) and glucose (8-20 DAA; Fig. 3.7H) were observed in TG1 seed coat compared to those of C1. It is possible that elevated levels of GA_1 in TG1 seed coats may have stimulated seed coat soluble invertase activity resulting in higher glucose levels in TG1 seed coats compared to the C1 control (as previously described for *le-3* seed coats).

Overall, it is likely that the enhanced seed growth as the result of *PsGA3ox1* overexpression increased the seed sink capacity in TG1 compared to that in C1.

Developing pea seeds synthesize and store large amounts of proteins within the vacuolar system in the cotyledon cells of the embryo (Craig, 1986). Protein accumulation in TG1 and C1 cotyledons was observed after reaching the contact point (at 14 DAA). No consistent trend in protein content on a mg per g dry weight basis was observed between TG1 and its control (C1) from 14 to 20 DAA (Fig. 3.18A). However, protein content per cotyledon pair was consistently higher in the cotyledons of TG1 (16 to 20 DAA) compared to that in C1 (Fig. 3.18B), suggesting that higher protein levels per seed for TG1 is a result of larger embryo size.

4.6 Summary and working hypothesis models

Two models are proposed from the data obtained in this thesis to gain an understanding of the roles of GAs in growth, cell expansion and carbohydrate partitioning in developing pea seeds. The first model (Fig. 4.1) summarizes the data obtained from pea plants that overexpress *PsGA3ox1* leading to increased levels of bioactive GA in developing

seed tissues. The second model (Fig. 4.2) summarizes the data obtained from pea plants that produced lower levels of bioactive GAs due to mutations in specific GA biosynthesis genes.

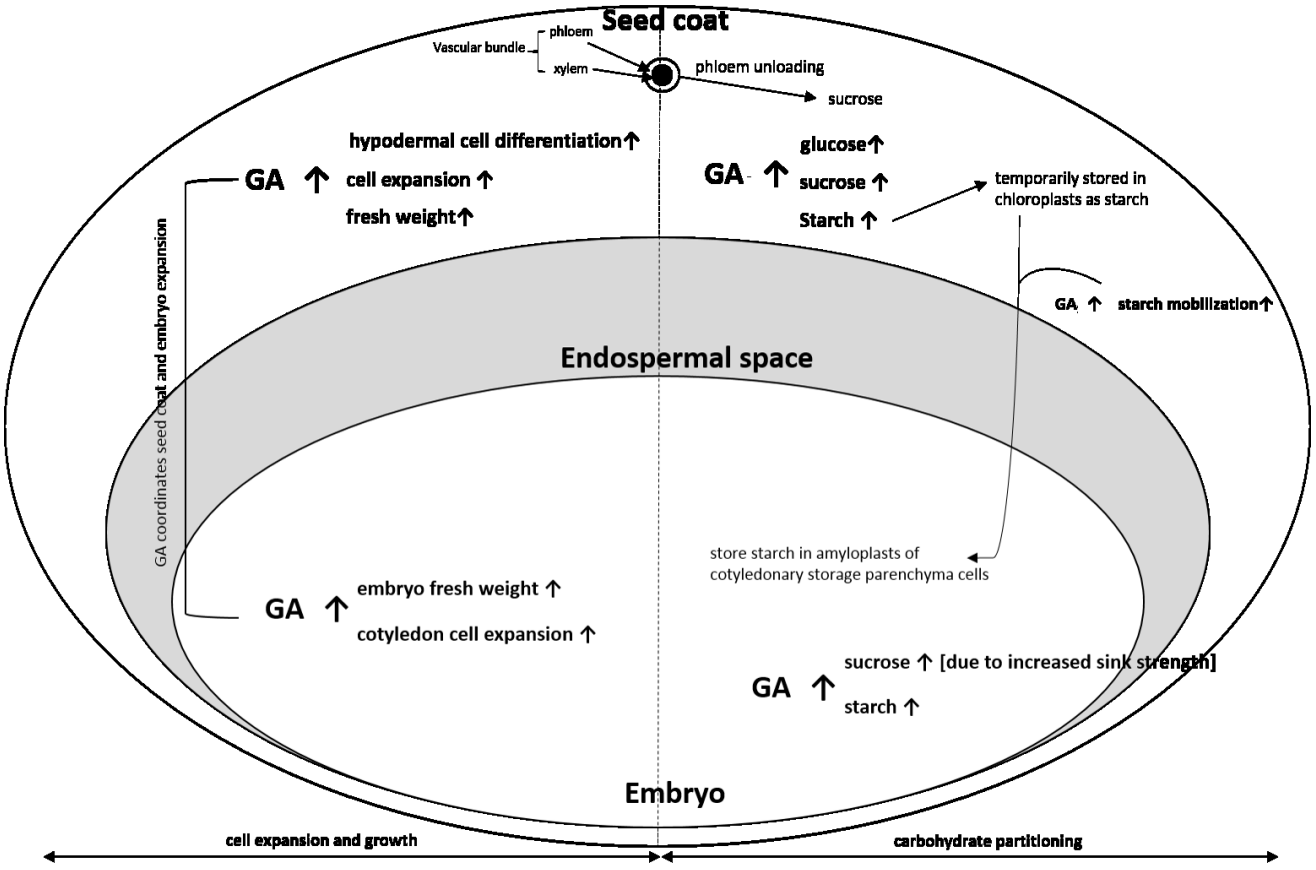

Figure 4.1: Effects of *PsGA3ox1* overexpression on growth, cell expansion and carbohydrate partitioning in developing pea seeds. Expression of *PsGA3ox1* increases the flow through bioactive GA_1, which, in turn, enhances seed coat and embryo cell expansion. GA-enhanced cell expansion in the seeds that overexpress *PsGA3ox1* leads to increased demand for energy to fuel the growth of the expanded cells. Under conditions of high energy demand, higher levels of phloem-derived sucrose are downloaded into the seed coat increasing starch, sucrose and glucose levels in this tissue prior to the contact point developmental phase. Concomitantly, greater cell expansion rates in the developing embryos of the *PsGA3ox1* overexpressor line also facilitates down-loading of sucrose into the seed coat to meet the energy demand of this tissue. This leads to higher sucrose levels in the embryo which can then be incorporated into starch in the cotyledon storage parenchyma cells.

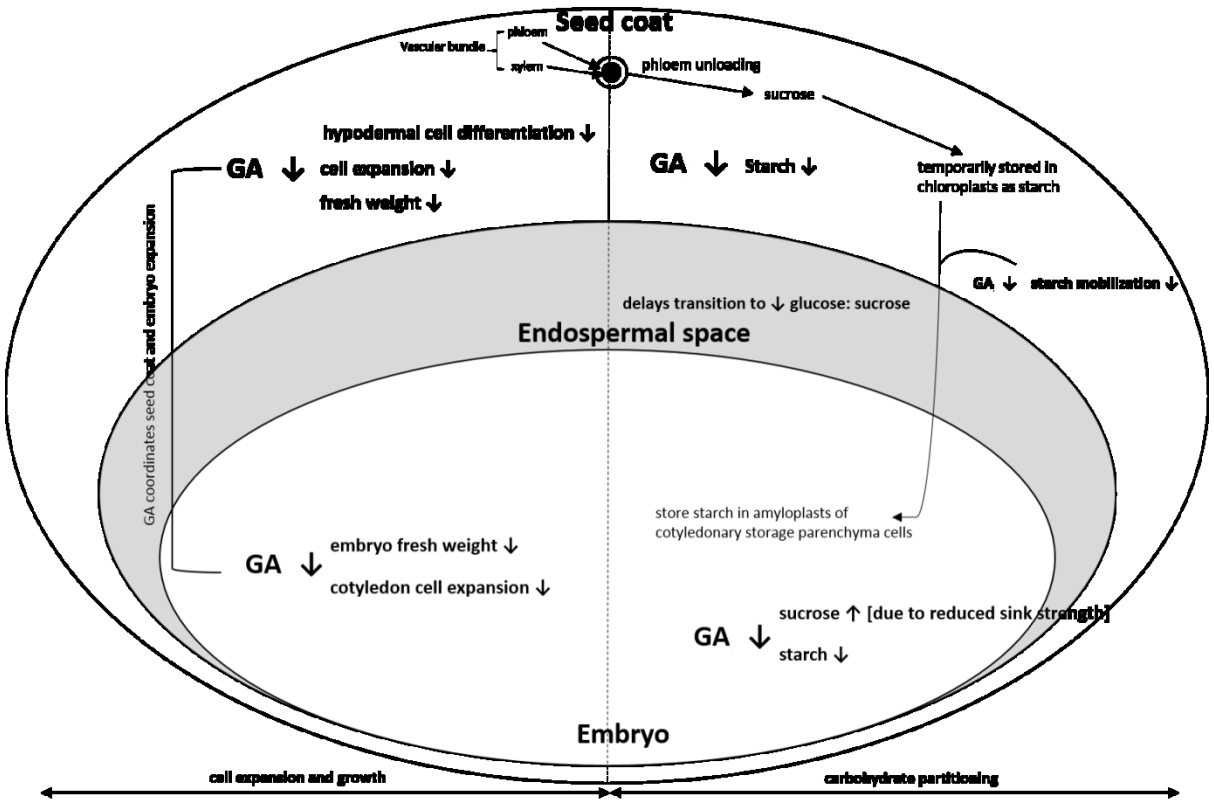

Figure 4.2: Effects of the GA biosynthesis mutation (*lh-2*) on growth, cell expansion and carbohydrate partitioning in developing pea seeds. Markedly lower bioactive GA levels (*lh-2* mutant) reduces cell expansion and growth of the seed coat and embryo during the mid-phase of seed development (8-20 DAA). As a result, seed coat and embryo development is delayed and the energy demand for the seed is reduced. The lower demand for sucrose by the *lh-2* seed is reflected in lower starch accumulation in the seed coat prior to contact point (14 DAA), and a reduced rate of sucrose utilization for starch synthesis in the embryo.

5. CONCLUSIONS

The growth and histology data of seed tissues obtained from plants that vary in their GA levels due to differences in their genetic backgrounds have led to the identification of GA-mediated processes that are involved seed growth and development in pea. Additionally, the role of GA as a regulator of carbohydrate partitioning in different seed tissues during seed development has been established. Together, these data show the link between GA-mediated growth responses and carbon partitioning in developing pea seeds, and suggest several possible directions for future research.

5.1 GA as a sink strength determinant

Carbohydrate distribution profiles, growth and histology data gathered from plants with varying GA levels (GA biosynthesis mutants and GA overexpressor lines) have shown the potential regulatory role of GA in seed development that may promote tissue development and cellular differentiation processes of developing seeds. Evidence presented here suggest that the level of bioactive GA_1 in developing seed is a determinant of seed coat and cotyledonary storage parenchyma cell expansion which has a strong impact on overall growth of the seed. However, it should be noted the effects of GAs on the cellular expansion and differentiation could be seen in high resolution under severe GA deficient or GA over-accumulation conditions in developing pea seeds. Furthermore, GA induced differentiation of cells in the hypodermal layer as well as the seed coat and cotyledon cell expansion during the phase of rapid growth of seed suggest the involvement of GAs at specific stages of the development. Since GA_1 is generally considered to enhance growth responses in the tissue where it is synthesized (Yamaguchi, 2008), it is highly likely that tissue-specific regulation of GA biosynthesis occurs to bring about unique developmental changes within each tissue of the seed at specific stages of the development. To investigate this possibility further, the expression pattern of GA biosynthesis genes within different cell layers of seed tissues needs to be analyzed; different cell layers of seed coats and cotyledons can be separated using "Laser Capture Microdissection" technique and transcript abundance of GA biosynthesis genes could be studied in each cell layer at different stages of seed development. Further, targeted metabolome profiling of each of the cell layers of seed coat and cotyledon tissues would provide a new insight about GA mediated metabolic switches that are operated in different tissue layers of developing seed.

The data presented here also suggest a role for GA as a sink strength determinant, which controls the amount of photoasssimilate imported into the seed during the developmental process. Elevated levels of bioactive GA enhance the seed coat cell expansion and thereby seed coat growth increasing the energy demand for the seed coat. Under this condition, higher level of phloem derived sucrose is imported into the seed coat. GA also mediates the growth and cell expansion of the embryo by increasing its size in coordination with that of the seed coat during seed development. Therefore, bigger the size of the embryo, the requirement of sucrose influx from the seed coat into the cotyledon is higher in order to meet the energy demand of the growing seed. Higher amount of sucrose imported into the embryo is reflected by the higher accumulation of starch in the cotyledon during its development.

5.2 Speculative roles of GA in regulating the carbohydrate status in developing pea seeds

It is most likely that GA-induced growth of cotyledon and seed coat also accelerates starch mobilization from the seed coat to the developing embryo as this process was enhanced in TG1 seeds that biosynthesize elevated levels of bioactive GA and delayed in *lh-2* seeds that have lower levels of bioactive GA with respect to their control backgrounds. This shows that GA indirectly controls the carbon partitioning between seed coat and embryo by controlling the growth of different tissues of seed during the development. However the direct involvement of GA in controlling this process cannot be excluded as it has been observed that GA_1 and/or GA_3 are localized around starch grains of seed coat cells in *Pharbitis nill* (Nakayama et al., 2002). Nakayama et al. (2002) also observed the localization of GA-inducible α-amylase transcripts (*PnAmy1*) to the starch grains of seed coat cells in *Pharbitis nill.* Therefore, it is highly likely that GA_1 present in pea seed may induce GA-inducible α-amylase starch grain digestion in the seed coat as part of the mechanism that is involved in starch mobilization from the seed coat to embryo during seed development. The examination of α-amylase activity in pea seed system of plants with different genetic backgrounds presented in our study would determine whether GA induces the starch grain digestion through α-amylase in seed coat.

Markedly elevated levels of glucose observed in TG1 seed coat could also be related to the increased activity of soluble invertase (SI) in the seed coat as it has been shown that post-bloom application of GA_3 to seed less “Sultana” grape increases hexose content and

soluble invertase activity throughout the growing period, compared to the GA_3 un-treated control (Pérez and Gómez, 2000).

Therefore, it is possible that GA overproduction in TG1 results in an increase in solute potential of the post-sieve symplastic pathway due to the higher content of glucose in the seed coat cells. Higher solute potential in the symplastic pathway promotes osmosis into seed coat cells increasing the hydrostatic pressure. This activates higher amount of nutrient release from the phloem into the post-phloem symplasmic route as bulk flow volume imported into seed is mainly determined by the hydrostatic pressure created at the seed-end of the phloem pathway. Examining the soluble invertase activity in pea seed system under *PsGA3ox1* overexpression conditions with respect to control genetic background should provide further insight about this possibility.

Figure 5.1 gives an overview about roles of GA in regulating tissue growth and carbohydrate partitioning in developing seeds. This model is proposed based on the results of this study and current knowledge on sugar metabolism in legume seed system. Possible direct involvement of GAs in regulating the carbohydrate states of seed tissues are also shown here.

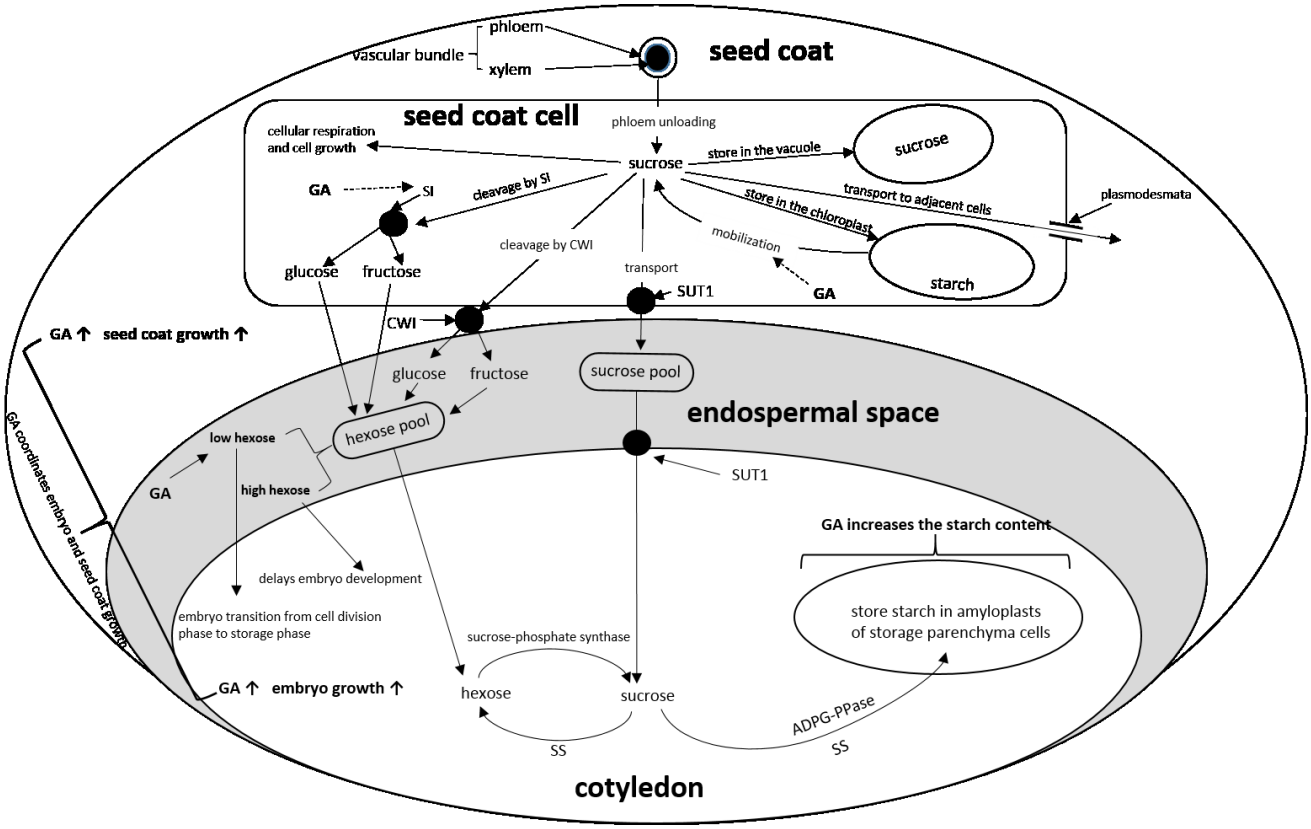

Fig. 5.1: Roles of GA in regulating tissue growth and carbohydrate partitioning in developing seeds. Arrows with broken lines show the speculative roles of GA in pea seed system. GA promotes the cellular expansion of seed coat and cotyledon cells and coordinates embryo and seed coat growth during the seed development. Sucrose is unloaded from the phloem symplastically into the ground parenchyma or chlorenchyma cells of the seed coat (Van Dongen et al., 2003). During the early phase of seed development, sucrose moves symplastically from cell to cell, through plasmodesmata toward the branched parenchyma cells and is further cleaved by cell wall invertase (CWI) in the apoplast (Murray, 1987). Direct transport of sucrose from the symplast of seed coat into the apoplast of the endosperm can also be occurred through sucrose transporters, SUT1 (Ayre, 2011). Within the seed coat cells, sucrose can be utilized for cellular respiration and cell growth related activities or sucrose is converted into glucose and fructose by soluble invertase (SI) or stored in the vacuole of the seed coat cells as soluble sucrose (Borisjuk et al., 2004). SI activity could be enhanced by GA which may lead to increase the levels seed coat glucose during the development. In the seed coat, sucrose can be converted into starch by the activities of sucrose synthase (SS) and ADP glucose pyrophosphorylase (ADPG-PPase; Webber et al., 1997) and is further temporarily stored in the chloroplasts of seed coat cells (Rochat and Boutin, 1992). Stored starch in the seed coat is re-converted into sucrose at later stages of seed development to be mobilized into the developing embryo (Rochat and Boutin, 1992). GA_1 presence in pea seed may induce GA-inducible α-amylase starch grain digestion in seed coat as

part of the mechanism that is involved in starch mobilization from the seed coat to embryo during seed development. Hexose to sucrose ratio in the surrounding environment of the embryo determines the developmental fate of the embryo. Developmentally regulated degradation of the branched parenchyma layer with the loss of CWI activity initiates the storage phase of the embryo through a switch from high to low ratios of hexose to sucrose in the endospermal space (Webber et al., 1997). Elevated levels of GA also play a role in decreasing the endosperm glucose level in pea which switches the endosperm from high to low ratio of hexose to sucrose and under this condition, embryo transition occurs from growth phase to storage phase. The sucrose metabolism in the cotyledons is controlled by synthesis and break down of sucrose involving sucrose-phosphate synthase and sucrose synthase, respectively (Weber et al., 1997). Sucrose is transported into cotyledon through SUT1 located in the epidermal cells of the cotyledon (Tegeder et al., 1999). Sucrose-phosphate synthase resynthesizes sucrose from imported hexoses whereas sucrose synthase breaks down sucrose to provide UDPglucose for starch synthesis (Preiss, 1992). ADPG-PPase further converts UDPglucose into ADPglucose, which serve as primers for amylose chain (Preiss, 1992). Synthesized starch granules are then stored in amyloplasts of cotyledonary storage parenchyma cells. GA plays a role in increasing the content of starch stored in cotyledons possibly through enhancing cotyledon growth.

LITERATURE CITED

A**it-Ali T, Swain SM, Reid JB, Sun T-P, Kamiya Y** (1997) The *LS* locus of pea encodes the gibberellin biosynthesis enzyme *ent*- kaurene synthase A. Plant J **11:** 443–454

Ayele BT, Ozga JA, Reinecke DM (2006) Regulation of GA biosynthesis genes during germination and young seedling growth of pea (*Pisum sativum* L.). J Plant Growth Regul **25:** 219-232

Borisjuk L, Rolletschek H, Radchuk R, Weschke W, Wobus U, Weber H (2004) Seed development and differentiation: a role for metabolic regulation. Plant Biol **6:** 375-386

Cooper DC (1938) Embryology of *Pisum sativum*. Bot Gaz **100:** 123-132

Craig S (1986) Fixation of a vacuole-associated network of channels in protein-storing pea cotyledon cells. Protoplasma **135:** 67-70

Cross BE, Grove JF, MacMillan J, Mulholland TPC (1956) Gibberellic acid, Part IV. The structures of gibberic and allogibberic acids and possible structures for gibberellic acid. Chem Ind (Lond) 954-955

Davidson SE, Elliott RC, Helliwell CA, Poole AT, Reid JB (2003) The pea gene *NA* encodes *ent*-kaurenoic acid oxidase. Plant Physiol **131:** 335-344

Davidson SE, Smith JJ, Helliwell CA, Poole AT, Reid JB (2004) The Pea gene *LH* encodes *ent*-kaurene oxidase. Plant Physiol **134:** 1123-1134

Denyer K, Smith AM (1992) The purification and characterisation of the two forms of soluble starch synthase from developing pea embryos. Planta **186**: 609-617

Depuydt S, Hardtke CS (2011) Hormone signalling crosstalk in plant growth regulation. Curr Biol **21:** 365-373

Ferraro K, Jin AL, Nguyen T-D, Reinecke DM, Ozga JA, Ro D-K (2014) Characterization of proanthocyanidin metabolism in pea (*Pisum sativum*) seeds. BMC Plant Biol **14:** 238

García-Martínez JL, López-Diaz I, Sánchez-Beltrán MJ, Phillips AL, Ward DA, Gaskin P, Hedden P (1997) Isolation and transcript analysis of gibberellin 20-oxidase genes in pea and bean in relation to fruit development. Plant Mol Biol **33:** 1073–1084

Garcia-Martinez JL, Sponsel VM, Gaskin P (1987) Gibberellins in developing fruits of *Pisum sativum* cv. Alaska: studies on their role in pod growth and seed development. Planta **170**: 130–137

Hardham AR (1976) Structural aspects of the pathways of nutrient flow to the developing embryo and cotyledons of *Pisum sativum* L. Aust J Bot **24:** 711–721

Hedden P (2012) Gibberellin Biosynthesis. eLS.John Wiley & Sons, Ltd, http://www.els.net/WileyCDA/ElsArticle/refId-a0023720.html

Hedden P, Kamiya Y (1997) Gibberellin biosynthesis: enzymes, genes and their regulation. Annu Rev Plant Physiol Plant Mol Biol **48:** 431–460

Hedden P, Phillips AL (2000) Gibberellin metabolism: new insights revealed by the genes. Trends Plant Sci **5:** 523-530

Helliwell CA, Sullivan JA, Mould RM, Gray JC, Peacock WJ, Dennis ES (2001) A plastid envelop location of *Arabidopsis ent*-kaurene oxidase links the plastid and endoplasmic reticulum steps of the gibberellin biosynthesis pathway. Plant J **28:** 201-208

Kasahara H, Hanada A, Kuzuyama T, Takagi M, Kamiya Y, Yamaguchi S (2002) Contribution of the melvonate and methylerythritol phosphate pathways to the biosynthesis of Gibberellins in *Arabidopsis*. J of Biol Chem **277:** 45188-45194

Lester DR, Ross JJ, Ait-Ali T, Martin DN, Reid JB (1996) A gibberellin 20-oxidase cDNA (accession no. U58830) from pea seed (PGR 96-050). Plant Physiol **111:** 1353

Lester DR, Ross JJ, Davies PJ, Reid JB (1997) Mendel's stem length gene (*Le*) encodes a gibberellin 3β-hydroxylase. Plant Cell **9:** 1435-1443

Lester DR, Ross JJ, Smith JJ, Elliott RC, Reid JB (1999) Gibberellin 2-oxidation and the *SLN* gene of *Pisum sativum*. Plant J **19:** 65-73

MacKenzie-Hose AK, Ross JJ, Davies NW, Swain SM (1998) Expression of gibberellin mutations in fruits of *Pisum sativum* L. Planta **204:** 397-403

Magome H, Nomura T, Hanada A,Takeda-Kamiya N, Ohnishi T, Shinma Y, Katsumata T, Kawaide H, Kamiya Y, Yamaguchi S (2013) *CYP714B1* and *CYP714B2* encode gibberellin 13-oxidases that reduce gibberellin activity in rice. Proc Natl Acad Sci USA **110:** 1947-1952

Marinos NG (1970) Embryogenesis of the pea (*Pisum sativum*): the cytological environment of the developing embryo. Protoplasma **70:** 261–279

Martin DN, Proebsting WM, Hedden P (1997) Mendel's dwarfing gene: cDNAs from the *Le* alleles and function of the expressed proteins. Proc Natl Acad Sci USA **94:** 8907-8911

Martin DN, Proebsting WM, Hedden P (1999) The *SLENDER* gene of pea encodes a gibberellin 2-oxidase. Plant Physiol **121:** 775-781

Martin DN, Proebsting WM, Parks TD, Dougherty WG, Lange T, Lewis MJ, Gaskin P, Hedden P (1996) Feed-back regulation of gibberellin biosynthesis and gene expression in *Pisum sativum* L. Planta **200:** 159–166

Melkus G, Rolletschek H, Radchuk R, Fuchs J, Rutten T, Wobus U, Altmann T, Jakob P, Borisjuk L (2009) The metabolic role of legume endosperm: a noninvasive imaging study. Plant Physiol **151:** 1139-1154

Murray DR (1987) Nutritive role of seedcoats in developing legume seeds. Am J Bot **74:** 1122-1137

Nadeau CD, Ozga JA, Kurepin LV, Jin A, Pharis RP, Reinecke DM (2011) Tissue-specific regulation of gibberellin biosynthesis in developing pea seeds. Plant Physiol **156:** 897-912

Nakayama A, Park S, Zheng-Jun X, Nakajima M, Yamaguchi I (2002) Immunohistochemistry of active gibberellins and gibberellin-inducible α-amylase in developing seeds of morning glory. Plant Physiol **129:** 1045–1053

Ozga JA, van Huizen R, Reinecke DM (2002) Hormonal and seed-specific regulation of pea fruit growth. Plant Physiol **128:** 1379-1389

Patrick JW, Offler CE (2001) Compartmentation of transport and transfer events in developing seeds. J Exp Bot **356:** 551-564

Pérez FJ, Gómez M (2000) Possible role of soluble invertase in the gibberellic acid berry-sizing effect in sultana grape. Plant growth Regul **30:** 111-116

Preiss J (1982) Regulation of the biosynthesis and degradation of starch. Annu Rev Plant Physiol **33:** 431-454

Radley M (1956) Occurrence of substances similar to gibberellic acid in higher plants. Nature **178:** 1070-1071

Reid JB (1986) Gibberellin mutants. *In* P King, A Blonstein, eds, Plant Gene Pesearch, a Genetic Approach to Plant Biochemistry, Vol 3, Springer-Vetlag, New Your, pp 1-34

Reid JB, Potts WC (1986) Internode length in *Pisum*. Two further mutants, *lh* and *ls*, with reduced gibberellin synthesis, and a gibberellin insensitive mutant, *lk*. Plant Physiol **66:** 417–426

Reid JB, Ross JJ (1993) A mutant based approach, using *Pisum sativum*, to understand plant growth. Int J Plant Sci **154:** 22-34

Reinecke DM, Wickramarathna AD, Ozga JA, Kurepin LV, Jin AL, Good AG, Pharis RP (2013) *Gibberellin 3-oxidase* gene expression patterns influence gibberellin biosynthesis, growth, and development in Pea. Plant Physiol **163:** 929-945

Rochat C, Boutin JP (1992) Temporary storage compounds and sucrose-starch metabolism in seed coats during pea seed development (*Pisum sativum*). Plant Physiol **85:** 567–572

Ross JJ, Davidson SE, Wolbang CM, Bayly-Stark E, Smith JJ, Reid JB (2003) Developmental regulation of the gibberellin pathway in pea shoots. Funct Plant Biol **30:** 83–89

Ross JJ, Reid JB (1991) Internode length in *Pisum*: *le*^{5839} is a less severe allele than Mendel's *le*. Pisum Genet **23:** 29-34

Santes CM, Hedden P, Sponsel VM, Reid JB, García-Martínez JL (1993) Expression of the *le* mutation in young ovaries of *Pisum sativum* and its effect on fruit development. Plant Physiol **101:** 759-764

Smith AM, Denyer K, Martin C (1997) The synthesis of the starch granule. Annu Rev Plant Physiol Plant Mol Biol **48:** 67–87

Sponsel VM, Hedden P (2010) Gibberellin biosynthesis and inactivation. *In* PJ Davies, Peter J, eds, Plant Hormones: Their Nature, Occurrence, and Functions, Kluwer academic publishers, Dordrecht/ Boston/ London, pp 63-94

Swain SM, Reid JB (1992) Internode length in *Pisum*: a new allele at the *Lh* locus. Physiol Plant **86:** 124–130

Swain SM, Reid JB, Kamiya Y (1997) Gibberellins are required for embryo growth and seed development in pea. Plant J **12:**1329–1338

Swain SM, Reid JB, Ross JJ (1993) Seed development in *Pisum*: the *lh*^{i} allele reduces gibberellin levels in developing seeds, and increases seed abortion. Planta **191:** 482-488

Swain SM, Ross JJ, Reid JB, Kamiya Y (1995) Gibberellins and pea seed development: expression of the *lh*^{i}, *ls* and *le*^{5839}mutations. Planta **195:** 426–433

Tegeder M, Wang X-D, Frommer WB, Offler CE, Patrick JW (1999) Sucrose transport into developing seeds of *Pisum sativum* L. Plant J **18:** 151–161

Ueguchi-Tanaka M, Nakajima M, Motoyuki MA, Matsuoka M (2007) Gibberellin receptor and its role in gibberellin signaling in plants. Annu Rev Plant Biol **58:** 183–198

Van Dongen JT, Ammerlaan AM, Wouterlood M, van Aelst AC, Borstlap AC (2003) Structure of the developing pea seed coat and the post-phloem transport pathway of nutrients. Ann Bot (Lond) **91:** 729–737

Wang TL, Hedley CL (1993) Genetic and developmental analysis of the seed. *In* R Casey, DR Davies, eds, Peas: Genetics, Molecular Biology and Biochemistry. CAB International, Cambridge, UK, pp 83–120

Weber H, Borisjuk L, Heim U, Buchner P, Wobus U (1995) Seed coat-associated invertases of fava bean control both unloading and storage functions: cloning of cDNAs and cell type-specific expression. Plant Cell **7:** 1835–1846

Weber H, Borisjuk L, Wobus U (1997) Sugar import and metabolism during seed development. Trends Plant Sci **2:** 169–174

Weston DE, Elliott RC, Lester DR, Rameau C, Reid JB, Murfet IC, Ross JJ (2008) The pea DELLA proteins LA and CRY are important regulators of gibberellin synthesis and root growth. Plant Physiol **147:** 199–205

Wickramarathna AD, (2009) Characterization of gibberellin overexpression lines in pea. PhD thesis. University of Alberta, Edmonton, Alberta, Canada

Yamaguchi S (2008) Gibberellin metabolism and its regulation. Annu Rev Plant Biol **59:** 225-251

APPENDIX

Appendix A: Approximate time required (DAA) for seeds to reach equivalent embryo and seed coat fresh weight

Table A.1: Approximate time required (DAA) for seeds to reach equivalent embryo and seed coat fresh weight for lines WT-107, *lh-2, lh-1, ls-1, le-3*, GA overexpressor (TG1) and transgenic control (C1).

Plant line	(DAA)
WT-107	14
lh-2	20
lh-1	14
ls-1	14
le-3	14-16
TG1	14
C1 *(le-1)*	14

Appendix B: Internode length differences between GA biosynthesis mutants lines *lh-1, lh-2, ls-1* and *le-3* and their isogenic wild-type (WT-107) line, and the GA overexpressor line TG1 and its transgenic control, C1, at plant maturity

B.1 Background

This appendix contains internode lengths measured from internode 1 to 20 from GA biosynthesis mutants; *lh-1, lh-2, ls-1* and *le-3* and their wild-type, WT-107, and the GA overexpressor line TG1 and its null control, C1, at plant maturity. WT-107, *lh-1*, *lh-2, le-3* and *ls-1* plant lines were grown under greenhouse conditions (experiment started on 2012 September 26 and finished seed harvesting on 2012 November 14; 8 hours controlled dark/ 15^0C-25^0C) and TG1 transgenic and C1 control lines were grown in Conviron growth chamber (Winnipeg, Canada) using cool-white fluorescent lamps (F54/I5/835/HO high fluorescent bulbs, Phillips, Holland) 16 h-light/8 h-dark photoperiod (19°C/17°C) with an average photon flux density of 385.5 μmol m^{-2} s^{-1} (measured with a QMSS-ELEC Quantum

meter, Apogee instruments, Logan, USA). The first internode was defined as the one between the cotyledon attachment (cotyledonary node) and the first stem node. Node and internode numbering system used in this study is shown in Fig. B.1.

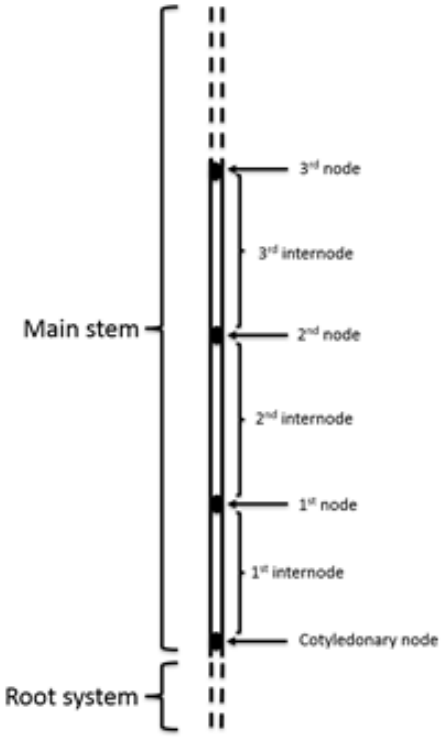

Figure B.1: Schematic representation of the node and internode numbering system used in this study.

B.2 Results

The WT-107 line produced longer internodes than *lh-1* (internodes 1 to 19) *lh-2* (internodes 1 to 17), *le-3* (internodes 1 to 20), and *ls-1* (internodes 1 to 20; Fig. B.2A and B). The *PsGA3ox1*-overexpressor line TG1 produced longer internodes than C1 (internodes 4 to 20) (Fig. B.2C).

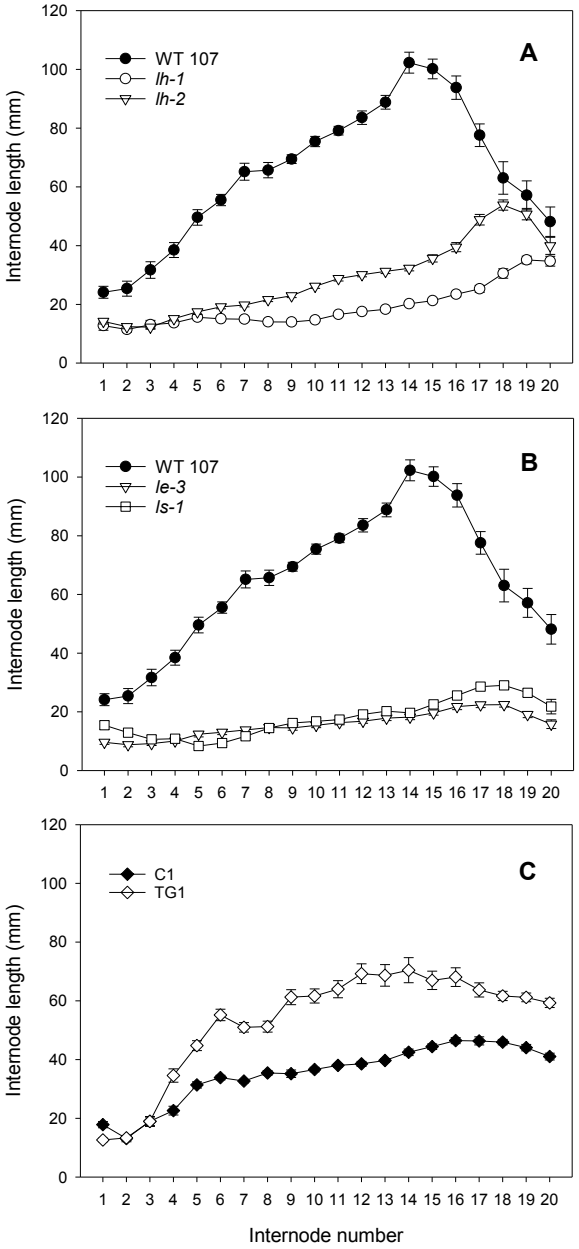

Figure B.2: Internode lengths at maturity. (A) GA biosynthesis mutants; *lh-1, lh-2,* and wild-type, WT- 107 (B) biosynthesis mutants; *ls-1* and *le-3* and wild-type, WT-107 (C) GA overexpressor line TG1 and its control, C1. Data are means ± SE, n= 33 for WT-107; n=29 for *lh-1*; n=29 for *lh-2*; n=31 for *le-3*; n=29 for *ls-1*; n=25 for C1; n=35 for TG1.

Appendix C: Phenotypic characterization of GA biosynthesis mutants; *lh-1, lh-2, ls-1* and *le-3* and their isogenic wild-type (WT-107)

C.1 Background

Plants of LS LH LE3 WT-107, *lh-1, lh-2, ls-1*-and *le-3* lines used to measure internode lengths (see section B.1) were further characterized at maturity for additional vegetative phenotypic parameters (total plant height, total number of nodes per plant, and nodes to first flower) and reproductive phenotypic parameters at the first and second flowering nodes (Table C.1).

C.2 Results

Table C.1: Phenotypic characterization of WT-107 control and *lh-1*, *lh-2*, *le-3* and *ls-1* mutants of GA biosynthesis in pea at maturity.

Data are means ± SE; np = not present; n = number of replicates. [a]Pericarp length at maturity (mm). [b]Number of seeds per fruit.

Parameter	WT-107	*lh-1*	*lh-2*	*le-3*	*ls-1*
Plant height (cm)	129.57 ± 3.28; n = 33	41.76 ± 1.56; n = 27	66.19 ± 1.36; n = 26	34.25 ± 0.92; n = 28	34.07 ± 0.61; n = 27
Nodes per plant	19.15 ± 0.27; n = 33	20.59 ± 0.37; n = 29	22.04 ± 0.30; n = 27	19.77 ± 0.24; n = 30	19.41 ± 0.31; n = 30
Nodes to first flower	14.67 ± 0.27	16.97 ± 0.27	16.85 ± 0.19	17.00 ± 0.22	15.93 ± 0.24
Number of seeds per pericarp	3.11 ± 0.09; n = 215	2.88 ± 0.13; n = 104	1.50 ± 0.08; n = 174	1.14 ± 0.08; n = 138	2.87 ± 0.12; n = 116
First flower node, Position 1*					
Pericarp length (no seed)	np	np	43.00 ± 1.00; n = 2	43.29 ± 1.33; n = 14	np
Pericarp length (one seed)	57; n = 1	np	50; n = 1	48.70 ± 0.83; n = 10	50.60 ± 1.78; n = 5
Pericarp length (two seeds)	50.00 ± 0.00; n = 2	49.57 ± 3.15; n = 7	47.57 ± 0.76; n = 14	49.20 ± 2.13; n = 5	52.60 ± 1.03; n = 5
Pericarp length (three seeds)	54.00 ± 1.87; n = 5	52.86 ± 1.56; n = 7	50.20 ± 0.58; n = 5	51; n = 1	52.67± 1.20; n = 3
Pericarp length (four seeds)	56.45 ± 0.79; n = 11	55.00 ± 0.88; n = 10	50.33 ± 0.33; n = 3	np	56.00 ± 0.99; n = 12
Pericarp length (five seeds)	60.21 ± 4.54; n = 14	58 ± 1.53; n = 3	50.00 ± 0.00; n = 2	np	61.00 ± 1.00; n = 2
First flower node, Position 2*					
Pericarp length (no seed)	np	np	np	42.00 ± 2.74; n = 8	np
Pericarp length (one seed)	44.00 ± 2.00; n = 2	np	np	45.00 ± 1.29; n = 11	np
Pericarp length (two seeds)	51.67 ± 1.67; n = 3	np	np	42.14 ± 1.51; n = 6	np
Pericarp length (three seeds)	50.83 ± 1.36; n = 12	np	46.00 ± 2.00; n = 2	np	49.00 ± 1.00; n = 2
Pericarp length (four seeds)	56.40 ± 0.75; n = 5	np	np	np	60; n = 1
Pericarp length (five seeds)	56.60 ± 1.03; n = 5	np	np	np	55; n = 1

Parameter	WT-107	*lh-1*	*lh-2*	*le-3*	*ls-1*
Second flower node, Position 1*					
Pericarp length (no seed)	np	np	45.00 ± 0.58; n = 3	43.00 ± 2.35; n = 7	np
Pericarp length (one seed)	np	48; n = 1	48.20 ± 1.10; n = 10	44.91 ± 1.68; n = 11	np
Pericarp length (two seeds)	52.50 ± 0.50; n = 2	52.67 ± 1.05; n = 6	47.22 ± 1.28; n = 9	47.14 ± 1.88; n = 7	53.00 ± 1.00; n = 4
Pericarp length (three seeds)	52.40 ± 0.73; n = 10	54.71 ± 0.94; n = 7	49.00 ± 0.77; n = 5	50.67 ± 2.19; n = 3	52.64 ± 1.53; n = 11
Pericarp length (four seeds)	54.31 ± 0.72; n = 16	54.18 ± 1.30; n = 11	np	52; n = 1	57.38 ± 1.13; n = 8
Pericarp length (five seeds)	55.00 ± 2.24; n = 5	59.25 ± 0.85; n = 4	np	np	59.17 ± 1.22; n = 6
Second flower node, Position 2*					
Pericarp length (no seed)	np	np	45; n = 1	43.75 ± 2.25; n = 4	np
Pericarp length (one seed)	50; n = 1	np	41; n = 1	46.75 ± 2.66; n = 4	np
Pericarp length (two seeds)	44.67 ± 3.53; n = 3	np	np	46.50 ± 1.32; n = 4	np
Pericarp length (three seeds)	51.00 ± 1.10; n = 12	np	np	50; n = 1	np
Pericarp length (four seeds)	54.29 ± 1.23; n = 7	np	np	np	np
Pericarp length (five seeds)	np	np	np	np	np

The first flower on the inflorescence is labeled as position 1 and second flower on the inflorescence is labeled as position 2.

Appendix D: Phenotypic characterization of transgenic control, C1 and *PsGA3ox1* overexpression transgenic, TG1 in pea at maturity

D.1 Background

Plants of TG1 and C1 lines used to measure internode lengths (see section B.1) were further characterized at maturity for additional vegetative phenotypic parameters (total plant height, total number of nodes per plant, nodes to first flower) and reproductive phenotypic parameters (Table D.1).

D.2 Results

Table D.1: Phenotypic characterization of transgenic control, C1 and *PsGA3ox1* overexpression transgenic, TG1 in pea at maturity.

Data are means ± SE; np = not present; n = number of replicates. [a]Pericarp length at maturity (mm). [b]Number of seeds per fruit.

Parameter	C1	TG1
Plant height (cm)	95.35 ± 1.75; n = 27	170.83 ± 2.08; n = 35
Nodes per plant	26.41 ± 0.41	35.23 ± 0.51
Nodes to first flower	23.15 ± 0.23	27.77 ± 0.25
Seeds per pericarp	2.62 ± 0.10; n = 137	3.71 ± 0.08; n = 242
Pericarp length (no seed)	np	42; n = 1
Pericarp length (one seed)	41.15 ± 1.94; n = 26	35.38 ± 2.41; n =8
Pericarp length (two seeds)	44.05 ± 1.00; n = 42	47.45 ± 1.39; n = 29
Pericarp length (three seeds)	52.32 ± 0.94; n = 38	52.46 ± 0.77; n = 69
Pericarp length (four seeds)	56.86 ± 1.06; n = 22	58.10 ± 0.64; n = 78
Pericarp length (five seeds)	61.63 ± 1.49; n = 8	63.26 ± 1.21; n = 39
Pericarp length (six seeds)	np	67.18 ± 1.42; n = 17

Appendix E: Toluidine blue stained micrographs of seed coat sections prepared from pea seeds cv. I_3 (Alaska-type)

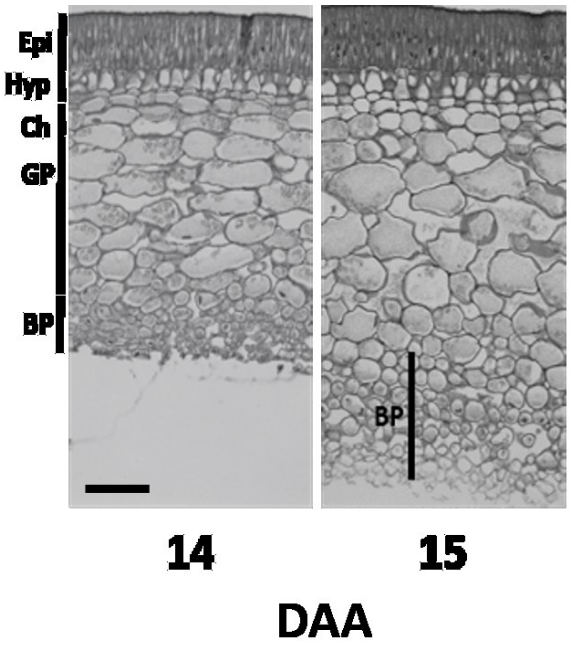

Figure E.1: Toluidine blue stained micrographs of seed coat sections prepared from cv. I_3 (Alaska-type) pea seeds from 14 and 15 DAA. Micrographs were taken at 20X magnification and scale bar is 100 µm. Epi, epidermis; Hyp, hypodermis; Ch, chlorenchyma; GP, ground parenchyma; BP, branched parenchyma.

Appendix F: Staining of starch granules in 25 DAA seed coat and cotyledon sections of *lh-2* mutant

F.1. Background

This appendix contains micrographs which were obtained by staining 25 DAA seed coat and cotyledon sections of *lh-2* with Gram's Iodine solution (1g of iodine and 2g of potassium iodide dissolved in 300 mL of water) to visualize starch granules. This experiment was conducted to see whether all the starch granules in the *lh-2* seed coat are mobilized to the cotyledons by 25 DAA, since a delay in the starch mobilization was observed in this line from 8 to 20 DAA, compared to the *LH*. For comparison, 20 DAA seed coat and cotyledon micrographs of *lh-2* mutant are also represented.

F.2 Results

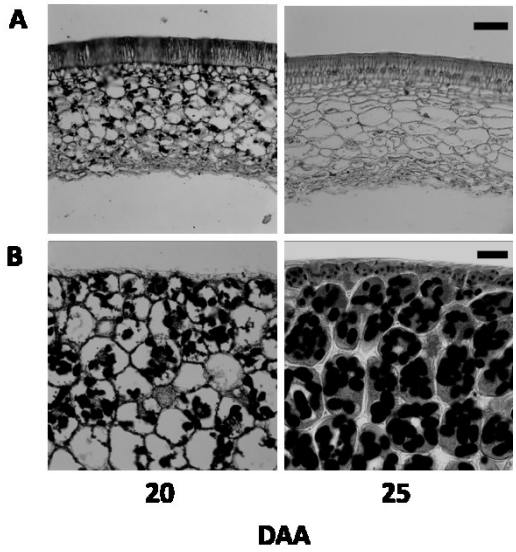

Figure F.1: Representative micrographs of pea seed coat and cotyledon cross-sections obtained from 20 and 25 DAA *lh-2* seeds. Sections were stained with Gram's Iodine solution for starch grain visualization. (A) Seed coats; (B) Cotyledons. Micrographs were taken at 20X (A) and 40X (B) magnifications and scale bars are 100 μm in A and 50 μm in B.

Minimal to no starch granules were visible in 25 DAA seed coats of *lh-2* suggesting relatively complete mobilization of the seed coat starch into the embryo by 25 DAA (Fig. F.1A). Consistently, starch content in storage parenchyma cells of *lh-2* cotyledons markedly increased from 20 to 25 DAA (Fig. F.1B). Therefore, the starch in the seed coats of the *lh-2* mutant is fully mobilized for transport to the embryo, but this process is markedly delayed compared to that observed in *LH*.

Appendix G: T-test tables

G.1 Introduction

Probability values (P-values) were calculated using two-tailed tests (assuming unequal variance) for the comparisons of WT-107 line with the GA-biosynthesis mutant lines *lh-1, lh-2, ls-1*, or *le-3,* and for the comparison of the GA overexpression line TG1 with the control C1 line for the following parameters:

a. Whole seed, seed coat and embryo fresh weight
b. Seed coat cellular expansion
c. Cotyledon cellular expansion
d. Seed coat carbohydrate analysis
e. Cotyledon carbohydrate analysis
f. Endosperm carbohydrate analysis
g. Cotyledon protein content analysis in TG1 and C1 embryos

G.2 Results

Table G.1: Probability values (P-values) for the comparison of the WT-107 (WT) line with the GA biosynthesis mutant lines, and the GA overexpressor TG1 line with its control (C1) line, using a two-tailed test (assuming unequal variance) for whole seed, seed coat and embryo fresh weight.

Whole seed

	Probablility (P) values for the comparison using a two-tailed test						
	DAA						
Comparison	**8**	**10**	**12**	**14**	**16**	**18**	**20**
WT-lh1	2.53088E-07	7.53684E-06	1.79863E-01	4.58505E-03	3.37792E-03	8.48548E-01	3.13338E-02
WT-lh2	1.58280E-14	1.29649E-08	1.19579E-06	1.55482E-09	3.04185E-07	9.15648E-13	6.12199E-12
WT-le3	2.41064E-03	3.48880E-01	1.86635E-02	5.84659E-10	1.48759E-05	3.48056E-06	1.67889E-02
WT-ls1	5.84189E-03	1.19240E-01	1.29506E-02	7.78552E-04	1.89772E-03	5.59361E-05	5.80178E-01
C1-TG1	1.45311E-05	9.13619E-01	1.15942E-03	2.33155E-01	2.29633E-09	8.64032E-04	1.03565E-04

Seed coat

	Probablility (P) values for the comparison using a two-tailed test						
	DAA						
Comparison	**8**	**10**	**12**	**14**	**16**	**18**	**20**
WT-lh1	5.66623E-04	5.56934E-06	9.88854E-01	2.88931E-03	8.40289E-02	8.73028E-01	6.32301E-02
WT-lh2	2.72870E-08	7.04426E-10	2.94458E-13	6.35744E-06	3.98514E-04	6.54130E-03	9.98733E-05
WT-le3	1.21136E-07	1.94776E-04	1.05068E-01	2.68686E-04	9.59640E-01	3.45421E-01	1.00000E+00
WT-ls1	7.75764E-06	3.39252E-05	4.36942E-01	3.80836E-01	1.70217E-02	5.57920E-01	5.71829E-03
C1-TG1	3.87258E-06	5.66806E-01	7.77697E-04	8.12277E-01	2.00251E-04	4.78776E-01	8.00527E-01

Embryo

	Probablility (P) values for the comparison using a two-tailed test				
	DAA				
Comparison	**12**	**14**	**16**	**18**	**20**
WT-lh1	1.02602E-02	4.63048E-03	6.77782E-03	5.16633E-01	1.34346E-02
WT-lh2	1.93347E-06	1.28104E-09	1.50963E-06	5.88645E-06	1.33169E-07
WT-le3	1.57150E-01	2.12905E-07	7.76222E-04	3.82210E-05	4.00151E-03
WT-ls1	6.60214E-02	1.61643E-03	5.41965E-03	4.74719E-04	8.53659E-01
C1-TG1	2.45272E-06	1.45961E-01	7.78897E-09	2.58196E-04	5.13456E-05

Table G.2: Probability values (P-values) for the comparison of the WT-107 (WT) line with GA biosynthesis mutant lines, and the GA overexpressor TG1 line with its control (C1) line, using a two-tailed test (assuming unequal variance) for cell expansion in seed coat epidermis, hypodermis, chlorenchyma, ground parenchyma and branched parenchyma layers.

Epidermis

	Probability (P) values for the comparison using a two-tailed test						
	DAA						
Comparison	8	10	12	14	16	18	20
WT-*lh1*	0.153553915	0.031057205	0.109570333	0.074980563	0.030558058	0.035422057	0.322506480
WT-*lh2*	0.001664982	0.010948452	0.001269458	0.000187934	0.188074300	0.071356989	0.044497662
WT-*le3*	0.140059237	0.007558298	0.638045562	0.151406270	0.604115864	0.033157932	0.212131746
WT-*ls1*	0.9306265	0.120485524	0.111150977	0.572295248	0.415193629	0.011318161	0.161011863
C1-TG1	0.119960249	0.000168802	0.026503111	0.002790641	0.028801046	0.478513956	0.107133167

Hypodermis

	Probability (P) values for the comparison using a two-tailed test						
	DAA						
Comparison	8	10	12	14	16	18	20
WT-*lh1*	0.882737396	0.125400545	0.782441153	0.129452588	0.178696791	0.008982076	0.011540835
WT-*lh2*	0.584492047	0.810111757	0.000336043	0.000078661	0.017957099	0.736565445	0.703796185
WT-*le3*	0.091799985	0.608721007	0.822364754	0.006490201	0.373540470	0.029698033	0.014422171
WT-*ls1*	0.555424014	0.058222116	0.715418408	0.167590017	0.031499430	0.017662361	0.114740081
C1-TG1	0.284670240	0.000311327	0.000221253	0.300366542	0.018037948	0.461654478	0.426839020

Cholenchyma

	Probability (P) values for the comparison using a two-tailed test						
	DAA						
Comparison	8	10	12	14	16	18	20
WT-*lh1*	0.297730329	0.000020007	0.629537682	0.776504233	0.504198484	0.587167204	0.370356737
WT-*lh2*	0.246849639	0.348031125	0.017965358	0.005379535	0.397158210	0.404102304	0.858346761
WT-*le3*	0.489725763	0.044837888	0.169443199	0.053961768	0.932310967	0.468922284	0.233650976
WT-*ls1*	0.241866323	0.011492516	0.018921208	0.254372999	0.777662706	0.287241835	0.069684857
C1-TG1	0.278231985	0.001585222	0.002726618	0.030160996	0.453205335	0.018917213	0.011185371

Ground Parenchyma

	Probability (P) values for the comparison using a two-tailed test						
	DAA						
Comparison	8	10	12	14	16	18	20
WT-*lh1*	0.000418020	0.275652807	0.295441582	0.507765983	0.943815343	0.944412641	0.697451413
WT-*lh2*	0.094381052	0.000536740	0.104604559	0.000179899	0.697393078	0.080546722	0.000341845
WT-*le3*	0.526866717	0.640666641	0.376370487	0.254946297	0.671679625	0.677683012	0.513659096
WT-*ls1*	0.167306171	0.378321968	0.001847039	0.107931141	0.249693846	0.040573484	0.011907778
C1-TG1	0.030332940	0.024299426	0.016787003	0.153770855	0.633002434	0.002079572	0.065768034

Branched Parenchyma

	Probability (P) values for the comparison using a two-tailed test				
	DAA				
Comparison	8	10	12	14	16
WT-*lh1*	0.086120137	0.262866737	0.184581724	0.361337782	0.216264074
WT-*lh2*	0.019060278	0.633548384	0.178814434	0.982023486	0.989602080
WT-*le3*	0.285953836	0.842386598	0.039115847	0.099598298	0.331360559
WT-*ls1*	0.062763735	0.130489105	0.083638756	0.076490775	0.006168939
C1-TG1	0.478739139	0.031108348	0.022347838	0.186070473	0.632829696

Table G.3: Probability values (P-values) for the comparison of the WT-107 (WT) line with the GA biosynthesis mutant lines, and the GA overexpressor TG1 line with its control (C1) line, using a two-tailed test (assuming unequal variance) for cotyledonary storage parenchyma cell expansion.

	Probability (P) values for the comparison using a two-tailed test				
	DAA				
Comparison	12	14	16	18	20
WT-*lh1*	0.13227402	0.77452291	0.76900211	0.84132787	0.92838847
WT-*lh2*	0.17485729	0.02855667	0.46192337	0.13933291	0.31846472
C1-TG1	0.0251245	0.13568602	0.00140239	0.00535617	0.67125311

Table G.4: Probability values (P-values) for the comparison of the WT-107 (WT) line with the GA biosynthesis mutant lines, and the GA overexpressor TG1 line with its control (C1) line, using a two-tailed test (assuming unequal variance) for seed coat starch, glucose and sucrose content.

Starch

	Probability (P) values for the comparison using a two-tailed test						
	DAA						
Comparison	**8**	**10**	**12**	**14**	**16**	**18**	**20**
WT-*lh1*	3.90269E-05	0.000138493	0.04501144	0.00361287	0.022494257	0.015201876	0.042179442
WT-*lh2*	4.5446E-05	3.25539E-06	0.001573749	0.043002183	0.001118829	0.000174522	4.18464E-06
WT-*le3*	0.000555869	4.97173E-06	0.000961863	0.011560591	0.000666234	0.591428194	0.095881884
WT-*ls1*	5.39531E-05	0.000383986	5.55616E-09	0.00209935	0.000994528	0.004016544	0.552783263
C1-TG1	0.297440872	0.003327168	0.280103332	0.126960795	0.018249124	0.000402428	0.047934474

Glucose

	Probability (P) values for the comparison using a two-tailed test						
	DAA						
Comparison	**8**	**10**	**12**	**14**	**16**	**18**	**20**
WT-*lh1*	0.066004886	0.06562276	0.000127649	0.018996021	0.030648907	0.250088305	0.341431936
WT-*lh2*	0.010639233	0.00529377	0.027236549	0.238059871	0.696473396	0.425501121	0.24409215
WT-*le3*	0.079314631	5.56401E-06	3.18886E-06	0.000523794	0.001373236	0.00842571	0.004793645
WT-*ls1*	0.096834606	0.014807601	3.16763E-05	0.006979434	0.001848927	0.129093974	0.105822172
C1-TG1	4.62937E-05	0.000243087	6.69539E-07	0.000111028	0.000878316	1.35167E-06	7.80453E-06

Sucrose

	Probability (P) values for the comparison using a two-tailed test						
	DAA						
Comparison	**8**	**10**	**12**	**14**	**16**	**18**	**20**
WT-*lh1*	0.011649766	0.043732295	0.018475178	0.865216545	0.019432855	0.000381342	2.55172E-05
WT-*lh2*	0.096446294	0.108005445	0.309091112	0.063671903	0.082506284	0.003883593	0.043070357
WT-*le3*	0.082362521	0.363201452	0.078612043	0.296584593	0.447072731	0.068869747	0.008332004
WT-*ls1*	0.025831034	0.037802243	0.016736844	0.032788017	0.047065248	0.043524326	0.012311439
C1-TG1	0.060966879	0.003474594	0.014199021	0.474939456	0.000923101	0.023665118	0.148794315

Table G.5: Probability values (P-values) for the comparison of the WT-107 (WT) line with the GA biosynthesis mutant lines, and the GA overexpressor TG1 line with its control (C1) line, using a two-tailed test (assuming unequal variance) for cotyledon starch, glucose and sucrose content.

Starch

	Probability (P) values for the comparison using a two-tailed test				
	DAA				
Comparison	**12**	**14**	**16**	**18**	**20**
WT-*lh1*	0.106744379	0.000929305	0.000221846	0.57400458	0.006923438
WT-*lh2*			2.30232E-07	0.005442417	0.001376221
WT-*le3*	0.027140444	0.001318464	0.000199501	0.043877345	0.00524551
WT-*ls1*	0.009306743	5.60792E-05	0.01364089	0.13351592	0.009150501
C1-TG1	6.75549E-05	0.000575452	0.005753145	0.002036722	0.006339117

Glucose

	Probability (P) values for the comparison using a two-tailed test				
	DAA				
Comparison	**12**	**14**	**16**	**18**	**20**
WT-*lh1*	9.11002E-05	0.001701524	0.041022323	0.068645457	0.003631366
WT-*lh2*			0.13663013	0.268173908	0.003053412
WT-*le3*	0.000400677	0.00068642	0.019048739	0.033786449	0.041975146
WT-*ls1*	0.00081938	0.011974433	0.047502006	0.889289639	0.000196733
C1-TG1	7.632E-05	0.145709244	0.29702951	0.602113141	0.617700746

Sucrose

	Probability (P) values for the comparison using a two-tailed test				
	DAA				
Comparison	**12**	**14**	**16**	**18**	**20**
WT-*lh1*	0.045358775	0.00308937	0.04649493	0.00061735	0.000473995
WT-*lh2*			0.103376956	0.003742806	0.000751617
WT-*le3*	0.001597823	0.03012352	0.030325201	0.000347546	0.001364278
WT-*ls1*	0.000580742	0.016430075	0.028459307	0.372315231	0.837587896
C1-TG1	0.028445936	6.40412E-05	0.008484702	0.015316844	0.24877149

Table G.6: Probability values (P-values) for the comparison of the WT-107 (WT) line with GA biosynthesis mutant lines, and the GA overexpressor TG1 line with its control (C1) line, using a two-tailed test (assuming unequal variance) for endosperm glucose and sucrose content.

Glucose

	Probability (P) values for the comparison using a two-tailed test	
	DAA	
Comparison	10	12
WT-*lh2*	0.016791033	6.65815E-05
C1-TG1	0.804946977	0.501821775

Sucrose

	Probability (P) values for the comparison using a two-tailed test	
	DAA	
Comparison	10	12
WT-*lh2*	0.003432759	6.74383E-05
C1-TG1	0.485176132	0.240490698

Sucrose: Glucose

	Probability (P) values for the comparison using a two-tailed test	
	DAA	
Comparison	10	12
WT-*lh2*	0.012536754	0.013381779
C1-TG1	0.34886447	0.114648714

Table G.7: Probability values (P-values) for the comparison of the GA overexpressor TG1 line with its control (C1) line using a two-tailed test (assuming unequal variance) for cotyledon protein content.

Protein content %

Probability (P) values for the comparison using a two-tailed test				
	DAA			
Comparison	10	12	14	16
C1-TG1	0.012724	0.001475	0.001021	0.001669

mg protein per cotyledon pair

Probability (P) values for the comparison using a two-tailed test				
	DAA			
Comparison	10	12	14	16
C1-TG1	0.001034	1.42E-05	4.23E-06	0.000202